CRYSTALLOGRAPHY OF $(Zn,Cd,Mn)_3(PO_4)_2$ COMPOUNDS

AN X-RAY CRYSTALLOGRAPHIC
STUDY OF
$(Zn,Cd,Mn)_3(PO_4)_2$ COMPOUNDS

By

JOHN SOMERSET STEPHENS, B. Sc.

A Thesis
Submitted to the Faculty of Graduate Studies
in Partial Fulfilment of the Requirements
for the Degree
Doctor of Philosophy

McMaster University
May 1967

DOCTOR OF PHILOSOPHY (1967) McMASTER UNIVERSITY
(Chemical Physics) Hamilton, Ontario

TITLE: An X-ray Crystallographic Study of $(Zn,Cd,Mn)_3(PO_4)_2$ Compounds

AUTHOR: John Somerset Stephens, B. Sc., (McMaster University)

SUPERVISOR: Professor C. Calvo

NUMBER OF PAGES: viii, 121

SCOPE AND CONTENTS: The crystal structures of four compounds of the type $(Zn,Cd,Mn)_3(PO_4)_2$ have been determined by X-ray diffraction methods. These structures are the high temperature (β) phase of $Zn_3(PO_4)_2$, the related structures of β^1-$Mn_3(PO_4)_2$ and β^1-$Cd_3(PO_4)_2$, and the structure of a member of a solid solution of median composition $Zn_2Cd(PO_4)_2$ which is similar in structure to the mineral graftonite. The orthophosphates of the small divalent metal ions have been separated into four structure classes and the stability of each of these classes is discussed in terms of cation concentration and the types of cation sites which exist in these structures. The correlation of a host crystal structure and the luminescence of Mn^{++} when this ion is added as an impurity is also discussed.

Acknowledgements

I am greatly indebted to my supervisor, Professor C. Calvo, for his guidance and for the close interest that he displayed throughout these studies. My thanks are also extended to the other members of the crystallography group, especially to Professor I. D. Brown, Mr. J. S. Rutherford and Mr. B. E. Robertson, for their very helpful discussions and collaboration in the preparation of computer programs.

I am grateful to the Government of the Province of Ontario for my personal financial support through the Ontario Graduate Fellowships.

TABLE OF CONTENTS

Page

I INTRODUCTION 1

II CRYSTAL STRUCTURE ANALYSIS

A. The Structure Factor and Electron Density 6

B. The Structure Factor and the Measured Intensity 7

C. The Patterson Function 8

D. Unitary Structure Factor Relationships 10

E. The Difference Synthesis 11

F. Least squares Refinement 13

III MEASUREMENT OF INTENSITIES

A. Photographic Methods 19

B. Diffractometer Method 20

C. Errors in Measurement 23

IV THE STRUCTURE OF $\beta\text{-}Zn_3(PO_4)_2$

A. Preliminary Investigations 28

B. Lattice parameters 29

C. Intensity Data and Absorption Corrections 30

D. The Trial Solution 31

E. The Refinement 32

F. Description of the Structure 38

V THE STRUCTURES OF $\beta^{1}\text{-}Mn_3(PO_4)_2$ AND $\beta^{1}\text{-}Cd_3(PO_4)_2$

A. Crystal Chemistry of $Mn_3(PO_4)_2$ 47

(continued)

TABLE OF CONTENTS (concluded)

Page

B. Preparation of $\beta^1\text{-}Cd_3(PO_4)_2$ 51

C. Lattice Parameters 51

D. Intensity Data 52

E. Superstructure in $\beta^1\text{-}Mn_3(PO_4)_2$ and $\beta^1\text{-}Cd_3(PO_4)_2$ 53

F. Solution of the Small Cell Structures 56

G. Solution and Refinement of the Large Cell Structure 57

H. Description of the Structure 69

VI THE GRAFTONITE STRUCTURE

A. Occurrence of the Graftonite Structure 78

B. Preparation 80

C. Lattice Parameters 82

D. Intensity Data 82

E. The Trial Solution 83

F. The Refinement 86

G. Description of the Structure 89

VII DISCUSSION AND SUMMARY

A. Discussion 102

B. Summary 113

BIBLIOGRAPHY 116

APPENDIX A 119

TABLE INDEX

Table Page

IV-1 β-$Zn_3(PO_4)_2$: Observed and calculated structure factors 34

IV-2 β-$Zn_3(PO_4)_2$: Atomic parameters 36

IV-3 β-$Zn_3(PO_4)_2$: Summary of residuals 37

IV-4 β-$Zn_3(PO_4)_2$: Bond distances and angles 40

IV-5 P-O bond distances in orthophosphate structures 45

IV-6 β-$Zn_3(PO_4)_2$: Bond angles subtended at the oxygen atoms 46

V-1 Lattice parameters of graftonite and Mn-graftonite 49

V-2 Lattice parameters of β-$Zn_3(PO_4)_2$, β^1-$Mn_3(PO_4)_2$ and β^1-$Cd_3(PO_4)_2$ 49

V-3 Residuals for $p=\pm 1$ during β^1-$Mn_3(PO_4)_2$ refinement 61

V-4 β^1-$Mn_3(PO_4)_2$ and β^1-$Cd_3(PO_4)_2$: Summary of residuals 61

V-5 β^1-$Mn_3(PO_4)_2$ and β^1-$Cd_3(PO_4)_2$: Atomic parameters 63

V-6 β^1-$Mn_3(PO_4)_2$: Observed and calculated structure factors 65

V-7 β^1-$Cd_3(PO_4)_2$: Observed and calculated structure factors 67

V-8 β^1-$Mn_3(PO_4)_2$ and β^1-$Cd_3(PO_4)_2$: P-O bond distances and angles 70

V-9 β^1-$Mn_3(PO_4)_2$, β^1-$Cd_3(PO_4)_2$ and β-$Zn_3(PO_4)_2$: Cation-oxygen bond distances and angles 71

V-10 β^1-$Mn_3(PO_4)_2$: Bond angles subtended at the oxygen atoms 77

VI-1 Lattice parameters of graftonite-like compounds 79

VI-2 B-graftonite: Atomic parameters 90

VI-3 B-graftonite: Summary of residuals 91

VI-4 B-graftonite: Observed and calculated structure factors 92

(continued)

TABLE INDEX (concluded)

Table		Page
VI-5	B-graftonite: Bond distances and angles	96
VI-6	B-graftonite: Bond angles subtended at the oxygen atoms	101
VII-1	Four structure classes among the small divalent metal ion orthophosphates	108
A-1	Dead-time correction evaluation	121

INDEX OF ILLUSTRATIONS

Figure		Page
I-1	Phase relationships in the $Zn_3(PO_4)_2$-$Cd_3(PO_4)_2$ system	3
III-1	Equi-inclination Weissenberg geometry	21
IV-1	Cation polyhedra linkages in β-$Zn_3(PO_4)_2$	42
IV-2	Spiral cation polyhedra chains in β-$Zn_3(PO_4)_2$	43
V-1	Cation polyhedra linkages in β^{1}-$Mn_3(PO_4)_2$	74
V-2	Spiral cation polyhedra chains in β^{1}-$Mn_3(PO_4)_2$	75
VI-1	Infinite sheet of $M(1)O_7$ polyhedra in B-graftonite	97
VI-2	Infinite chains of $M(3)O_5$ polyhedra in B-graftonite	98
VI-3	Interlocking sheets of cation polyhedra in B-graftonite	99

CHAPTER I

INTRODUCTION

The first comprehensive study of the phase behaviour of the orthophosphates of Zn^{++}, Cd^{++} or Mn^{++} was that of Hummel and his co-workers. In a study of the phase behaviour in the $ZnO-P_2O_5$ system(1), they found that pure $Zn_3(PO_4)_2$ exists in two modifications. The low temperature modification, or α phase, is stable at temperatures below 942°C. Above this temperature the β phase is stable. The transition between these two phases is reversible, but is sluggish, and the β phase can thus be obtained as a metastable crystalline solid at room temperature by quenching from above the transition temperature.

Further studies in the $ZnO-MnO-P_2O_5$ system(2) showed that a solid solution extending up to 30 mole per cent of $Mn_3(PO_4)_2$ in $Zn_3(PO_4)_2$ above 940°C. gave an X-ray powder diffraction pattern which corresponded to that of $\beta-Zn_3(PO_4)_2$. At temperatures below this, only a small amount of $Mn_3(PO_4)_2$ could be disolved in $\alpha-Zn_3(PO_4)_2$. With $Mn_3(PO_4)_2$ concentrations between about 5 and 25 mole per cent, a third distinct structure was noted, and this solid solution was called $\gamma-Zn_3(PO_4)_2$. The existence of this phase had been previously reported by Smith(3) together with the α and β phases, but their phase relationship was not well characterized.

The $(Zn, Cd)_3(PO_4)_2$ system was also studied in some detail and a phase diagram derived(4). As in the $(Zn, Mn)_3(PO_4)_2$ studies, $Zn_3(PO_4)_2$ and $Cd_3(PO_4)_2$ were found to form a limited solid solution with the $\beta-Zn_3(PO_4)_2$ structure at temperatures above about 900°C. At lower temperatures, three distinct solid solution regions were reported between the two end members. This phase diagram is reproduced in Fig. (I-1). The "A" solid solution was recognized to have the γ-$Zn_3(PO_4)_2$ structure, showing that this structure is stabilized by $Cd_3(PO_4)_2$ as well as $Mn_3(PO_4)_2$. "B" and "C" solid solutions were noted to have similar X-ray powder patterns, but a discontinuous change in the d-spacings of some of the lines, as the Zn-Cd ratio was changed, indicated that these were two distinct phases. The sixth phase in this system is a solid solution region with less than 6 mole per cent $Zn_3(PO_4)_2$, which evidently has the same structure as pure $Cd_3(PO_4)_2$.

Investigation of the $Zn_3(PO_4)_2$-$Mg_3(PO_4)_2$ system$^{(5)}$ showed that the γ-$Zn_3(PO_4)_2$ solid solution series is also stabilized by the addition of more than 3 mole per cent $Mg_3(PO_4)_2$, and that this solid solution extends all the way to the Mg end member.

These phase studies were combined with studies of the luminescence of Mn^{++} when the different phases were doped with this ion. This luminescence is either red, in the case of β-$Zn_3(PO_4)_2$, γ-$Zn_3(PO_4)_2$ (including $Mg_3(PO_4)_2$) and in all the $(Zn,Cd)_3(PO_4)_2$ phases, or a yellowish green in the case of α-$Zn_3(PO_4)_2$.

In an attempt to explain the different luminescent behaviour of Mn^{++} in silicate glasses, Linwood & Weyl$^{(6)}$ and Schulman$^{(7)}$ had suggested that the emission wavelength increased as the coordination number of the luminescing ion increased. Specifically, the green luminescence was thought to be due to tetrahedrally coordinated Mn^{++}, and the red luminescence to the ion in a site of octahedral coordination. This generalization has been supported by the determination of the crystal structures of

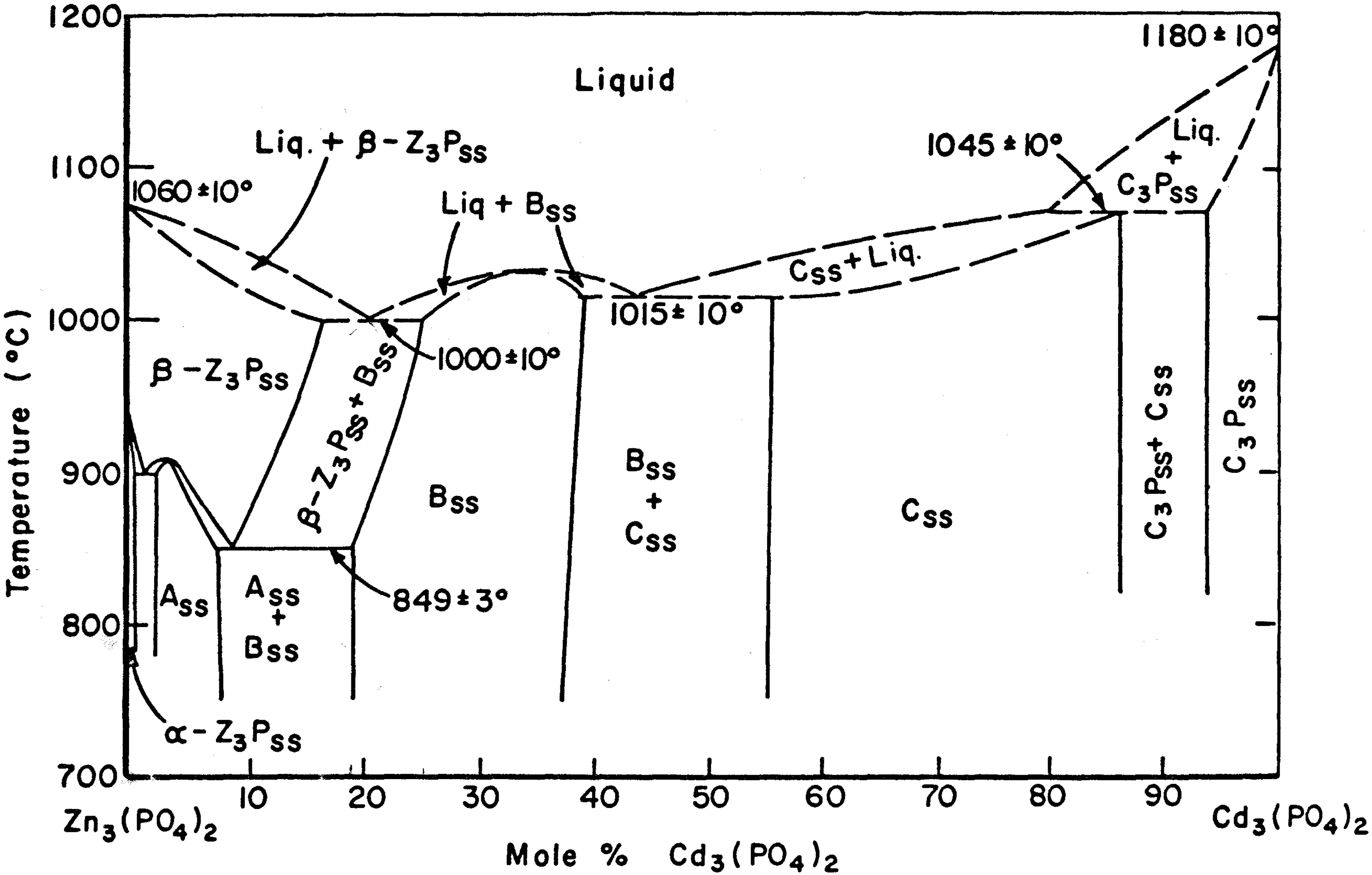

FIG. (1-1) Phase relationships on the $Zn_3(PO_4)_2$-$Cd_3(PO_4)_2$ join α-$Zn_3(PO_4)_2$(8) and γ-$Zn_3(PO_4)_2$(9). It was found that in the α phase, all of the cations are tetrahedrally coordinated, but that in the γ phase, one-third of the cations are situated in octahedral sites.

One can explain, in a qualitative manner, this observed relationship between coordination number and emission wavelength. In the Mn^{++} ion, the energy of the lowest excited state, arising from the ^4G state of the free ion, is depressed by a cubic crystal field, such as that found in an octahedral or tetrahedral environment(10). The field is stronger in the octahedral case, resulting in a lower energy for the transition to the ^6S ground state. Thus, the emission wavelength might be expected to increase as the strength of the crystal field increases with increasing coordination number.

If the Mn^{++} substitutes directly for a cation in the host lattice, as is likely in these divalent orthophosphate systems when $Mn_3(PO_4)_2$ forms solid solutions with the host structure, then the coordination number of a Mn^{++} ion in the host lattice should be the same as that of the host cation in the same site. If the relationship between coordination number and luminescent wavelength is a general one, this "coordination number hypothesis" might prove useful in providing information on the cation environment in a host lattice from a knowledge of the luminescent behaviour of Mn^{++} when this ion is added to the host crystal as an impurity.

The study of the structure of β-$Zn_3(PO_4)_2$ was initially undertaken to complete the structural knowledge of the phases of pure $Zn_3(PO_4)_2$, and also to test the applicability of the coordination number hypothesis in predicting the existence of an octahedral cation site from the red luminescence of Mn^{++}.

In the course of this study, the structural similarity of

$\beta^1\text{-}Cd_3(PO_4)_2$ and $\beta^1\text{-}Mn_3(PO_4)_2$ was noted, and a determination of these structures undertaken concurrently. $\beta^1\text{-}Mn_3(PO_4)_2$ was found to be one of two stable phases of pure $Mn_3(PO_4)_2$, the second phase having the same structure as the mineral graftonite$^{(11)}$ a mixed orthophosphate of Fe^{++}, Mn^{++} and Ca^{++}. Also, having this "graftonite" structure are the two solid solutions, B and C, in the $(Zn,Cd)_3(PO_4)_2$ system. The graftonite-like structure was also determined, using a crystal of the B solid solution.

The structure determinations of the four structures, $\beta\text{-}Zn_3(PO_4)_2$, $\beta^1\text{-}Mn_3(PO_4)_2$, $\beta^1\text{-}Cd_3(PO_4)_2$, and graftonite, are presented in Chapters IV, V and VI. In Ch. VII, the different structures are discussed with respect to their stability as a function of temperature and cation constitutents, and some conclusions are drawn concerning the preferred environments for the different cations, Zn^{++}, Cd^{++} and Mn^{++}. The applicability of the coordination number hypothesis in predicting cation environments is also discussed. In Ch. II the general methods of a crystal structure analysis are briefly outlined, and the experimental procedure used to measure the diffracted X-ray intensities is described in Ch. III.

CHAPTER II

CRYSTAL STRUCTURE ANALYSIS

A. The Structure Factor and Electron Density

X-rays are scattered by the electrons in a crystal. The amplitude of this scattering is given by the Fourier transform of the electron density $\rho(\underline{r})$. This amplitude, usually called the structure factor, or structure amplitude, can be written as (12)

$$F(\underline{H}) = \sum_{j=1}^{N} f_j(H) \exp 2\pi i(\underline{H}\cdot\underline{r}_j) \exp(-\underline{H}\cdot\underline{\underline{\beta}}_j\cdot\underline{H}) \qquad \text{(II-1)}$$

where $\underline{r}_j = x_j\underline{a} + y_j\underline{b} + z_j\underline{c}$ defines the position of the jth atom which has a scattering factor $f_j(H)$. $\underline{H}$ is a vector which is proportional to the change in momentum of a scattered photon, and thereby defines the direction of scattering. The scattering factor $f_j(H)$ is the Fourier transform of the electron density, at absolute zero, of the jth atom, which is assumed to be spherically symmetric, and which has been tabulated for different ionic species over the useful range of $|\underline{H}|$.(13) The factor $\exp(-\underline{H}\cdot\underline{\underline{\beta}}_j\cdot\underline{H})$ corrects $f_j(H)$ for the reduction in scattering amplitude due to the anisotropic thermal motion of the jth atom. $\underline{\underline{\beta}}_j$ or its isotropic counterpart, B_j, are referred to as the "temperature factors" of the jth atom.

The translational periodicity of the electron density in the crystal, where $\underline{a}$, $\underline{b}$, and $\underline{c}$ are chosen to be a set of fundamental translation vectors, restricts the vector $\underline{H}$ (for coherent, elastic scattering) to

$$\underline{H} = h\underline{a}^* + k\underline{b}^* + \ell\underline{c}^* \qquad \text{(II-2)}$$

where h, k and ℓ are integers. The relationship between the vectors $\underline{a}$, $\underline{b}$ and $\underline{c}$ which define the unit cell of volume V, and the corresponding reciprocal cell of volume $V^* = 1/V$, defined by the vectors $\underline{a}^*$, $\underline{b}^*$ and $\underline{c}^*$ are (12)

$$\underline{a}^* = \frac{\underline{b} \times \underline{c}}{V} \quad \text{and} \quad \underline{a} = \frac{\underline{b}^* \times \underline{c}^*}{V^*} \tag{II-3}$$

plus all cyclic permutations of a, b and c.

As the electron density is periodic, it can be represented by means of a Fourier series. The coefficients of this series are the structure factors,(12)

$$\rho(\underline{r}) = \frac{1}{V} \sum_{\underline{H}} F(\underline{H}) \exp -2\pi i(\underline{H} \cdot \underline{r}) \tag{II-4a}$$

or alternatively,

$$\rho(x,y,z) = \frac{1}{V} \sum_{h,k,\ell} F_{hk\ell} \exp -2\pi i(hx+ky+\ell z) \tag{II-4b}$$

B. The Structure Factor and the Measured Intensity

The structure amplitude defined in Eqn. (II-1) is in general a complex quantity. Only the magnitude of this quantity can be determined experimentally, as the integrated intensity of a reflection is given by(12)

$$I(\underline{H}) = k \left|F(\underline{H})\right|^2 \cdot A \cdot L \cdot p \tag{II-5}$$

The constant k depends on the volume of the unit cell, and the intensity and wavelength of the incident X-ray beam, all of which are independent of $\underline{H}$. L is the Lorentz factor, and this takes into account the different speeds with which the reflections pass through the reflecting condition. The Lorentz factor is purely geometric in origin, and the analytic expressions for its calculation have been derived for the geometries normally used for recording the X-ray intensity data.(12) The polarization factor, p, arises from the partial polarization of the X-ray beam upon "reflection" from the crystal.(12)

The term A in Eqn. (II-5) results from the attenuation of the incident and diffracted X-ray beams as they pass through the crystal. This reduction in intensity is of the form(12)

$$A = \frac{1}{V} \int_{V} \exp(-\mu x)\ dV \qquad \text{(II-6)}$$

where x is the total path length of the X-rays within a volume element dV in the crystal, and μ is the linear absorption coefficient of the crystal for the particular X-ray wavelength. Absorption corrections are usually only calculated for crystals of high external symmetry, such as spherical or cylindrical, for which the necessary corrections have been tabulated as a function of scattering angle.(12) If the crystal used in the intensity measurements is sufficiently small, and μ not too large, these corrections can often be ignored.

The electron density cannot be calculated in terms of experimentally determined quantities, as the phases of the structure factors are not initially known, and the solution of a crystal structure becomes the problem of determining these phases. If the structure contains a centre of symmetry, the structure factors must be real, and the problem is reduced to determining whether the structure factors are positive or negative.

C. The Patterson Function

If the electron density function is convoluted with itself, displaced by a vector $\underline{s} = u\underline{a} + v\underline{b} + w\underline{c}$, we have,

$$P(uvw) = V \int_{000}^{111}\!\!\int\!\!\int \rho(xyz)\, \rho(x+u,\, y+v,\, z+w)\, dx\, dy\, dz \qquad \text{(II-7)}$$

which with the aid of Eqn. (II-4b), reduces to

$$P(uvw) = \frac{1}{V} \sum_{hk\ell} |F_{hk\ell}|^2 \cos 2\pi(hu + kv + \ell w) \qquad \text{(II-8)}$$

This function, called the Patterson function after A. L. Patterson who derived it in 1934,(14) can be calculated with the information obtained directly from the measured intensities. The projection of this function down one of the unit cell axes, say $\underline{c}$, is given by

$$P(uv) = c \int_0^1 P(uvw)\, dw \qquad \text{(II-9)}$$

which, from Eqn. (II-8) becomes,

$$P(uv) = \frac{1}{A} \sum_{hk} |F_{hk0}|^2 \cos 2\pi(hu + kv) \qquad \text{(II-10)}$$

where A is the area of the projection.

Analogous expressions exist for the projected electron density, $\rho(xy)$.

As the electron density contains maxima at the positions of the atoms, and has relatively low values elsewhere, the Patterson function will contain a peak corresponding to each interatomic vector, at the point $\underline{s}$, where $\underline{s} = \underline{r}_j - \underline{r}_i$. If there are N atoms in the unit cell, each with Z_j electrons, j = 1, 2, ..N, the Patterson function will contain N^2 peaks of weight Z_iZ_j; N peaks of weight Z_i^2 at the origin, and N(N-1) peaks elsewhere in the function.

It has been shown(15) that a complete knowledge of the locations of all the Patterson peaks is sufficient to determine the positions of the atoms themselves. In practice, however, the $N(N-1)$ non-origin peaks are seldom all resolved in three dimensions, let alone in projection. Usually only the peaks corresponding to vectors between the heaviest atoms (a heavy atom refers to one with a large number of electrons, Z) are sufficiently well resolved to permit a solution for their positions to be obtained.

There are many techniques for solving Patterson functions to obtain trial coordinates for the heavier atoms,(15) and these will not be described here. The use of the Patterson function has been the most fruitful method for obtaining trial structures, and is the method most often used. There are, however, other methods of determining the phases of the structure factors directly from their magnitudes. These "direct methods" employ relationships which arise from the existence of symmetry operations which relate the atomic positions, and also from criteria such as the fact that the electron density is a real and positive function at all points in the unit cell.

D. Unitary Structure Factor Relationships

Although most of the trial solutions for the structures determined in these studies were obtained by finding solutions to their respective Patterson projections, the structure of β^1-$Mn_3(PO_4)_2$ was elucidated partly through the use of inequality relationships between the unitary structure factors.

A unitary structure factor is defined as(16)

$$U_{\underline{H}} = \frac{F(\underline{H})}{\sum_{j=1}^{N} f_j(H)\, \exp\,(-\underline{H}\cdot\underline{\underline{\beta}}_j\cdot\underline{H})} \qquad \text{(II-11)}$$

This is approximately the value that the structure factor would have if the ith atom were replaced by a stationary point scattering mass of $Z_i / \sum_{j=1}^{N} Z_j$ electrons. The term $\exp(-\underline{H}\cdot\underline{\underline{\beta}}_j\cdot\underline{H})$ in Eqn. (II-11) corrects for the thermal motion which is inherent in the value of $F(\underline{H})$. The maximum value of $U_{\underline{H}}$ is now unity, and corresponds to all of the atoms scattering in phase.

The existence of symmetry elements relating the positions of the atoms can be used to generate inequality relationships among the unitary structure factors. The particular inequalities used in the β^1-$Mn_3(PO_4)_2$ structure determination were (16)

$$(|U_{\underline{H}}| + |U_{\underline{H}'}|)^2 \leqq (1+U_{\underline{H}}U_{\underline{H}'}U_{\underline{H}+\underline{H}'})(1+U_{\underline{H}}U_{\underline{H}'}U_{\underline{H}-\underline{H}'}) \qquad \text{(II-12)}$$

which are valid for any structure which contains a centre of symmetry. If the unitary structure factors are large enough, this relationship can be used to show that either

$$U_{\underline{H}}U_{\underline{H}'}U_{\underline{H}+\underline{H}'} > 0, \text{ or } U_{\underline{H}}U_{\underline{H}'}U_{\underline{H}-\underline{H}'} > 0, \text{ or both.}$$

Relationships between the phases (signs) of the structure factors can thus be generated and these phases used with the $|F(\underline{H})|$ to calculate the electron density, from which the atomic coordinates are inferred.

E. The Difference Synthesis

When a trial structure has been found, it can be improved by two particularly useful procedures, (i) the difference electron density synthesis (difference synthesis), and (ii) the least squares refinement of the atomic parameters. The latter method is discussed in the next section.

The difference synthesis$^{(17)}$ is analogous to the electron density calculation (Eqn. (II-4)). Here, one must distinguish between $F_o(\underline{H})$, the observed structure factor, and $F_c(\underline{H})$, the structure factor calculated from Eqn. (II-1) using the atomic coordinates of the trial structure. Ideally, the difference synthesis is expressed as

$$\Delta\rho(\underline{r}) = \rho_o(\underline{r}) - \rho_c(\underline{r}) = \frac{1}{V}\sum_{hk\ell}\left[F_o(\underline{H})-F_c(\underline{H})\right] \exp-2\pi i(\underline{H}\cdot\underline{r}) \qquad \text{(II-13a)}$$

The phase of $F_o(\underline{H})$ is taken to be the same as that of $F_c(\underline{H})$, on the assumption that the trial structure is close enough to the correct structure to affect only the magnitude of the structure factors. It is necessary to weight the terms in a difference synthesis according to the reliability of the phase calculated for $F_c(\underline{H})$, and the actual calculation is of the form

$$\Delta\rho(\underline{r}) = \sum_{hk\ell} w_{\underline{H}}\left[F_o(\underline{H}) - F_c(\underline{H})\right] \exp-2\pi i(\underline{H}\cdot\underline{r}) \qquad \text{(II-13b)}$$

In practice, $w_{\underline{H}}$ is usually 0 or 1, depending on the assessed reliability of the phase.

If the jth atom is incorrectly located, there will be a negative peak in $\Delta\rho$ at the point $x_j y_j z_j$, and a positive peak at the correct location. If the displacement from the correct location is small, there will be a steep gradient in $\Delta\rho$ at the trial location. The atom should be shifted "up the slope" by a small amount. The amount of this shift can be calculated from the electron density gradient and the atomic number, Z_j, of the atom involved.$^{(17)}$

Difference syntheses were used extensively in the refinements described in the following chapters, both with three dimensional data and in projection. The difference synthesis is especially useful in locating the lighter atoms in a structure when the positions of the heavier ones have been determined, using only those reflections (usually the stronger ones) whose phases have been determined with a fair degree of certainty. Difference syntheses have an advantage over an electron density synthesis in such a situation as they are less affected by "ripples" caused by series termination effects, due to the omission of reflections with large values of H from the calculation. These reflections are weaker on the average, and their phases will not be as well determined as those of the stronger, lower-angle reflections.

The main limitation of the difference synthesis, or any Fourier method, is that only the positional coordinates can be determined with any certainty. This limitation is not inherent in the least squares method of refining the parameters, and these two methods can be used together to complement each other, especially in the early stages of a refinement, when all the atoms may not have been located. In the later stages, the two methods are equivalent, but only the least squares method provides a convenient estimation of the reliability of the parameters.

F. Least Squares Refinement

The advantages of the least squares procedure lie in its directness, and in its quantitative determination of the estimated standard deviations (esd's) of the atomic parameters. It allows the determination of anisotropic temperature factors, which was virtually impossible with Fourier methods.

The least squares process(12) varies the atomic parameters, $x_1, x_2, \ldots x_M$, to minimize the residual R_2, where

$$R_2 = \left[\frac{\sum_{i=1}^{N} w_i(|F_o| - |F_c|)_i^2}{\sum_{i=1}^{N} w_i|F_o|_i^2} \right]^{1/2} \qquad \text{(II-14)}$$

where $|F_o|$ and $|F_c|$ are the observed and calculated values of $|F(\underline{H})|$, and the summation is over N reflections. If there are M parameters to be varied simultaneously, the least squares process requires the solution of the M simultaneous equations (the "normal equations"),

$$\frac{\delta R_2}{\delta x_k} = 0 \qquad k = 1, 2 \cdots M \qquad \text{(II-15)}$$

If $F_c(x_1, x_2, \cdot\cdot x_M)$ is the structure factor calculated using a set of trial parameters $x_1, x_2, \cdot\cdot x_M$, then an improved value for the structure factor can be written

$$F_c(x_1+\Delta x_1 \ldots x_M+\Delta x_M) = F_c(x_1 \ldots x_M) + \sum_{k=1}^{M} \frac{\delta F_c(x_1 \ldots x_M)}{\delta x_k} \cdot \Delta x_k + \ldots \qquad \text{(II-16)}$$

If the Taylor expansion in Eqn. (II-16) is truncated, the normal equations (Eqn.(II-15)) are linear in the parameter corrections Δx_k and can be readily solved. The trial parameters must be close enough to the parameters which describe the structure to justify the neglect of the higher order terms in the expansion.

The success with which a structure refinement is progressing is gauged, in part, by the value of R_2. A crude gauge of the correctness of a trial structure is afforded by the quantity

$$R_1 = \sum_{i=1}^{N} \left| |F_o| - |F_c| \right|_i \Big/ \sum_{i=1}^{N} |F_o|_i \tag{II-17}$$

but R_2 is to be preferred as a reliability index.

In the least squares refinement, each reflection is given a weight w_i, and the full power of the least squares method is attained only when the proper weights are used. The weight should be(12)

$$w_i = 1/\sigma_i^2 \tag{II-18}$$

where σ_i is the standard deviation of $|F_o|_i$. It is often not feasible to determine the esd of each measured intensity, and it is then necessary to substitute some appropriate weighting scheme.

The simplest scheme is to apply equal weight (unit weights) to each reflection. This scheme is generally recognized to be disadvantageous, especially in the later stages of a refinement, as it makes the strongest reflections the dominant terms in the refinement. This is not desirable in the final stages as these strong reflections are primarily of low angle (θ), where they do not provide the resolution necessary to correct small errors in the atomic positions. These reflections are also the most likely to suffer from extinction effects, thereby adversely affecting the temperature factors. Unit weights are suitable however in the "initial" and "middle" stages of a refinement; at least until all the atoms are unequivocably located.

Several other weighting schemes have been proposed to circumvent the actual determination of σ_i, and which are more realistic than unit weights. When the intensities are estimated visually from films, the relative accuracy of the estimation is approximately constant for all but the very strong and very weak reflections, where the relative errors are usually higher. This would imply that $\sigma_i \propto |F_o|_i$ would be applicable for most of the data. The greater relative errors in the weaker reflections could be taken into account by a constant esd, $\sigma_i = C$, and the very strong reflections assigned esd's of the form $\sigma_i \propto |F_o|_i^2$. While an assignment of weights based on this scheme may be slightly artificial, it is at least more realistic than unit weights.

A better weighting scheme is the method advocated by Cruickshank$^{(20)}$, which requires that the average weighted discrepancy,

$$\langle w_i \Delta_i^2 \rangle = \langle w_i \, \big||F_o| - |F_c|\big|_i^2 \rangle \qquad \text{(II-19)}$$

be a constant function of some systematic parameter, such as $|F_o|$ or $\frac{\sin\theta}{\lambda}$. The functional form for the weight is usually taken to be

$$w_i^{-1} = a_o + |F_o|_i + a_1 |F_o|_i^2 \qquad \text{(II-20)}$$

where a_o and a_1 are constants determined to satisfy the criterion with respect to $|F_o|$. This method of weighting ascribes the entire discrepancy, Δ^2, to random errors in the observed structure factors. This scheme is only justified in the final few cycles of a least squares refinement.

In all structures refined in these studies, the average Δ^2 was calculated as a function of $|F_o|$, and was fitted by a polynomial of the form

$$w_i^{-1} = \sum_{n=0}^{m} a_n |F_o|_i^n \qquad \text{(II-21)}$$

The order of the polynomial, m, was usually taken to be 2, but higher order terms are not to be precluded 'a priori'.

In any crystal structure investigation, a certain fraction of the total possible number of reflections will remain unobserved. The intensity of such a reflection must lie within the range $0<I<I_{min}$ where I_{min} is the minimum detectable intensity in this region of reciprocal space. The corresponding structure factor, $|F_{min}|$, is the only quantity whereby the agreement of the calculated structure factor, $|F_c|$, can be assessed.

If $|F_c| < |F_{min}|$, the two are in agreement, and it is preferable to assign zero weight to such a reflection. If the weight is non-zero, then some assumption regarding the most probable value of $|F_o|$ must be made, and the sign of the discrepancy, $\Delta = |F_o| - |F_c|$, used in the least squares refinement, would only be randomly correct. If $|F_c| > |F_{min}|$ however, an estimation of the most probable vaue of $|F_o|$ is desirable, and a value $k|F_{min}|$ is usually chosen. The most usual choices for k are $1/\sqrt{2}$, 1/2 or 2/3, depending on the assumed probability distribution for $|F_o|$.

As the refinement progresses, the value of k should be increased towards unity. The reason for this increase is that when a trial structure is refined towards the correct structure, the number of unobserved reflections which are calculated to be in disagreement decreases.

Those that are still not in agreement have an increasingly greater probability of lying just below $|F_{min}|$ in magnitude. In the structures investigated here, the value of k was initially set at 1/2, and, when the weighting schemes were changed from unit weights, k was gradually increased to a final value of 0.85 or 0.9.

CHAPTER III

MEASUREMENT OF INTENSITIES

A. Photographic Methods

The intensities of the X-rays diffracted from a crystalline substance are generally recorded on photographic films or by electronic means with a scintillation counter, for example, and pulse counting circuitry.

When the diffracted intensities are recorded on film, the densities of the spots are proportional (for optical densities less than about unity) to the incident X-ray intensity.(21) The relative densities of these images can be estimated by inter-comparison, using a series of photographs exposed for different lengths of time. The main drawback in this method is the difficulty in judging the equality in integrated density of two spots of different size and/or shape. In accurate X-ray structure analysis, it is necessary to measure the integrated intensity of a reflection, not just the peak intensity.(22) This can only be done with any degree of confidence when the spots being compared are of similar size and shape.

The integrated intensity can be recorded photographically by means of an "integrating camera". Such a camera records the diffraction pattern a large number of times, shifting the film between each exposure by a small amount. The resulting overlap of the photographic images provides an integration over the density profile of the spot, and the density of the centre of the spot is now proportional to the integrated intensity of the reflection. This peak density is usually measured by means of a microdensitometer, which provides greater consistency than does a visual estimation of the density. This "integrated photograph/microdensitometer" method was used to measure many of the intensity data collected in the course of the investigations reported in the following chapters.

B. Diffractometer Method

The second method, which was used in these studies to record most of the final intensity data, utilized a scintillation counter and a manual single crystal diffractometer. The diffractometer was basically a Weissenberg camera, manufactured by the Charles A. Supper Co., to which a scintillation counter had been mounted with freedom to move on the surface of a cone. The axis of the cone was the spindle axis of the camera. The usual equi-inclination Weissenberg geometry(37) was employed, (see Fig. III-1), with the crystal being rocked across the reflecting condition for the reflection being measured. During this rocking motion, or scan, the counter was stationary, having been preset to the required angle ϕ. This corresponds to the ω-scan, or "moving crystal, stationary counter" mode of operation described more fully elsewhere.(22)

The scintillation counter consisted of a scintillator, photomultiplier and preamplifier, which produced a pulse for each X-ray photon detected. The amplitude of the pulse was proportional to the energy of the photon. These pulses were amplified by a linear amplifier, and passed to a discriminator circuit. This circuit could be set to reject all pulses whose amplitude was below a certain "threshold" value (threshold mode), or to reject all pulses that did not lie within a specified

ν is the equi-inclination angle

ϕ is the angle between the diffracted X-ray beam and the plane defined by the incident X-ray beam and the spindle axis

2θ is the angle through which the X-ray beam is diffracted

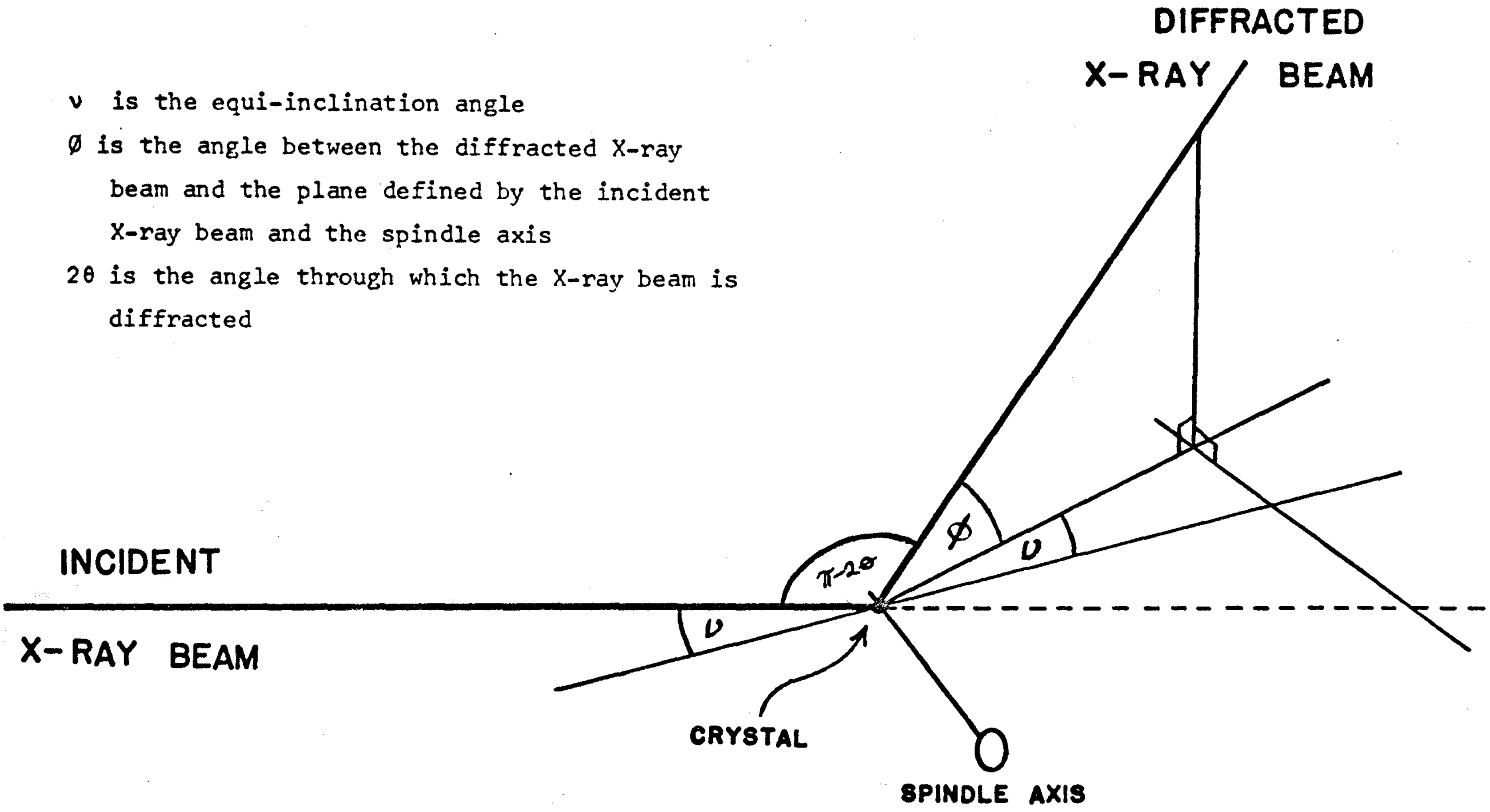
DIFFRACTED
X-RAY BEAM
ϕ
ν
$\pi-2\theta$
INCIDENT
X-RAY BEAM
ν
CRYSTAL
SPINDLE AXIS

FIGURE (III-1) Equi-inclination Weissenberg geometry range of amplitudes, called the "window" (channel mode). Those pulses which were accepted were counted on a decimal scalar which could record up to 10^5 pulses, and were fed to a rate-meter and chart recorder. The chart drive and the scalar were cued into the scanning operation in such a manner that they were operative only while the scan was in progress.

When operating in the threshold mode, the threshold level was set midway between the amplitudes of the desired Kα X-ray pulses, and the low energy noise pulses which originate in the photomultiplier. For channel mode operation, the Kα count-rate profile was determined as a function of amplitude. The discriminator amplitude to be used for the intensity measurements was set at the maximum of this profile, and the amplitude "window" set to include about 80-90 per cent of the Kα pulses. The channel mode of operation is preferable to the threshold mode as the background counts are markedly depressed in the former. Extraneous high-amplitude noise pulses produced by nearby electrical equipment were also eliminated using the channel mode, whereas they could have caused difficulties when operating in the threshold mode.

Before each layer line was to be measured, an ordinary Weissenberg photograph was taken for about 24 hours. This length of exposure required about the same minimum intensity for a spot to be visible, as the scintillation counter required in order to detect a reflection above the background. Approximate values for the angular coordinates ϕ and ω were measured for each reflection from these photographs. The counter was set to the approximate ϕ angle for each reflection, and the spindle turned slowly in the neighbourhood of the measured ω angle until the maximum count rate was obtained. The counter was then repositioned so that the diffracted beam passed through the centre of the counter aperture. The spindle was displaced by one-half of the scanning angle, and the scan started. After the completion of the two minute scan, the number of counts was recorded and the scalar reset. The spindle was then displaced so that the background could be counted in an angular range immediately adjacent to the reflection.

C. Errors in Measurement

(i) Ø or ω set improperly

If ω is misset, the full integrated intensity is not obtained. This condition can be seen readily from the chart recorder, which will show that the count rate did not fall off to background level at both extremes of the scan. If this condition was noted, the scan was repeated after resetting ω.

The counter aperture, ΔØ was fairly large (2°). A deviation of more than ±0.5° in Ø was thus quite permissable as the divergence of the X-ray beam was less than 1°, and the Ø arc could easily be set more accurately than this. Only on measuring very weak reflection, for large values of Ø, could this have posed any problem.

(ii) Incorrect determination of background

The main sources of background radiation are, (i) external sources, such as cosmic rays and adjacent diffraction equipment, (ii) incoherent scattering of X-rays by the crystal, and (iii) coherent scattering of unwanted wavelengths from any reciprocal lattice point in the crystal. By counting the background adjacent to each reflection, the first two sources of background were effectively eliminated. The third type of unwanted radiation posed a greater problem. The two most important sources of this type were contributions from the white radiation streak from other reflections and the white streak from the reflection being measured. This white streak consists mainly of longer wavelengths than the Kα, as these wavelengths are passed by the normal β filter. The scintillation pulses produced by these wavelengths, although of lower amplitude than the desired Kα pulses, were not sufficiently low to be rejected by the discriminator circuit.

The white streak from the reflection being measured caused difficulty because the wavelength dispersion is a function of the scattering angle θ:

$$\frac{d\theta}{d\lambda} = \frac{\tan\theta}{\lambda} \qquad \text{(III-1)}$$

The ω-scan method provides a constant aperture in the 2θ direction for each layer line, and hence the range of wavelengths which can be diffracted through this aperture is a function of 2θ, and therefore a function of ϕ. Thus, if the counter aperture was to be sufficient to allow the Kα_1 and Kα_2 wavelengths to be detected for a high angle reflection, this same aperture would result in the recording of a considerable portion of the white streak in the case of low angle reflections.

Any irregularities caused by the inclusion of these white streaks, or the white streaks from a nearby reflection, were apparent from an examination of the chart tracings of the intensity and background scans. If the error seemed to be excessive, an approximate correction was made by a visual estimation of the "correct" background for the reflection from the areas under the chart tracings, and the assumption that the reflection profile was approximately Gaussian.

(iii) "Dead-time" effects

Any apparatus which detects the passage of a photon has a finite resolution time within which it is incapable of detecting the passage of another photon. In scintillation counters these times are quite short, usually less than a microsecond. The electronic apparatus into which the pulses are fed by a photomultiplier also has a certain resolving time within which it is unable to process two separate input pulses and record both. The apparent count rate is thus always less than the true count rate due to coincidence losses.

There are two methods of correcting for these coincidence losses; (i) insert attenuating filters into the X-ray beam (either incident or diffracted) which reduce the count rate to a point where the coincidence losses do not constitute a significant error, or (ii) correct the observed count rate for the coincidence losses by means of some analytic relationship between observed and true count rates. The former method is cumbersome, and has the disadvantage that the attenuation of an absorbing filter is usually a function of the wavelength. The attenuation factor must therefore be determined as a function of scattering angle for each filter, due to the wavelength dispersion discussed earlier.(23) The latter method was used in correcting all intensity data for coincidence losses.

For a statistically constant count rate, the relationship

$$i = \frac{i'}{1-i'\tau} \qquad \text{(III-2)}$$

is applicable$^{(24)}$ provided that the correction does not exceed approximately 20 per cent. Here, i is the true count rate which, due to the resolution time τ, gives rise to the observed rate i'. This relationship depends on the assumption that τ is independent of the count rate i, and it is this assumption that limits the validity of Eqn. (III-2) to corrections of less than approximately 20 per cent.

This expression relates the true and observed count rates and does not strictly apply to the total number of counts obtained when measuring the integrated intensity of a reflection, as the count rate is not constant. An approximate dead-time correction can still be made to the observed integrated intensity using the analogous relation

$$I = \frac{I'}{1-I'\psi} \tag{III-3}$$

where I and I' refer to the integrated intensities and ψ is an effective resolution time, which is related to the actual resolving time τ of the apparatus and to the intensity profile as a function of time.

ψ was determined separately for each layer line by repeatedly scanning the strongest reflection in the layer with a succession of attenuating filters of known relative thickness inserted in the X-ray beam. If there had been no coincidence losses, the plot of ln(I') vs. the relative filter thickness would have been linear, as the intensity passed by an attenuator of thickness x and attenuation coefficient μ is

$$I = I_0\exp(-\mu x) \tag{III-4}$$

where I_0 is the incident intensity. Coincidence losses caused the curve to be depressed for high count rates, and an extrapolation of the straight portion of the curve, for which these losses were negligible, determined the true unattenuated intensity. The effective resolution time ψ was calculated from Eqn. (III-3).

The corrected integrated intensities of all weaker reflections in the layer were then calculated using Eqn. (III-3) and the value of ψ just determined. As all other corrections were smaller than that for the strongest reflection, errors arising from the use of this relation are necessarily of second order, and in fact, negligible. An analysis of the applicability of this method is given in Appendix A, where a theoretical correction based on a Gaussian intensity profile is used for comparison. The discrepancy between the theoretical corrections and those obtained using Eqn. (III-3) is less than 0.5% when the coincidence losses for the strongest reflection are 27.5%. In all layer lines measured, the strongest reflection suffered losses of less than 15%, for which the error in the approximation is negligible.

CHAPTER IV

THE STRUCTURE OF β-$Zn_3(PO_4)_2$

A. Preliminary Investigations

$Zn_3(PO_4)_2$ was prepared by reacting stoichiometric amounts of zinc oxide and phosphoric acid, according to the equation,

$$3ZnO + 2H_3PO_4 \longrightarrow Zn_3(PO_4)_2 + 3H_2O \qquad \text{(IV-1)}$$

Crystals of the β phase were grown from the melt, which was cooled slowly through the freezing point (1060°C.),(1) and then quenched to room temperature. This quenching was necessary to prevent the conversion of the sample to the α form, which is the stable phase below 942°C.

The crystals of β-$Zn_3(PO_4)_2$ occurred in the form of white, almost colourless, flat plates, with definite striations of the faces of these plates. Preliminary X-ray photographs showed that these crystals had monoclinic symmetry, and that they could be indexed on the basis of a unit cell with $P\text{-}2_1/c$ symmetry, as this space group was unambiguously defined by the systematically absent reflections: $h0\ell$ for ℓ odd, and $0k0$ for k odd. The density of the crystals was measured with a pycnometer,(25) and found to be 4.17(1) gm/cm^3.

A small single-crystal fragment was selected and mounted on a goniometer head to rotate around the b axis. This crystal was approximately spherical, with a mean radius of 0.09 mm, and was used in the measurement of the lattice parameters, and for the recording of all the intensity data.

B. Lattice Parameters

The length of the b axis of β-$Zn_3(PO_4)_2$ was determined from a rotation photograph which was calibrated by means of a superimposed rotation photograph of a single-crystal of TiO_2 (rutile). The lattice constants for the TiO_2 crystal were taken to be(26) a = 4.5929(5)Å and c = 2.9591(3)Å.

The relationship between the rotation axis length and the distance between the layer lines on a rotation photograph is(27)

$$\sin\left[\tan^{-1}\left(\frac{d}{D}\right)\right] = \frac{n\lambda}{A} \qquad \text{(IV-2)}$$

where D is the diameter of the cylindrical film, d is the distance between the n and $\bar{n}$ layer lines, λ is the wavelength, and A is the length of the rotation axis. The value of D determined from the TiO_2 interlayer spacing was 56.96(1) mm. This value of D was then used to calculate the length of the rotation axis (b) of β-$Zn_3(PO_4)_2$. The value obtained was 9.17(1) Å.

The remaining cell constants were determined from the values of a*, c*, and cosβ*, which were determined from an h0ℓ Weissenberg photograph, using Cu-Kα radiation. This photograph was calibrated by means of the Debye-Scherrer (powder) lines of α-Al_2O_3 (corundum) which were superimposed near both edges of the single-crystal photograph. The hexagonal lattice constants of α-Al_2O_3 were taken to be(28) a = 4.75903(3)Å and c = 12.9908(2)Å, and the values for the wavelengths of the Cu-Kα doublet were(13) α_1 = 1.54081Å and α_2 = 1.54433Å.

Only the θ values of the high-angle reflections were measured, where the α_1 and α_2 components were completely resolved. The powder lines were indexed, and the θ values calculated for these lines were used to correct the θ values for the β-$Zn_3(PO_4)_2$ reflections.

The values of a*, c* and cosβ* were determined by means of a least squares fit to these corrected values of θ. 98 independent measurements of θ were used in this refinement, and the final values for the parameters are, $a^* = 0.13115(1)\mathring{A}^{-1}$, $c^* = 0.14182(1)\mathring{A}^{-1}$ and $\cos\beta^* = -0.58395(8)$. The corresponding real cell parameters for β-$Zn_3(PO_4)_2$ are $a = 9.393(1)\mathring{A}$, $b = 9.17(1)\mathring{A}$, $c = 8.686(1)\mathring{A}$ and $\beta = 125.7(1)^\circ$.

The volume of the unit cell is $607.3\ \mathring{A}^3$. The measured density of $4.17\ gm/cm^3$ implies that there are four formula weights of $Zn_3(PO_4)_2$ per unit cell, (F. W. = 386.1 gm), which corresponds to a calculated density of $4.21\ gm/cm^3$. As the multiplicity of a general position in the space group $P\text{-}2_1/c$ is also four, none of the atoms in the structure are constrained to lie in special positions.

C. Intensity Data and Absorption Corrections

All intensity data were recorded using Zr-filtered Mo-Kα radiation from a Phillips PW1010 X-ray generator, set at 50 kV and 12 ma. Mo-Kα radiation was selected as its shorter wavelength allowed more of the reciprocal lattice to be explored than would have been possible with Cu-Kα for example, and because errors due to absorption would be smaller.

The reciprocal lattice planes, $hN\ell$, where $N=0,1,..6$, were measured on the Weissenberg diffractometer, operating in the threshold mode, and the intensities corrected for "dead-time" effects, as described in Ch. III. The 0kℓ, hk0 and hk$\bar{h}$ planes were recorded on film with an integrating precession camera. The peak densities of these integrated spots were measured on a Leeds & Northrup microdensitometer.

The linear absorption co-efficient for β-$Zn_3(PO_4)_2$ is 118 cm^{-1}. As the average radius of the crystal was 0.09 mm, the absorption parameter μR was 1.06, and absorption corrections corresponding to this value of μR for a spherical crystal were applied to all intensity data(12). Lorentz and polarization corrections were calculated and the values of $|F_o|$ obtained.

D. The Trial Solution

Patterson projections were prepared from the data contained in the three principal zones. A satisfactory solution for the positions of the three cations was obtained only for the b axis projection.

The y coordinates of the cations and the two phosphorus atoms were taken from those determined for the similar structure of β^1-$Cd_3(PO_4)_2$. The details of this determination are given in Ch. V. The cation coordinates could be determined easily from Patterson projections in the case of β^1-$Cd_3(PO_4)_2$ due to the considerably greater scattering power of Cd^{++} which has 46 electrons, compared to Zn^{++} with only 28.

Using the y coordinates obtained from the β^1 structure and the x and z coordinates from the β-$Zn_3(PO_4)_2$ b axis projection, three dimensional electron density and difference syntheses were calculated. These density maps showed peaks which corresponded to the positions of all the oxygen atoms. A subsequent least squares refinement and a second difference synthesis confirmed the locations of all 13 atoms in the asymmetric zone, and reduced the reliability index R_2 to 0.20 .

E. The Refinement

The initial cycles of least squares refinement were carried out with unit weights and isotropic temperature factors. During these cycles, the shifts in the positions of the oxygen atoms were large, sometimes in excess of 0.1 Å, and the temperature factors on some of these atoms became overly large (>10.). These temperature factors were reset to a value of 1.0 and held constant until the positional parameters of the oxygen atoms were well established.

The criterion used to determine whether the oxygen atom coordinates were well established was the nearly regular tetrahedral geometry exhibited by PO_4 groups in other orthophosphate structures$^{(29)}$. In these structures, the average P-O bond distance is 1.54 Å, with individual P-O bond lengths deviating by no more than 0.05 Å from this average value. Consequently, only when all the P-O distances in β-$Zn_3(PO_4)_2$ remained between 1.49 Å and 1.59 Å were the temperature factors on the oxygen atoms allowed to vary in the least squares cycle. The best value of R_2 obtained with unit weights and isotropic temperature factors was 0.091 .

The temperature factors were then converted to the corresponding anisotropic form, and the refinements continued. At this stage the scale constants were sufficiently well determined so that multiply-measured reflections could be averaged. This averaging was performed, and the average values of $|F_o|$ were assigned at random to one of the two (or three) scale constants involved. If a reflection had been classed as observed in one measurement, and unobserved in another, the observed value of $|F_o|$ was always retained. When this averaging was complete, there were 1633 independent reflections, of which 648 were classed as unobserved.

The weighting scheme was then changed from unit weights to the scheme suggested by Cruickshank(20), which was outlined in Ch. II. The expression used to calculate the weights was,

$$w_i^{-1} = 8.54 - 0.187|F_o|_i + 0.0022|F_o|_i^2 \qquad \text{(IV-3)}$$

A final few cycles of refinement using this weighting scheme and varying all 127 parameters (10 scales, 39 positional, and 78 thermal) were performed. During the last cycle the parameter shifts were approximately 1/10 of the esd's calculated for the parameters. The refinement was considered to be complete, and the final value for the residual R_2 was 0.048 .

A total of 22 reflections had been classed as "unreliable", and given zero weight in the refinement. Of these 22 reflections, 13 were suspected to have suffered from extinction effects(30), as they were all large in magnitude, of low angle, and in each case $|F_c|$ exceeded $|F_o|$ by at least 10%.

The final values of the atomic parameters, together with their esd's, are listed in Table (IV-2), and the reliability indices, R_1 and R_2, are summarized in Table(IV-3). The agreement between the

TABLE (IV–I) OBSERVED AND CALCULATED STRUCTURE FACTORS (X10)

UNOBSERVED REFLECTIONS ARE MARKED WITH AN ASTERISK (*), AND UNRELIABLE REFLECTIONS WITH THE SYMBOL (#).

K=0

H	L	|FOBS|	FCALC
2	0	414	390
3	0	#1102	1224
4	0	*139	49
5	0	697	779
6	0	169	140
7	0	1234	1294
8	0	260	228
9	0	181	-101
10	0	221	-163
11	0	*265	-148
12	0	*282	-74
13	0	*297	21
14	0	291	276
0	2	941	-929
1	2	806	724
2	2	*133	44
3	2	586	-574
4	2	1940	-2049
5	2	547	547
6	2	579	-597
7	2	572	-590
8	2	196	210
9	2	426	-398
10	2	*272	-109
11	2	419	-392
12	2	*301	-70
1	-2	698	619
2	-2	870	812
3	-2	#2121	-2344
4	-2	573	556
5	-2	737	767
6	-2	616	597
7	-2	657	678
8	-2	85	98
9	-2	882	889
10	-2	638	-657
11	-2	*245	-86
12	-2	616	620
13	-2	*280	27
14	-2	*275	205
15	-2	*306	144
0	4	789	-768
1	4	325	316
2	4	1300	-1326
3	4	352	-343
4	4	235	186
5	4	1054	-1048
6	4	*233	-3
7	4	*250	103
8	4	*266	-47
9	4	*282	-138
10	4	*297	257
1	-4	1525	-1526
2	-4	1670	-1662
3	-4	354	-358
4	-4	535	-514
5	-4	2005	-2088
6	-4	487	463
7	-4	*169	-79
8	-4	485	-474
9	-4	1023	-1056
10	-4	244	-227
11	-4	207	156
12	-4	736	-755
13	-4	671	669
14	-4	*282	-75
15	-4	232	-229
16	-4	*307	53
0	6	151	-117
1	6	*195	105
2	6	1059	1035
3	6	434	403
4	6	*236	107
5	6	230	276
6	6	425	409
7	6	*282	-78
8	6	294	290
9	6	506	478
1	-6	971	1003
2	-6	218	-188
3	-6	468	447
4	-6	601	-582
5	-6	1170	1132
6	-6	117	84
7	-6	1188	-1196
8	-6	1109	1104
9	-6	775	-776
10	-6	377	-394
11	-6	*227	110
12	-6	*242	211
13	-6	*258	-73
0	8	626	657
1	8	*233	-132
2	8	514	547
3	8	*259	-53
4	8	346	354
5	8	*286	-109
6	8	390	-387
7	8	*307	279
1	-8	*212	-14
2	-8	*204	-91
3	-8	1228	1206
4	-8	*194	53
5	-8	450	437
6	-8	637	640
7	-8	769	755
8	-8	569	-560
9	-8	305	299
10	-8	958	951
11	-8	261	-258
12	-8	341	346
13	-8	*258	227
14	-8	*271	122
0	10	409	-403
1	10	251	-239
2	10	*283	-8
3	10	*293	-46
4	10	394	-382
5	10	*310	-19
1	-10	469	-481
2	-10	*243	46
3	-10	825	-819
4	-10	205	246
5	-10	451	427
6	-10	872	-865
7	-10	*225	-21
8	-10	*227	-73
9	-10	*231	-194
10	-10	149	-164
11	-10	*245	187
12	-10	*255	208
13	-10	*265	-307
14	-10	*276	86
15	-10	*287	-129
0	12	*296	-37
1	12	*303	147
2	12	*309	-220
3	12	*313	221
1	-12	383	-402
2	-12	*280	-156
3	-12	*273	151
4	-12	*266	91
5	-12	296	-317
6	-12	252	-258
7	-12	482	-513
8	-12	552	-517
9	-12	228	227
10	-12	376	-372
11	-12	277	258
12	-12	368	-370
13	-12	*302	109
14	-12	*287	-93
15	-12	602	-582
16	-12	*302	173
0	14	*313	-164
1	14	*313	-40
2	14	340	349
1	-14	389	401
2	-14	*308	-55
3	-14	*303	237
4	-14	373	397
5	-14	*294	44
6	-14	*290	227
7	-14	*288	-252
8	-14	*286	316
9	-14	*286	-44
10	-14	*287	127
11	-14	409	436
12	-14	*292	91
13	-14	*296	1
14	-14	*300	-207
10	-16	327	401
11	-16	*308	-89
12	-16	*309	81
13	-16	*310	135
14	-16	*312	-231
15	-16	*313	75
16	-16	*313	142

K=1

H	L	|FOBS|	FCALC
2	0	86	-68
3	0	497	-464
4	0	#1474	1681
5	0	210	-177
6	0	268	237
7	0	499	493
8	0	160	133
9	0	256	208
10	0	306	-296
11	0	499	475
12	0	*253	139
13	0	*266	-52
0	1	220	180
1	1	#387	159
2	1	281	255
3	1	426	-423
4	1	705	740
5	1	758	767
6	1	314	-315
7	1	231	-252
8	1	258	277
9	1	465	-443
10	1	*232	-48
11	1	321	290
1	-1	#280	-158
2	-1	#752	640
3	-1	#1747	2178
4	-1	390	-364
5	-1	211	247
6	-1	971	1057
7	-1	*164	-65
8	-1	175	-170
9	-1	636	646
10	-1	282	279
11	-1	*228	158
12	-1	279	261
13	-1	*258	133
14	-1	*270	-65
0	2	#1931	2260
1	2	897	-867
2	2	1112	1110
3	2	600	596
4	2	194	-201
5	2	766	788
6	2	212	210
7	2	372	392
8	2	341	-360
9	2	*228	190
10	2	*244	27
11	2	*258	-224
1	-2	1011	-978
2	-2	834	-850
3	-2	505	-501
4	-2	619	-582
5	-2	917	-998
6	-2	591	596
7	-2	787	-827
8	-2	311	-323
9	-2	*188	-74
10	-2	230	-194
11	-2	*220	54
12	-2	*235	-134
13	-2	368	353
14	-2	302	-279
15	-2	*275	-76
0	3	293	-312
1	3	1690	-1720
2	3	665	-638
3	3	350	-308
4	3	316	-300
5	3	218	-192
6	3	155	-143
7	3	*210	-65
8	3	612	-619
9	3	*241	-155
10	3	*255	61
1	-3	596	543
2	-3	548	-507
3	-3	971	-995
4	-3	377	344
5	-3	689	-725
6	-3	1304	-1400
7	-3	78	88
8	-3	236	247
9	-3	414	-452
10	-3	303	305
11	-3	#208	-4
12	-3	*228	-58
13	-3	*244	-104
14	-3	*258	-78
15	-3	*270	148
0	4	296	257
1	4	419	407
2	4	1053	-1047
3	4	428	-389
4	4	601	-591
5	4	367	366
6	4	488	-521
7	4	240	-188
8	4	215	213
9	4	532	-510
1	-4	1196	1174
2	-4	1185	-1157
3	-4	663	641
4	-4	152	-135
5	-4	*149	21
6	-4	93	64
7	-4	650	-671
8	-4	437	416
9	-4	934	-963
10	-4	179	180
11	-4	261	251
12	-4	233	-214
13	-4	*238	-81
14	-4	*252	-63
15	-4	*265	40
16	-4	259	-222
17	-4	*280	70
0	5	183	-176
1	5	274	265
2	5	381	-372
3	5	206	-160
4	5	343	341
5	5	208	245
6	5	*224	70
7	5	*238	1
8	5	*252	72
1	-5	414	-413
2	-5	925	894
3	-5	174	178
4	-5	1565	-1581
5	-5	*158	4
6	-5	290	-285
7	-5	641	-647
8	-5	154	-147
9	-5	219	233
10	-5	197	-198
11	-5	428	-412
12	-5	404	-407
13	-5	*234	-57
14	-5	172	-164
15	-5	*261	-202
16	-5	*272	177
0	6	514	-531
1	6	*175	59
2	6	668	-682
3	6	158	154
4	6	348	-353
5	6	457	-438
6	6	474	466
7	6	*253	-44
1	-6	251	-241
2	-6	590	590
3	-6	1182	1145
4	-6	396	-399
5	-6	1322	1318
6	-6	100	106
7	-6	178	150
8	-6	214	-212
9	-6	375	391
10	-6	521	537
11	-6	310	-290
12	-6	524	537
13	-6	*231	-91
14	-6	*245	-76
15	-6	*258	63
0	7	758	756
1	7	356	-357
2	7	298	290
3	7	426	428
4	7	*228	-29
5	7	274	297
6	7	*254	215
1	-7	650	646
2	-7	*192	38
3	-7	728	740
4	-7	794	801
5	-7	292	-301
6	-7	288	266
7	-7	505	513
8	-7	678	681
9	-7	207	182
10	-7	*193	68
11	-7	333	336
12	-7	171	-164
13	-7	212	-226
14	-7	312	270
15	-7	*256	168
16	-7	*267	-106
0	8	*207	41
1	8	481	470
2	8	402	428
3	8	*232	-219
4	8	245	212
5	8	*256	160
1	-8	354	-358
2	-8	*198	76
3	-8	651	-655
4	-8	860	864
5	-8	245	-234
6	-8	787	-767
7	-8	466	464
8	-8	541	-526
9	-8	294	311
10	-8	*198	12
11	-8	176	199
12	-8	*219	38
13	-8	285	-306
14	-8	316	288
15	-8	236	-264
16	-8	*266	45
17	-8	*274	105
0	9	461	-483
1	9	*227	98
2	9	*238	-139
3	9	377	-395
4	9	*259	93
1	-9	*208	97
2	-9	266	219
3	-9	*199	-79
4	-9	168	-172
5	-9	*202	45
6	-9	*202	31
7	-9	*208	-34
8	-9	*192	109
9	-9	523	538
10	-9	188	183
11	-9	241	-258
12	-9	226	209
13	-9	282	264
14	-9	155	-153
15	-9	305	265
16	-9	365	315
17	-9	*274	-115
0	10	472	490
1	10	245	-214
2	10	147	190
3	10	*263	62
1	-10	144	-115
2	-10	183	-198
3	-10	193	-130
4	-10	*214	-80
5	-10	482	-456
6	-10	160	178
7	-10	708	-693
8	-10	132	-110
9	-10	391	402
10	-10	482	-497
11	-10	213	217
12	-10	293	-308
13	-10	*238	-4
14	-10	192	-177
15	-10	246	-265
16	-10	269	292
17	-10	162	-192
18	-10	*279	51
0	11	*251	55
1	11	219	-244
2	11	*267	-174
1	-11	169	-115
2	-11	*235	-200
3	-11	167	-159
4	-11	295	-262
5	-11	347	-365
6	-11	374	-376
7	-11	175	-154
8	-11	*225	61
9	-11	517	-507
10	-11	*232	-9
11	-11	*228	65
12	-11	578	-586
13	-11	*243	-60
14	-11	*251	125
0	12	*265	-124
1	-12	326	319
2	-12	*251	-138
3	-12	307	368
4	-12	300	244
5	-12	287	-287
6	-12	*231	126
7	-12	*230	30
8	-12	347	361
9	-12	*231	-155
10	-12	244	225
11	-12	*238	197
12	-12	*243	-199
13	-12	*250	95
14	-12	*257	-141
3	-13	*260	144
4	-13	*254	-192
5	-13	*250	102
6	-13	221	228
7	-13	*244	-112
8	-13	*243	99
9	-13	*244	221
10	-13	262	-277
11	-13	*248	-154
12	-13	*252	127
13	-13	*257	-211
14	-13	*263	-40
5	-14	*264	195
6	-14	*260	-62
7	-14	*258	-15
8	-14	*256	140
9	-14	*256	80
10	-14	*257	202
11	-14	223	-251
12	-14	203	224
13	-14	*265	-57
14	-14	*269	-69
6	-15	*272	158
7	-15	311	369
8	-15	*268	18
9	-15	*267	44
10	-15	*267	126
11	-15	*268	35
12	-15	*270	16
13	-15	*272	216
14	-15	*275	141
15	-15	*277	43

K=2

H	L	|FOBS|	FCALC
0	0	*93	-21
1	0	890	894
2	0	568	-542
3	0	*78	27
4	0	*86	83
5	0	738	-766
6	0	943	978
7	0	270	-260
8	0	385	367
9	0	*113	-3
10	0	249	-226
11	0	*335	315
0	1	*98	-27
1	1	1548	1626
2	1	962	1009
3	1	775	799
4	1	304	-279
5	1	895	965
6	1	381	387
7	1	353	-342
8	1	799	812
9	1	657	625
10	1	*327	-13
1	-1	#202	-68
2	-1	1079	-1032
3	-1	*137	58
4	-1	262	-214
5	-1	#1288	-1433
6	-1	178	-207
7	-1	433	439
8	-1	404	-411
9	-1	*276	-25
10	-1	427	436
0	2	337	-329
1	2	529	-532
2	2	1017	1007
3	2	806	-822
4	2	339	330
5	2	*233	-96
6	2	*255	-184
7	2	*277	177
8	2	*299	-119
9	2	*322	70
10	2	*343	-134
1	-2	1375	1391
2	-2	1258	-1302
3	-2	381	364
4	-2	1209	-1223
5	-2	392	400
6	-2	341	388
7	-2	*222	-188
8	-2	324	352
9	-2	381	-382
10	-2	#163	236
11	-2	278	-265
12	-2	*332	163
0	3	843	833
1	3	*173	80
2	3	*192	-116
3	3	738	698
4	3	391	383
5	3	678	-704
6	3	*274	-197
7	3	*296	97
8	3	*318	39
9	3	*339	-287
1	-3	325	259
2	-3	555	479
3	-3	786	-815
4	-3	1019	-1051
5	-3	143	130
6	-3	982	-1018
7	-3	770	-799
8	-3	361	385
9	-3	203	-199
10	-3	679	-682
11	-3	243	-257
12	-3	*322	-217
13	-3	365	-336
0	4	751	743
1	4	572	-559
2	4	*215	59
3	4	*234	-142
4	4	293	264
5	4	*274	11
6	4	*295	-254
7	4	*316	219
8	4	*337	-290
1	-4	866	-801
2	-4	481	428
3	-4	269	-226
4	-4	538	-526
5	-4	775	758
6	-4	927	-936
7	-4	606	608
8	-4	385	-402
9	-4	367	-372
10	-4	292	302
11	-4	441	-451
12	-4	*315	82
0	5	1554	-1630
1	5	512	-510
2	5	310	307
3	5	493	-495
4	5	444	-433
5	5	*295	6
6	5	335	-326
7	5	472	-458
8	5	286	-265
1	-5	465	463
2	-5	305	297
3	-5	1126	1143
4	-5	643	626
5	-5	544	-528
6	-5	998	1009
7	-5	849	845
8	-5	*233	125
9	-5	542	553
10	-5	*269	109
11	-5	*289	17
12	-5	296	-290
0	6	399	348
1	6	*247	-81
2	6	*263	-236
3	6	441	445
4	6	315	-316
5	6	*318	360
6	6	*337	-52
1	-6	350	-327
2	-6	664	646
3	-6	193	-194
4	-6	461	433
5	-6	*208	98
6	-6	211	-216
7	-6	*225	32
8	-6	*238	-127
9	-6	547	552
10	-6	502	-500
11	-6	*288	153
12	-6	*307	74
0	7	668	670
1	7	*271	-57
2	7	397	-398
3	7	482	514
4	7	#364	497
1	-7	904	892
2	-7	*235	-47
3	-7	763	-737
4	-7	*225	77
5	-7	*225	182
6	-7	444	421
7	-7	134	127
8	-7	802	769
9	-7	302	299
10	-7	214	-214
11	-7	*289	191
12	-7	397	368
0	8	285	-269
1	8	*295	191
2	8	*311	-123
3	8	*328	52
1	-8	*269	194
2	-8	*258	-6
3	-8	*251	18
4	-8	579	576
5	-8	727	-717
6	-8	462	454
7	-8	*250	0
8	-8	*110	-42
9	-8	509	503
10	-8	*280	-159
11	-8	*294	278
12	-8	*309	-159
13	-8	*326	218
0	9	*306	-120
1	9	*320	-174
2	9	437	437
1	-9	691	-706
2	-9	623	-593
3	-9	199	-186
4	-9	761	-743
5	-9	560	-549
6	-9	*264	-62
7	-9	*266	42
8	-9	546	-559
9	-9	615	-632
10	-9	*289	-88
11	-9	403	-391
12	-9	372	-379
13	-9	314	310
0	10	372	-384
1	-10	*318	153
2	-10	*307	-226
3	-10	*298	20
4	-10	*291	-94
5	-10	*286	-93
6	-10	*284	1
7	-10	310	-315
8	-10	440	431
9	-10	474	-467
10	-10	236	213
11	-10	*310	59
12	-10	*322	-178
3	-11	*322	-303
4	-11	*314	205
5	-11	441	428
6	-11	*305	56
7	-11	*304	-147
8	-11	*305	127
9	-11	*309	-159
10	-11	582	-574
11	-11	*322	8
12	-11	*332	215
13	-11	383	-359
4	-12	*337	-351
5	-12	*331	317
6	-12	*326	-108
7	-12	*324	-128
8	-12	*324	-14
9	-12	*326	-259
10	-12	*330	160
11	-12	*336	-147
12	-12	*343	35
5	-13	*352	101
6	-13	543	552
7	-13	*344	389
8	-13	*343	-296
9	-13	*343	303
10	-13	*346	251
11	-13	*350	58
12	-13	*356	230
13	-13	*363	356

K=3

H	L	|FOBS|	FCALC
2	0	#1328	-1452
3	0	582	583
4	0	351	361
5	0	401	410
6	0	191	186
7	0	135	134
8	0	600	580
9	0	418	-402
10	0	290	253
0	1	611	629
1	1	667	-644
2	1	376	-330
3	1	*183	150
4	1	783	-813
5	1	*233	103
6	1	247	251
7	1	*281	-50
8	1	*305	-54
1	-1	290	305
3	-1	852	-924
4	-1	272	258
5	-1	*202	-124
6	-1	457	-503
7	-1	193	225
8	-1	*275	-186
9	-1	*299	-147
10	-1	437	-432
0	2	172	193
1	2	460	441
2	2	324	303
3	2	1183	1212
4	2	370	-377
5	2	215	192
6	2	1267	1306
7	2	313	-304
8	2	*324	84
1	-2	#1605	-1766
2	-2	491	-467
3	-2	504	-525
4	-2	#1322	-1482
5	-2	472	480
6	-2	773	-823
7	-2	*240	-183
8	-2	903	-946
9	-2	*287	-45
10	-2	*311	95
11	-2	612	-584
12	-2	*359	156
0	3	206	-147
1	3	1187	1178
2	3	*208	-76
3	3	343	-330
4	3	263	288
5	3	191	202
6	3	*297	32
7	3	*320	239
1	-3	449	427
2	-3	846	835
3	-3	#163	-44
4	-3	218	226
5	-3	370	-337
6	-3	866	909
7	-3	283	316
8	-3	*256	-63
9	-3	386	388
10	-3	*301	-115
11	-3	*325	-104
12	-3	*348	61
13	-3	*371	204
0	4	734	-709
1	4	*215	112
2	4	288	-258
3	4	1498	-1533
4	4	431	439
5	4	*296	-219
6	4	406	-417
7	4	*341	38
1	-4	354	-336
2	-4	424	411
3	-4	670	-643
4	-4	1305	1349
5	-4	*197	21
6	-4	422	-434
7	-4	*232	77
8	-4	221	-182
9	-4	210	-208
10	-4	412	-439
11	-4	467	483
12	-4	237	-226
13	-4	386	-357
14	-4	292	282
0	5	113	122
1	5	*241	-28
2	5	*258	-117
3	5	*278	258
4	5	*298	-182
5	5	350	-354
6	5	*341	213
1	-5	282	262
2	-5	407	-391
3	-5	*200	-111
4	-5	*202	68
5	-5	*94	26
6	-5	*221	32
7	-5	384	388
8	-5	589	624
9	-5	349	-349
10	-5	*292	63
11	-5	321	346
12	-5	*334	-35

TABLE (IV-I) CONCLUDED

			|FOBS|	FCALC
11	-5	•	356	207
0	6		719	696
1	6		986	-990
2	6	•	294	-154
3	6	•	303	-4
4	6		385	-395
5	6	•	343	-257
1	-6		242	259
2	-6		365	359
3	-6		1065	1017
4	-6		888	874
5	-6		175	-180
6	-6		1440	1451
7	-6		357	-342
8	-6	•	258	-59
9	-6		1029	1047
10	-6	•	247	-159
11	-6		509	501
12	-6		313	303
0	7		371	-371
1	7	•	293	-7
2	7	•	310	110
3	7	•	328	-168
4	7	•	148	22
5	7	•	367	-96
1	-7		374	-362
2	-7		253	-235
3	-7		224	-203
4	-7		602	-579
5	-7	•	244	-50
6	-7	•	248	110
7	-7		508	-477
8	-7		421	-427
9	-7	•	280	-30
10	-7	•	296	-205
11	-7		385	-385
0	8		609	607
1	8		622	628
2	8	•	336	150
3	8	•	354	126
4	8	•	372	-169
5	8		498	499
1	-8	•	291	261
2	-8		780	-783
3	-8	•	271	-2
4	-8		363	354
5	-8		459	-445
6	-8		497	-475
7	-8		358	-349
8	-8		336	337
9	-8		765	-747
10	-8		608	596
11	-8		323	318
0	9	•	331	102
1	9	•	346	-84
1	-9	•	317	6
2	-9	•	306	-126
3	-9	•	296	111
4	-9		416	402
5	-9	•	286	137
6	-9		325	-300
7	-9		211	216
8	-9		320	-332
9	-9		293	-288
10	-9	•	313	119
11	-9	•	325	-50
12	-9	•	340	-53
0	10	•	357	186
1	-10		323	-314
2	-10		305	319
3	-10	•	322	223
4	-10		952	-948
5	-10		331	320
6	-10		435	-425
7	-10		626	-599
8	-10	•	311	-220
9	-10	•	317	-60
10	-10		93	86
11	-10		429	-406
12	-10	•	348	18
13	-10		419	-417
5	-11		384	402
6	-11	•	330	43
7	-11	•	328	-23
8	-11	•	330	31
9	-11		345	335
10	-11	•	340	111
11	-11	•	348	182
12	-11	•	358	223
7	-12		525	534
8	-12	•	350	-125
9	-12		403	393
10	-12	•	356	68
11	-12	•	363	105
12	-12	•	371	40
13	-12		402	-412
8	-13	•	370	-84
9	-13	•	371	26
10	-13	•	373	66
11	-13	•	378	243
12	-13	•	384	-36
13	-13	•	391	-19
9	-14		488	472
10	-14	•	390	-82
11	-14	•	393	10
12	-14	•	397	68
13	-14	•	402	163
14	-14	•	408	21

H	L			K=4
0	0		1219	-1257
1	0		1129	-1168
2	0		213	221
3	0		1170	-1237
4	0		973	-1026
5	0		585	586
6	0		821	-846
7	0		543	-557
8	0		370	-373
9	0		154	154
10	0		188	-174
11	0	•	378	-141
12	0	•	400	312
0	1		572	550
1	1		550	552
2	1		345	356
3	1		338	331
4	1		199	192
5	1		288	272
6	1		292	290
7	1	•	294	13
8	1	•	320	164
9	1		450	460
10	1	•	370	-301
11	1	•	393	67
2	-1		378	-350
3	-1		229	-232
4	-1		440	488
5	-1		717	-746
6	-1		205	230
7	-1		307	316
8	-1	•	288	-153
9	-1	•	313	103
10	-1	•	338	155
0	2		970	941
1	2		512	497
2	2		1040	-1031
3	2		1128	1163
4	2		546	564
5	2		330	341
6	2		144	185
7	2	•	314	263
8	2	•	339	103
9	2	•	363	-212
10	2		559	543
1	-2		810	-829
2	-2		162	130
3	-2	•	154	60
4	-2		1002	1057
5	-2	■	1261	-1374
6	-2		298	-285
7	-2		425	471
8	-2		856	-874
9	-2	•	300	94
10	-2	•	325	-96
0	3		1210	1188
1	3		425	-403
2	3		448	431
3	3	•	240	45
4	3		172	-212
5	3	•	287	111
6	3		405	-416
7	3	•	335	111
8	3	•	359	28
1	-3	•	164	53
2	-3	•	159	95
3	-3		332	-317
4	-3		537	-522
5	-3	•	201	-104
6	-3		431	-424
7	-3		457	-484
8	-3		315	327
9	-3		367	-390
10	-3	•	315	-24
11	-3	•	340	38
12	-3	•	364	-133
0	4		1028	-1005
1	4		749	734
2	4		293	293
3	4		406	381
4	4		273	264
5	4		426	408
6	4		587	572
7	4		459	-472
1	-4		1642	1688
2	-4		1341	1367
3	-4	•	186	5
4	-4		1122	1185
5	-4		374	368
6	-4		542	547
7	-4		370	-364
8	-4		917	926
9	-4		694	723
10	-4		238	-240
11	-4		480	475
12	-4	•	356	115
13	-4	•	379	15
0	5		892	-904
1	5		358	362
2	5		349	-354
3	5	•	291	-119
4	5		303	-286
5	5	•	334	-44
6	5	•	357	-133
1	-5		341	351
2	-5		252	-220
3	-5		1017	964
4	-5		406	-390
5	-5	•	98	-31
6	-5		262	282
7	-5		217	-210
8	-5	•	265	89
9	-5	•	284	99
10	-5	•	305	21
11	-5	•	327	-18
12	-5	•	350	-127
13	-5	•	372	-72
0	6		315	-299
1	6		511	-487
2	6		721	-719
3	6		488	-468
4	6		330	334
5	6		476	-457
1	-6	•	250	-137
2	-6		480	-470
3	-6		1045	1024
4	-6		682	-669
5	-6		1013	-990
6	-6		233	206
7	-6	•	255	-42
8	-6	•	270	98
9	-6	•	287	-134
10	-6		740	754
11	-6	•	326	-85
12	-6		359	-362
13	-6		226	218
0	7	•	79	27
1	7	•	307	15
2	7		213	-244
3	7	•	343	190
1	-7		271	271
2	-7	•	266	234
3	-7		342	-338
4	-7	•	255	216
5	-7		320	305
6	-7		188	-152
7	-7		481	462
8	-7	•	279	-65
9	-7		221	237
10	-7	•	309	165
11	-7	•	327	-324
12	-7		328	307
13	-7	•	367	-164
14	-7	•	386	49
0	8		146	-151
1	8		574	-605
2	8	•	352	111
1	-8	•	305	137
2	-8	•	293	60
3	-8		535	-529
4	-8		680	-651
5	-8	•	277	116
6	-8		1238	-1245
7	-8	•	283	-231
8	-8		207	191
9	-8	•	303	-186
10	-8	•	317	-168
11	-8		540	-527
12	-8	•	349	96
13	-8		673	-660
14	-8	•	386	-94
15	-8		316	289
0	9	•	346	21
1	9	•	361	-209
1	-9		431	-423
2	-9	•	320	-36
3	-9		324	-314
4	-9	•	304	34
5	-9	•	300	-129
6	-9	•	299	-68
7	-9	•	302	186
8	-9	•	308	-174
9	-9	■	101	-22
10	-9	•	327	-195
11	-9	•	340	129
0	10		573	574
1	-10	•	359	-50
2	-10		563	557
3	-10	•	337	145
4	-10	•	329	95
5	-10	•	324	-67
6	-10	•	322	134
7	-10		662	645
8	-10		369	-367
9	-10		615	606
10	-10		180	195
11	-10		376	-374

H	L			K=5
1	0		320	-322
2	0		784	818
3	0		344	-370
4	0		358	318
5	0		879	-955
6	0	•	109	46
7	0	•	112	43
8	0		504	-465
9	0		515	486
10	0	•	356	-163
0	1		696	-702
1	1		821	-864
2	1	•	207	-101
3	1		179	-172
4	1		391	-390
5	1		697	-701
6	1		726	747
7	1		277	245
8	1	•	335	-202
9	1		345	357
10	1	•	372	-61
1	-1		1068	1066
3	-1	■	1226	-1403
4	-1		266	-287
5	-1		583	-636
6	-1		440	-482
7	-1		285	-334
8	-1		260	271
9	-1		775	-785
10	-1		418	-392
11	-1	•	366	-2
0	2		541	527
1	2		829	-838
2	2		200	197
3	2		136	-120
4	2		380	-377
5	2		373	376
6	2		653	-647
7	2	•	317	9
8	2	•	342	59
9	2	•	366	20
1	-2		1386	1455
2	-2		305	298
3	-2		141	-132
4	-2		623	666
5	-2		451	-456
6	-2	•	235	45
7	-2		234	255
8	-2		421	437
9	-2	•	296	-3
10	-2	•	314	-15
11	-2	•	330	182
12	-2		327	-308
0	3		905	907
1	3		1220	1207
2	3		736	711
3	3	•	272	-112
4	3		697	680
5	3		426	414
6	3	•	312	106
7	3		361	378
8	3		487	488
1	-3		184	169
2	-3		961	958
3	-3		790	801
4	-3		1068	-1052
5	-3		748	804
6	-3		743	796
7	-3	•	277	176
8	-3	•	284	-229
9	-3	•	288	158
10	-3	•	305	38
11	-3		467	-471
12	-3	•	367	155
0	4	•	71	-66
1	4	•	258	72
2	4	•	270	57
3	4		398	363
4	4	•	290	-52
5	4	•	313	288
6	4	•	336	-1
7	4	•	360	134
1	-4		210	-182
2	-4	•	224	-90
3	-4		590	580
4	-4		1069	-1060
5	-4		343	329
6	-4		440	442
7	-4		432	-438
8	-4		684	695
9	-4		282	-285
10	-4	•	312	208
11	-4	•	335	-121
12	-4	•	358	-143
13	-4	•	381	160
0	5		690	702
1	5		274	-269
2	5	•	280	153
3	5		269	261
4	5		359	-367
5	5	•	337	-263
6	5	•	360	-105
1	-5		373	367
2	-5		251	-241
3	-5		352	-341
4	-5		1298	1271
5	-5		312	255
6	-5	•	263	-86
7	-5		1098	1117
8	-5		232	231
9	-5	•	282	21
10	-5	•	296	-9
11	-5	•	311	276
12	-5	•	324	308
13	-5	•	337	-86
14	-5		488	450
0	6		336	-306
1	6		717	716
2	6		283	-271
3	6	•	320	76
4	6	•	341	216
5	6	•	362	-86
1	-6	•	283	-82
2	-6		603	-600
3	-6	•	272	22
4	-6		321	-323
5	-6	•	282	162
6	-6		523	-505
7	-6		371	363
8	-6		356	-341
9	-6	•	284	-103
10	-6	•	292	63
11	-6		343	-346
0	7		734	-730
1	7		246	191
2	7	•	328	-334
3	7		296	-269
4	7	•	366	-208
1	-7		940	-897
2	-7	•	300	-27
3	-7		723	-691
4	-7		543	-497
5	-7	•	288	-29
6	-7	•	293	61
7	-7		528	-510
8	-7		576	-562
9	-7		280	255
10	-7		454	-442
0	8		139	-93
1	8		311	-293
2	8	•	351	-33
3	8	•	356	-9
1	-8	•	321	-240
2	-8		636	616
3	-8		490	-483
4	-8	•	305	253
5	-8	•	303	205
6	-8	•	301	-190
7	-8		283	303
8	-8		381	-360
9	-8		265	238
10	-8	•	320	20
0	9	•	349	-23
1	9	•	364	53
2	9	•	380	95
3	9		488	474
1	-9	•	335	-32
2	-9	•	323	-303
3	-9	•	313	28
4	-9		538	538
5	-9		362	-352
6	-9	•	315	-77
7	-9	•	318	-40
8	-9		178	-170
9	-9		573	-574
10	-9	•	320	-50
11	-9		336	320
2	-10	•	350	-8
3	-10	•	340	-19
4	-10	•	332	182
5	-10	•	327	-67
6	-10	•	324	174
7	-10	•	325	-5
8	-10	•	328	193
9	-10	•	334	1
10	-10		235	-233
11	-10		425	428
3	-11		436	417
4	-11	•	358	105
5	-11		480	498
6	-11	•	348	291
7	-11	•	347	-208
8	-11	•	348	113
9	-11	•	352	251
10	-11	•	358	238
11	-11	•	339	54
12	-11		473	452

H	L			K=6
0	0		1546	-1618
1	0		520	483
2	0		177	-174
3	0		487	-484
4	0		167	-160
5	0		243	-222
6	0	•	157	57
7	0		502	-488
8	0	•	109	-26
9	0	•	329	-119
10	0	•	354	-124
0	1		86	95
1	1		454	-455
2	1	■	1536	-1694
3	1	•	232	20
4	1		602	-633
5	1		641	-651
6	1	•	287	135
7	1	•	302	-67
8	1	•	314	-307
9	1		561	-572
10	1	•	369	-41
1	-1		479	466
3	-1		216	-254
4	-1		219	249
5	-1	■	966	1111
6	-1	•	285	-111
7	-1	•	306	-13
8	-1	•	324	-129
9	-1	•	330	-26
10	-1	•	330	-115
11	-1	•	338	-262
12	-1		393	414
0	2		433	424
1	2	•	202	-132
2	2	•	223	-87
3	2	•	241	-86
4	2		815	835
5	2		430	-418
6	2		334	319
7	2	•	315	153
8	2	•	340	-229
9	2	•	363	242
1	-2	•	131	69
2	-2		336	-354
3	-2		697	747
4	-2		234	-245
5	-2	•	212	-154
6	-2	•	233	23
7	-2	•	254	-80
8	-2	•	271	121
9	-2		434	-428
10	-2	•	327	196
11	-2	•	351	-24
0	3		888	-895
1	3	•	232	-39
2	3		447	437
3	3		818	-816
4	3		257	-251
5	3		287	268
6	3		362	383
7	3	•	336	-154
8	3	•	359	276
9	3	•	382	128
1	-3		875	-847
2	-3		441	453
3	-3		693	742
4	-3		786	794
5	-3		581	601
6	-3	•	234	-37
7	-3		658	686
8	-3	•	264	-259
9	-3	•	281	39
10	-3		566	581
11	-3	•	341	199
0	4		348	324
1	4		573	-568
2	4		546	532
3	4	•	283	28
4	4	•	297	-121
5	4		602	602
6	4	•	334	-172
7	4	•	357	56
8	4	•	379	-37
1	-4		342	402
2	-4		423	407
3	-4		335	327
4	-4		194	-194
5	-4		813	847
6	-4	•	241	-134
7	-4	•	244	116
8	-4		347	340
9	-4		359	374
10	-4	•	287	138
11	-4	•	303	-91
12	-4		427	404
0	5		948	939
1	5		491	482
2	5	•	294	146
3	5	•	305	-19
4	5		751	750
5	5	•	334	-129
6	5	•	343	85
7	5		698	692
1	-5		670	-642
2	-5	•	251	129
3	-5		728	-721
4	-5	•	248	91
5	-5		139	-130
6	-5		485	-462
7	-5		738	-746
8	-5	•	261	-117
9	-5		262	272
10	-5		507	-516
11	-5		376	372
0	6	•	110	18
1	6	•	298	-99
2	6		523	-508
3	6	•	319	13
4	6	•	339	-50
5	6	•	359	-14
1	-6		578	-528
2	-6		363	381
3	-6		407	-391
4	-6		194	224
5	-6		564	-569
6	-6		365	-350
7	-6		610	589
8	-6		605	-616
9	-6		408	405
10	-6	•	307	163
0	7		157	186
1	7	•	309	-220
2	7	•	376	160
3	7	•	344	-130
4	7		465	-457
1	-7	•	295	-59
2	-7		426	-411
3	-7		523	482
4	-7		230	207
5	-7		884	-840
6	-7	•	286	128
7	-7		249	-239
8	-7		470	-442
9	-7		190	-224
10	-7		328	329
0	8		363	-367
1	8	•	335	207
2	8	•	352	-232
3	8	•	369	56
1	-8	•	318	170
2	-8	•	309	62
3	-8		399	-388
4	-8	•	295	109
5	-8		424	-408
6	-8	•	289	-182
7	-8		531	-520
8	-8		270	252
9	-8	•	291	-42
10	-8		567	-539
0	9	•	344	43
1	9	•	349	40
2	9		404	-413
1	-9	•	336	367
2	-9		445	424
3	-9	•	327	186
4	-9	•	325	105
5	-9		924	895
6	-9	•	323	-267
7	-9	•	319	-60
8	-9		634	627
9	-9		175	-167
10	-9		389	395
2	-10	•	348	-89
3	-10		524	510
4	-10	•	330	-100
5	-10	•	325	-43
6	-10		389	384
7	-10	•	323	-65
8	-10	•	327	184
9	-10	•	333	47
10	-10		114	138

H	L			K=7
1	-1		641	-645
2	-2		876	917
3	-3	•	105	-3
4	-4		573	-586
5	-5		576	-570
6	-6		344	-336
7	-7		185	167
8	-8		173	173
9	-9		175	172

H	L			K=8
1	-1		303	301
2	-2		688	675
3	-3		818	804
4	-4		203	-205
5	-5		384	365
6	-6		100	115
7	-7		166	163
8	-8		94	83

H	L			K=9
1	-1	•	109	17
2	-2	•	109	-43
3	-3		167	167
4	-4	•	246	-81
5	-5		214	-232
6	-6		154	-138
7	-7		584	594
8	-8		223	-268

H	L			K=10
1	-1		265	-238
2	-2		285	230
3	-3		589	-600
4	-4		533	-530
5	-5		482	-509
6	-6		188	-195
7	-7		153	-162

H	L			K=11
1	-1		373	-363
2	-2		288	-257
3	-3		286	-282
4	-4		653	673
5	-5		272	-292

H	L			K=12
1	-1		173	-157

H	K			L=0
1	7		211	181
2	7		193	150
3	7		833	843
4	7		982	-999
5	7		434	-428
6	7		143	151
7	7		498	-473
8	7		153	-150
9	7		166	183
0	8		1043	1050
1	8		331	288
2	8	•	110	-8
3	8		267	270
4	8	•	305	317
5	8		140	117
6	8	•	110	-42
7	8		925	932
1	9		137	-104
2	9		334	374
3	9		373	-339
4	9	•	110	69
5	9	•	109	-59
6	9		208	-203
7	9	•	110	68
0	10		579	555
1	10		527	531
2	10	•	110	-58
3	10		315	301
4	10		576	539
5	10		143	-135
6	10		215	230
1	11		266	265
2	11		298	-300
3	11	•	101	-22
4	11		226	225
5	11		426	429
0	12		410	-402
1	12		244	-223
2	12		108	130
3	12		142	-142

K	L			H=0
7	1		431	392
7	2		1054	-1097
7	3		130	-95
7	4	•	77	9
7	5		449	-437
7	6	•	110	80
7	7	•	91	-50
8	1		499	489
8	2	•	109	55
8	3	•	77	68
8	4	•	109	69
8	5		579	573
8	6		223	-211
8	7		404	-416
9	1		277	-264
9	2		205	200
9	3	•	78	-11
9	4	•	77	47
9	5	•	75	-52
9	6	•	69	59
9	7		288	320
10	1		387	-381
10	2		241	-226
10	3	•	92	24
10	4		373	354
10	5		255	-262
11	1		255	253
11	2		221	205
11	3	•	98	-13
11	5		343	-409

TABLE (IV-2)

β-$Zn_3(PO_4)_2$ atomic parameters; positional and thermal

Atom	x=X/a	y=Y/b	z=Z/c	U_{11}(Å^2)	U_{22}(Å^2)	U_{33}(Å^2)	U_{12}(Å^2)	U_{13}(Å^2)	U_{23}(Å^2)
Zn(1)	0.9843(1)	0.3898(1)	0.3550(1)	0.0175(4)	0.0108(8)	0.0103(4)	-.0019(5)	0.0058(3)	0.0005(5)
Zn(2)	0.7065(1)	0.1115(1)	0.2636(1)	0.0111(4)	0.0085(7)	0.0099(4)	0.0016(5)	0.0044(3)	0.0020(5)
Zn(3)	0.4187(1)	0.2325(1)	0.3868(1)	0.0147(4)	0.0106(8)	0.0149(4)	-.0040(5)	0.0108(3)	-.0037(5)
P(1)	0.6439(2)	0.4412(3)	0.3365(3)	0.0066(7)	0.0079(13)	0.0071(7)	-.0006(8)	0.0040(6)	-.0002(8)
O(1)	0.8385(8)	0.4813(8)	0.4446(8)	0.0128(24)	0.0177(42)	0.0141(25)	-.0017(28)	0.0076(21)	-.0027(28)
O(3)	0.4699(7)	0.0729(8)	0.2686(8)	0.0113(22)	0.0096(37)	0.0119(23)	0.0030(27)	0.0066(19)	0.0002(27)
O(5)	0.6064(7)	0.3845(8)	0.4766(7)	0.0119(21)	0.0091(38)	0.0097(21)	-.0020(28)	0.0071(18)	0.0008(26)
O(7)	0.6086(7)	0.3163(7)	0.2000(8)	0.0107(21)	0.0023(32)	0.0099(21)	0.0019(24)	0.0043(18)	0.0014(25)
P(2)	0.1416(2)	0.1143(3)	0.4624(3)	0.0081(7)	0.0078(12)	0.0068(7)	0.0004(10)	0.0042(6)	0.0008(9)
O(2)	0.2509(7)	0.3987(9)	0.1801(7)	0.0138(22)	0.0184(42)	0.0024(17)	-.0009(28)	0.0016(17)	0.0002(27)
O(4)	0.2239(8)	0.2219(9)	0.4041(9)	0.0194(28)	0.0253(50)	0.0210(29)	-.0035(31)	0.0145(25)	0.0048(32)
O(6)	0.8720(8)	0.4610(8)	0.1058(9)	0.0202(28)	0.0097(36)	0.0157(26)	0.0041(30)	0.0102(24)	0.0040(28)
O(8)	0.9573(7)	0.1808(8)	0.3790(8)	0.0118(23)	0.0105(39)	0.0130(24)	0.0026(26)	0.0068(21)	0.0038(27)

TABLE (IV-3)

Summary of residuals for β-$Zn_3(PO_4)_2$

Residual	# of refl.	Conditions	Value of residual
R_2	1633	all reflections	0.049
R_1	1633	all reflections	0.045
R_2	988	obs. refl. only	0.047
R_1	988	obs. refl. only	0.038

observed and calculated structure factors is shown in Table (IV-1). In this table, the unobserved reflections are marked with an asterisk (*), and the 22 unreliable reflections with the symbol Ø. The value of $|F_o|$ quoted for the unobserved reflections is $|F_{min}|$.

For the calculation of structure factors for β-$Zn_3(PO_4)_2$ and also for all of the other structures studied, the scattering factors, ($f_j(H)$ in Eqn. (II-1)), were those for the ionic species M^{++}, P^o and O^-, obtained by linear interpolation from the values given in the International Tables for X-ray Crystallography(13).

F. Description of the Structure

The most informative way of describing the structure of an orthophosphate is to consider the near-neighbour cation environment, which can be classified as a MO_n polyhedron, and the way in which these individual polyhedra link together to form the basic structural framework. There are two ways in which two of these polyhedra can be directly linked; by sharing one, or two, oxygen atoms. The former linkage is termed corner-sharing, and the latter edge-sharing. It is geometrically possible for two neighbouring cation polyhedra to share a face, three oxygen atoms, but this would place the cations so close together that metal-metal bonding would result. Such face-sharing is not found among the divalent metal ion orthophosphates.

Zn(1) is strongly bonded to four oxygen atoms which are located at the corners of an irregular tetrahedron. A pair of these tetrahedra are linked by a shared edge, across a centre of symmetry. The average bond distance in these tetrahedra is 1.98±0.08†Å. Zn(2) is bonded to five oxygen atoms with an average bond distance of 2.09±0.10 Å. This group shares a corner, O(8), with Zn(1) and an edge, O(5) and O(7), with the remaining cation, Zn(3). Additional corners, O(2) and O(3), are shared with two other neighbouring Zn(3) sites, Zn(3) is also bonded to five oxygen atoms, with the average Zn-O distance in this group being 2.08±0.12 Å. The near-neighbour bond distances and angles for the cations, and also for the two phosphate groups, are listed in Table (IV-4).

The two five-coordinate cations, Zn(2) and Zn(3), also have markedly irregular environments. The $Zn(3)O_5$ polyhedron can be described as an irregular trigonal bipyramid, where O(2) and O(7) are the axial ligands, while O(3), O(4), and O(5) lie rigourously in the equatorial plane. It can be seen from Table (IV-4) that the three equatorial bonds are significantly shorter than the two axial ones. The polyhedron of oxygen atoms surrounding Zn(2) cannot be described as a trigonal bipyramid, and is perhaps closer to a highly distorted tetragonal pyramid.

There are two additional Zn-O bonds in this structure, which because of their length must be very weak. These two distances,

---

† The ±0.08 Å refers to the root mean square (rms) deviation from the mean of the four bonds to Zn(1). Similar rms deviations are quoted in the same manner for other averaged quantities.

TABLE (IV-4)

Bond distances and angles in β-$Zn_3(PO_4)_2$

Bonded atoms	Distance (Å)	Bonded atoms	Angle (°)	Bonded atoms	Angle (°)
Zn(1)-O(6)	1.886(7)	O(6)-Zn(1)-O(1')	115.	O(1')-Zn(1)-O(1)	80.
Zn(1)-O(1')	1.953(6)	O(6)-Zn(1)-O(8)	116.	O(1')-Zn(1)-O(4)	90.
Zn(1)-O(8)	1.960(8)	O(6)-Zn(1)-O(1)	104.	O(8)-Zn(1)-O(1)	101.
Zn(1)-O(1)	2.105(9)	O(6)-Zn(1)-O(4)	104.	O(8)-Zn(1)-O(4)	63.
Zn(1)-O(4)	2.549(8)	O(1') -Zn(1)-O(8)	126.	O(1)-Zn(1)-O(4)	152.
Zn(2)-O(2)	1.994(8)	O(2)-Zn(2)-O(7)	166.	O(7)-Zn(2)-O(3)	82.
Zn(2)-O(7)	2.021(7)	O(2)-Zn(2)-O(8)	100.	O(7)-Zn(2)-O(6)	116.
Zn(2)-O(8)	2.049(7)	O(2)-Zn(2)-O(5)	101.	O(8)-Zn(2)-O(5)	100.
Zn(2)-O(5)	2.089(6)	O(2)-Zn(2)-O(3)	84.	O(8)-Zn(2)-O(3)	154.
Zn(2)-O(3)	2.276(8)	O(2)-Zn(2)-O(6)	63.	O(8)-Zn(2)-O(6)	76.
Zn(2)-O(6)	2.509(7)	O(7)-Zn(2)-O(8)	93.	O(5)-Zn(2)-O(3)	105.
		O(7)-Zn(2)-O(5)	81.	O(5)-Zn(2)-O(6)	163.
				O(3)-Zn(2)-O(6)	83.
Zn(3)-O(4)	1.924(9)	O(4)-Zn(3)-O(3)	122.	O(3)-Zn(3)-O(2)	111.
Zn(3)-O(3)	2.001(8)	O(4)-Zn(3)-O(5)	132.	O(3)-Zn(3)-O(7)	102.
Zn(3)-O(5)	2.013(7)	O(4)-Zn(3)-O(2)	81.	O(5)-Zn(3)-O(2)	83.
Zn(3)-O(2)	2.174(7)	O(4)-Zn(3)-O(7)	91.	O(5)-Zn(3)-O(7)	77.
Zn(3)-O(7)	2.262(6)	O(3)-Zn(3)-O(5)	107.	O(2)-Zn(3)-O(7)	145.
P(1)-O(3)	1.515(7)	O(3)-P(1)-O(1)	110.	O(1)-P(1)-O(7)	107.
P(1)-O(1)	1.534(7)	O(3)-P(1)-O(7)	112.	O(1)-P(1)-O(5)	110.
P(1)-O(7)	1.539(7)	O(3)-P(1)-O(5)	110.	O(7)-P(1)-O(5)	108.
P(1)-O(5)	1.541(8)				
P(2)-O(6)	1.502(8)	O(6)-P(2)-O(4)	115.	O(4)-P(2)-O(2)	111.
P(2)-O(4)	1.512(9)	O(6)-P(2)-O(2)	105.	O(4)-P(2)-O(8)	104.
P(2)-O(2)	1.542(6)	O(6)-P(2)-O(8)	112.	O(2)-P(2)-O(8)	111.
P(2)-O(8)	1.558(7)				

Zn(1)-O(4)=2.55 Å and Zn(2)-O(6)=2.51 Å, are underlined in Table (IV-4) and are shown with dashed bonds in Fig. (IV-1). Both of these bonds are significantly longer than the typical Zn-O bond distances of about 2.05 Å found elsewhere in the structure. These two bonds will therefore not be considered as contributing to the linkages between the MO_n polyhedra.

As shown in Fig. (IV-1), the corner-sharing of O(2) and the edge-sharing of O(5) and O(7), together with the centre of symmetry at (½,½,½), result in a closed ring of two $Zn(2)O_5$ and two $Zn(3)O_5$ polyhedra. This ring lies approximately in the $(10\bar{1})$ plane, and is connected by O(8) to the $Zn(1)O_4$ tetrahedra to form an infinite chain which runs along the body diagonal [111] of the unit cell. An identical chain, derived from this one by the c glide operation, and not shown in Fig. (IV-1), runs in the $[1\bar{1}1]$ direction. These two chains are linked together by sharing O(3).

Fig. (IV-2) shows part of the structure projected down the b axis of the unit cell. Here, the corner-sharing of O(3) is seen to result in chains of polyhedra which spiral around the 2_1 axes in the crystal. The result of the two types of infinite chains, as shown in Fig. (IV-1) and Fig. (IV-2) respectively, is a complete three dimensional framework of ZnO_n polyhedra. This is in immediate contrast to the structures of α and γ-$Zn_3(PO_4)_2$ which exhibit isolated chains and sheets of polyhedra respectively.(8), (9)

The two PO_4 groups occur as slightly irregular, independent tetrahedra, with average P-O bond distances of 1.533±0.011 Å and 1.528±0.023 Å. All of the O-P-O angles lie between 103° and 115°

Fig. (IV-1) Cation polyhedra linkages in β-$Zn_3(PO_4)_2$. The ring formed by two $Zn(2)O_5$ and two $Zn(3)O_5$ polyhedra is shown sharing opposite corners with pairs of edge-sharing $Zn(1)O_4$ tetrahedra. The dashed bonds denote the two "long" Zn-O bond distances of 2.5 Å. The two PO_4 groups are shown as solid tetrahedra.

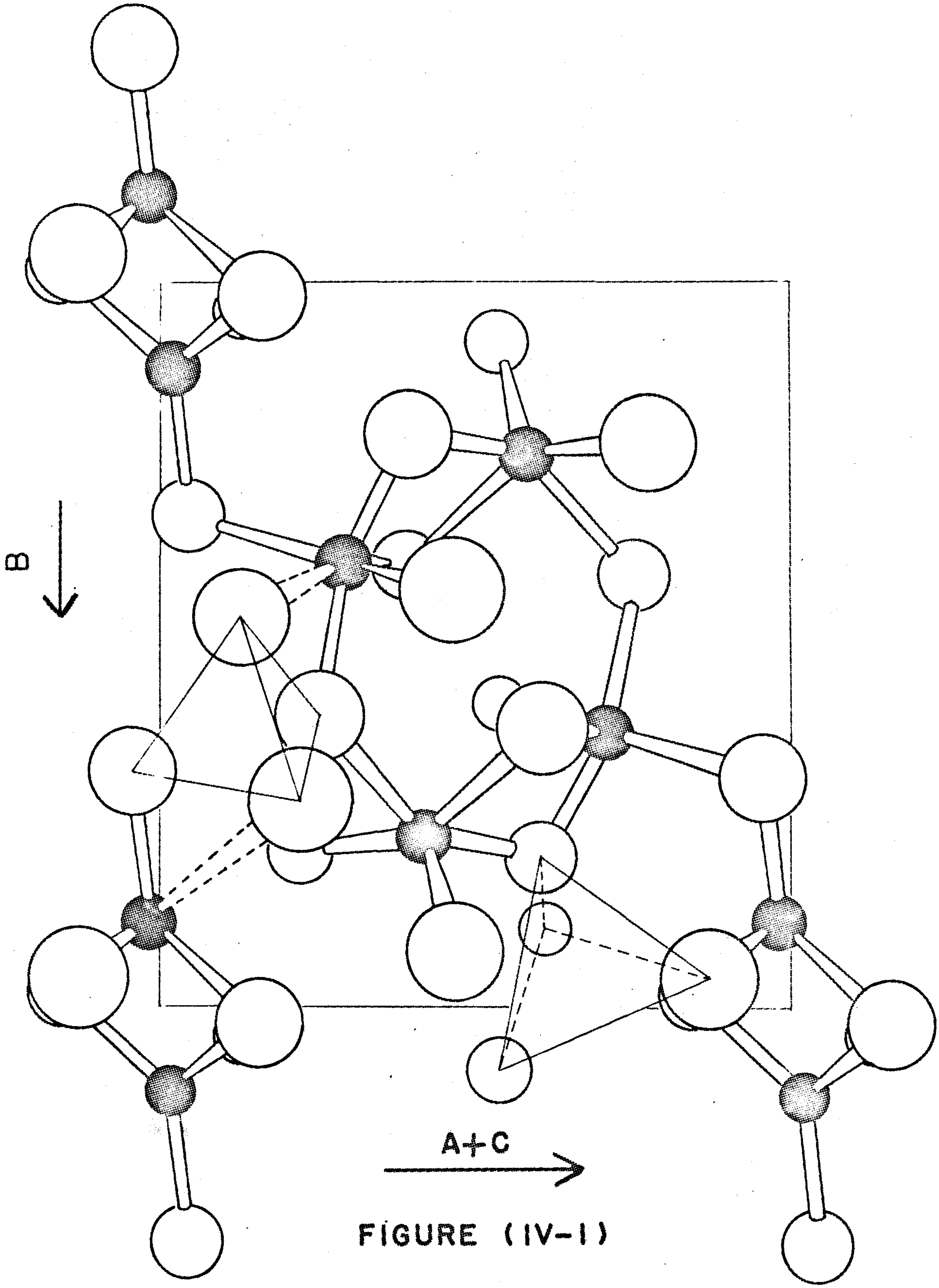

FIGURE (IV-1)

Fig. (IV-2) Spiral cation polyhedra chains in β-$Zn_3(PO_4)_2$. The interconnected spiral chains are shown in projection down the b axis. The concentric oxygen atoms, where the lower one is shown in broken outline, are related by b, showing the spiral nature of the chains. The two weak Zn-O bonds of 2.5 Å in length are not shown in this figure.

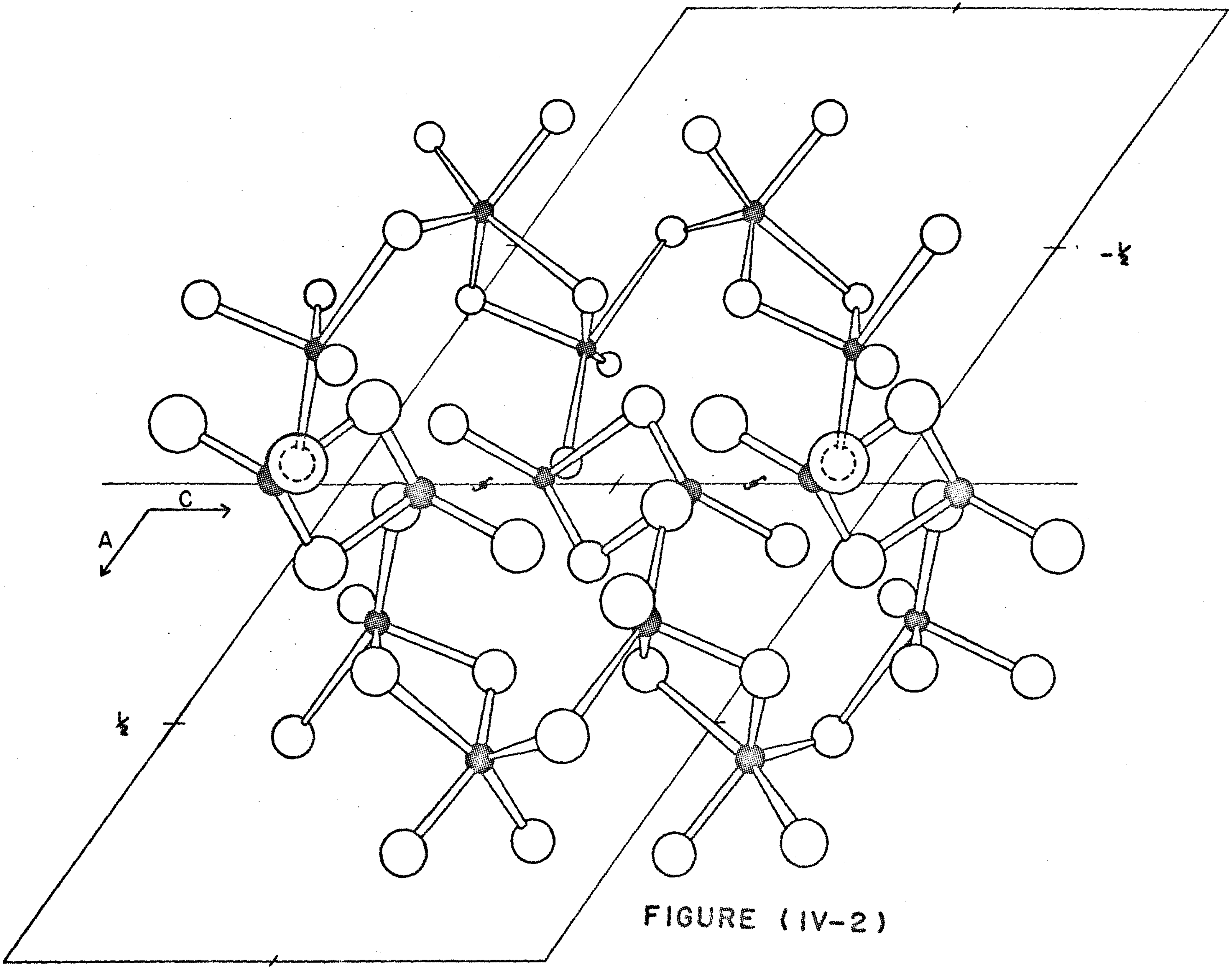

FIGURE (IV-2)

with a mean value of 109.5°. The variations in the P-O bond distances are significant, however, and can be correlated with the further bonding of the oxygen atoms to cations in the structure. This variation is most apparent for O(4) and O(6), which are strongly bonded to only one cation. In the case of these two atoms, the P-O distances have decreased to 1.50 Å and 1.51 Å respectively. Despite these two short bonds, the average bond distance in this PO_4 group is only slightly reduced. This tendency of tetrahedral anions, such as $(PO_4)^{3-}$, to maintain a constant average bond length despite the differences in individual bond lengths, is well known.(31) Table (IV-5) lists the individual and average P-O bond distances in several accurately determined orthophosphate structures.

Each of the oxygen atoms lies accurately in the plane formed by the three atoms to which it is bonded; a phosphorus atom and two cations. Even with O(4) and O(6), to which the second cation is only weakly bonded, this planarity still exists. The accuracy with which an oxygen atom lies in its coordination plane can be gauged by comparing the sum of the three bond angles subtended at the atom to 360°. Any deviation of the oxygen atom from the plane will result in a decrease in this sum from 360°. These angles and their sums are listed in Table (IV-6) for the eight oxygen atoms in the β-$Zn_3(PO_4)_2$ structure.

TABLE (IV-5)

P-O bond distances in 4 accurately refined orthophosphate structures

β-$Zn_3(PO_4)_2$				$Cu_3PO_4(OH)_3$ (29a)		$Fe_3(PO_4)_2 \cdot 4H_2O$ (29b)		$CuAl_6(PO_4)_4(OH)_8 \cdot 4H_2O$ (29c)			
Bond	Dist. (Å)	Bond	Dist. (Å)	Bond	Dist. (Å)	Bond	Dist. (Å)	Bond	Dist. (Å)	Bond	Dist. (Å)
P(1)-O(1)	1.534	P(2)-O(2)	1.542	P-O(1)	1.539	P-O(1)	1.542	P(1)-O(3)	1.541	P(2)-O(1)	1.534
P(1)-O(3)	1.515	P(2)-O(4)	1.512	P-O(2)	1.532	P-O(2)	1.549	P(1)-O(8)	1.521	P(2)-O(2)	1.533
P(1)-O(5)	1.542	P(2)-O(6)	1.501	P-O(3)	1.504	P-O(3)	1.542	P(1)-O(11)	1.539	P(2)-O(7)	1.543
P(1)-O(7)	1.539	P(2)-O(8)	1.558	P-O(4)	1.536	P-O(4)	1.536	P(1)-O(14)	1.556	P(2)-O(13)	1.550
<P(1)-O>	1.533	<P(2)-O>	1.528	<P-O>	1.528	<P-O>	1.542	<P(1)-O>	1.539	<P(2)-O>	1.540

Average P-O distance in all tetrahedra, 1.535 Å.

TABLE (IV-6)

Bond angles subtended at the oxygen atoms in β-$Zn_3(PO_4)_2$

Bonded atoms	Bond Angles (°)	Sum of bond angles (°)	Bonded atoms	Bond Angles (°)	Sum of bond angles (°)
P(1)-0(1)-Zn(1)	118.6	359.8	P(2)-0(2)-Zn(2)	105.7	355.2
P(1)-0(1)-Zn(1)'	141.4		P(2)-0(2)-Zn(3)	126.9	
Zn(1)-0(1)-Zn(1)'	99.8		Zn(2)-0(2)-Zn(3)	122.6	
P(1)-0(3)-Zn(2)	117.8	359.5	P(2)-0(4)-Zn(1)	82.9	360.0
P(1)-0(3)-Zn(3)	126.5		P(2)-0(4)-Zn(3)	139.0	
Zn(2)-0(3)-Zn(3)	115.2		Zn(1)-0(4)-Zn(3)	138.1	
P(1)-0(5)-Zn(2)	141.7	359.4	P(2)-0(6)-Zn(1)	129.7	360.0
P(1)-0(5)-Zn(3)	118.7		P(2)-0(6)-Zn(2)	86.0	
Zn(2)-0(5)-Zn(3)	99.0		Zn(1)-0(6)-Zn(2)	144.3	
P(1)-0(7)-Zn(2)	128.5	359.4	P(2)-0(8)-Zn(1)	104.7	359.3
P(1)-0(7)-Zn(3)	137.5		P(2)-0(8)-Zn(2)	138.9	
Zn(2)-0(7)-Zn(3)	93.4		Zn(1)-0(8)-Zn(2)	115.7	

CHAPTER V

THE STRUCTURES OF β^1-$Mn_3(PO_4)_2$ AND β^1-$Cd_3(PO_4)_2$

A. Crystal Chemistry of $Mn_3(PO_4)_2$

A sample of $Mn_3(PO_4)_2$ had been prepared$^{(32)}$ whose powder pattern was very similar to that of β-$Zn_3(PO_4)_2$. Initial attempts to prepare single crystals of $Mn_3(PO_4)_2$ with this structure were unsuccessful. A form of $Mn_3(PO_4)_2$ which gave a powder pattern similar to that of the mineral "graftonite" (an anhydrous orthophosphate of Fe^{++}, Mn^{++} and Ca^{++}),$^{(11)}$ resulted from all such attempts.

This form of $Mn_3(PO_4)_2$, which will be referred to as Mn-graftonite, was prepared by reacting stoichiometric amounts of manganous carbonate and phosphoric acid, according to the equation,

$$3MnCO_3 + 2H_3PO_4 \longrightarrow Mn_3(PO_4)_2 + 3CO_2 + 3H_2O \qquad (V\text{-}1)$$

The reaction was performed by adding the acid to a water slurry of the carbonate, and heating gently until CO_2 evolution was complete. The water was then removed by evaporating the sample to dryness. Single crystals were grown from the melt in a vycor tube, by cooling slowly through the freezing point and then quenching to room temperature. The dark colour of the resulting sample indicated that there had been considerable oxidation of Mn^{++}. The same procedure was repeated with the final fusing and crystallization being carried out in a graphite crucible with a fitted cover. The amount of oxidation in this case was minimal, and the crystals of Mn-graftonite were a light greenish-brown in colour. These crystals were needle-shaped and preliminary X-ray photographs showed that the space group was $P\text{-}2_1/c$, and that the long axis of the crystals coincided with the c axis of the unit cell. The approximate lattice parameters of Mn-graftonite are listed in Table (V-1), together with those of the mineral for comparison(33).

Crystals of $Mn_3(PO_4)_2$ with a structure similar to $\beta\text{-}Zn_3(PO_4)_2$ were grown in a later attempt. The material used was "$Mn_3(PO_4)_2 \cdot 7H_2O$", supplied by Fisher Scientific Co., which was heated to remove the water, and fused in a vycor tube by heating with an oxy-gas flame. Flat plate-like crystals, which varied in colour from a dirty brown to almost colourless, were produced. Preliminary X-ray photographs taken using a fairly large single crystal showed that the structure was similar to $\beta\text{-}Zn_3(PO_4)_2$. Consequently, this phase of $Mn_3(PO_4)_2$ was denoted as $\beta^1\text{-}Mn_3(PO_4)_2$.

An attempt was then made to determine the conditions which resulted in the formation of the β^1 phase rather than the graftonite-like phase. It was felt that the sample of "$Mn_3(PO_4)_2 \cdot 7H_2O$" was probably contaminated with the acid or the basic phosphate, and that the resultant depression of the melting point might have crossed a phase boundary between the two forms. If this were true, then the Mn-graftonite was obtained as a metastable phase by quenching, in the same manner as $\beta\text{-}Zn_3(PO_4)_2$.

To test this possibility, a series of samples were prepared according to the following equation, with the parameter x taking the values, 1.1, 1.0, 0.9, 0.8, 0.7 and 0.6 .

TABLE (V-1)

Approximate lattice parameters for Mn-graftonite and the mineral

Parameter	Mineral(33)	Mn-graftonite
a (Å)	8.87	8.81
b (Å)	11.57	11.45
c (Å)	6.17	6.27
β (°)	99.2	99.
space group	$P\text{-}2_1/c$	$P\text{-}2_1/c$

TABLE (V-2)

Lattice parameters of $\beta\text{-Zn}_3(\text{PO}_4)_2$, $\beta^1\text{-Mn}_3(\text{PO}_4)_2$ and $\beta^1\text{-Cd}_3(\text{PO}_4)_2$

Parameter	$\beta\text{-Zn}_3(\text{PO}_4)_2$	$\beta^1\text{-Mn}_3(\text{PO}_4)_2$	$\beta^1\text{-Cd}_3(\text{PO}_4)_2$
a (Å)	9.393(1)	8.94(3)	9.221(1)
b (Å)	9.17(1)	10.04(2)	10.335(1)
c (Å)	8.686(1)	24.14(12)	24.90(5)
β (°)	125.7(1)	120.8(1)	120.7(2)
V (Å^3)	607.3(7)	1861.(12)	2030.(6)
Z	4	12	12
space group	$P\text{-}2_1/c$	$P\text{-}2_1/c$	$P\text{-}2_1/c$

$$xMnCO_3 + Mn_2P_2O_7 \longrightarrow \begin{cases} xMn_3(PO_4)_2 + (1-x)Mn_2P_2O_7 + xCO_2 & \text{if } x \leqq 1 \\ Mn_3(PO_4)_2 + (x-1)MnO + xCO_2 & \text{if } x \geqq 1 \end{cases} \qquad (V-2)$$

Each sample was mixed intimately with mortar and pestle, and fused in a covered graphite crucible to minimize oxidation of Mn^{++}. After cooling, the samples with x equal to 1.1, 1.0 and 0.9 all contained the distinctive needle-like crystals of Mn-graftonite, and the bulk of the polycrystalline mass was also this phase. This was confirmed by powder X-ray diffractometer tracings taken with Mn-filtered FeKα radiation, and single crystal rotation photographs with MoKα radiation. The samples with x equal to 0.8, 0.7 and 0.6 were polycrystalline, and did not give diffractometer tracings which could be completely identified. There was certainly $Mn_2P_2O_7$ in these samples, but the presence of Mn-graftonite could not be confirmed. No evidence of β^1-$Mn_3(PO_4)_2$ could be found in any of the samples, however.

The conclusive test of the hypothesis that β^1-$Mn_3(PO_4)_2$ is stable at temperatures below the stability region of Mn-graftonite would be to obtain a quantity of pure β^1-$Mn_3(PO_4)_2$ and fuse it, followed by the same cooling and quenching process used previously to obtain Mn-graftonite. If the hypothesis is true, Mn-graftonite crystals should be formed. Unfortunately it was not possible to perform this experiment as pure β^1-$Mn_3(PO_4)_2$ could not be prepared in sufficient quantity.

B. Preparation of β^1-$Cd_3(PO_4)_2$

$Cd_3(PO_4)_2$ was prepared by reacting stoichiometric amounts of ammonium acid phosphate and cadmium carbonate, according to the equation,

$$3CdCO_3 + 2(NH_4)H_2PO_4 \longrightarrow Cd_3(PO_4)_2 + 3CO_2 + 3H_2O + 2NH_3 \qquad \text{(V-3)}$$

Single crystals were grown from the melt by cooling the sample through the freezing point (1180°C).(4)

Preliminary X-ray photographs indicated that these crystals were of monoclinic symmetry, and the systematically absent reflections, $h0\ell$ for ℓ odd and $0k0$ for k odd, defined the space group to be $P\text{-}2_1/c$. These photographs showed that the lattice parameters were very close to those of β^1-$Mn_3(PO_4)_2$ and the similarity between the intensity data indicated that these compounds were isostructural. This form of $Cd_3(PO_4)_2$ was therefore denoted as β^1-$Cd_3(PO_4)_2$.

C. Lattice Parameters

(i) β^1-$Mn_3(PO_4)_2$

A small flake, broken from a larger flat single crystal of β^1-$Mn_3(PO_4)_2$ was mounted on a glass fibre and aligned to rotate around the $\underline{b}$ axis. The length of the $\underline{b}$ axis was determined from a TiO_2-calibrated rotation photograph, as described earlier. Precession photographs were taken of the $0k\ell$ and $hk0$ zones, and, as the crystal was aligned with the $\underline{b}$ axis parallel to the camera spindle axis, the β angle could be determined directly from the spindle settings for these two photographs. The reciprocal axis lengths, a^*, b^* and c^*

were measured from these precession photographs, which were calibrated for film shrinkage (assumed to be isotropic) by scaling the b* measurements to the value of b determined from the rotation photograph. The corresponding real lattice parameters for β^1-$Mn_3(PO_4)_2$ are listed in Table (V-2), together with those of β-$Zn_3(PO_4)_2$ and β^1-$Cd_3(PO_4)_2$ for comparison.

(ii) β^1-$Cd_3(PO_4)_2$

A small crystal of β^1-$Cd_3(PO_4)_2$ was mounted on a glass fibre and aligned on the Weissenberg camera with the c axis parallel to the rotation axis of the goniometer. The values of a* and b* were determined from a Weissenberg photograph, which was calibrated by superimposed rotation photographs of a TiO_2 crystal, by the same least squares procedure used for the β-$Zn_3(PO_4)_2$ parameters. Precession photographs of the 0kℓ and h0ℓ zones were taken, and these were measured to provide values for β, b* and c*. The c* values were corrected for film shrinkage by scaling to the value of b* obtained from the calibrated Weissenberg photograph, again assuming that any shrinkage was isotropic. The corresponding real lattice parameters are listed in Table (V-2) together with those of β-$Zn_3(PO_4)_2$ and β^1-$Mn_3(PO_4)_2$.

D. Intensity Data

(i) β^1-$Mn_3(PO_4)_2$

The same crystal for which the lattice parameters were determined was used in all intensity measurements. The h0ℓ plane was photographed on the Weissenberg camera using MoKα radiation and the hk0 and 0kℓ planes were recorded on film with the precession camera, also using MoKα radiation. Each plane was photographed for periods of 4, 12, and 36 hours, and, in the case of the 0kℓ photograph, 108 hours. The intensities of the reflections were estimated by visual intercomparison, using the logarithmic method.(34) The usual Lorentz and polarization corrections(12) were made to the data, but no corrections for absorption were applied.

(ii) β^1-$Cd_3(PO_4)_2$

As with β^1-$Mn_3(PO_4)_2$, the same crystal used in the lattice parameter measurements was used to collect all the intensity data. Precession photographs of the h0ℓ and 0kℓ zones were taken with MoKα radiation and the intensities estimated visually. The hk0 and hk3 planes were photographed on the Weissenberg camera. These photographs were used to determine the values of ω and ∅ for the reflections, whose intensities were measured on the diffractometer, using the technique described in Ch. III. For the hk0 measurements, the discriminator was operated in the threshold mode. As a result, the background level was quite high, and there were many weak reflections that, although clearly visible on the hk0 photograph, were obscured by the background. The intensities of these weak hk0 reflections were estimated visually, and assigned a separate scale constant. The usual Lorentz and polarization corrections were made to the data, but no corrections for absorption.

E. Superstructure in β^1-$Mn_3(PO_4)_2$ and β^1-$Cd_3(PO_4)_2$

In both β^1-$Mn_3(PO_4)_2$ and β^1-$Cd_3(PO_4)_2$ the reflections with

$\ell=0$ modulo 3 (0mod3) are, on the average, much weaker than those with $\ell\neq 0$mod3. This implies the existence of a translational sub-periodicity of $\underline{c}/3$. The gross structural features should therefore be very similar in the three adjacent "sub-cells" which together make up the true unit cell. The similarity between these β^1 structures and the structure of β-$Zn_3(PO_4)_2$ is apparent from the similarity between the intensities of the $\ell=0$mod3 reflections of the β^1 structures, and the β-$Zn_3(PO_4)_2$ reflections.

The position vectors of three identical atoms which are almost related by the translation vector $\underline{c}/3$ can be written as

$$\underline{R}_{jn} = \underline{r}_j + \underline{\varepsilon}_{jn} + n\underline{c}/3 \qquad \text{(V-4)}$$

where n identifies the particular sub-cell. The vector $\underline{r}_j$ is chosen so that

$$\sum_{n=0}^{2} \underline{\varepsilon}_{jn} = 0 \qquad \text{(V-5)}$$

For a centrosymmetric structure with this form of "tripling", the expression for the structure factor becomes, from Eqn. (II-5), assuming that the thermal motions are independent of n and have been incorporated into $f_j(H)$,

$$F(\underline{H}) = \sum_{j=1}^{N/3} f_j(H) \sum_{n=0}^{2} \cos 2\pi(\underline{H}.(\underline{r}_j+\underline{\varepsilon}_{jn}+n\underline{c}/3)) \qquad \text{(V-6)}$$

If the displacements $\underline{\varepsilon}_{jn}$ are sufficiently small, Eqn. (V-6) reduces to

$$F(\underline{H}) = \sum_{j=1}^{N/3} f_j(H)\left\{\cos 2\pi(\underline{H}\cdot\underline{r}_j)[1 + 2\cos\left(\frac{2\pi\ell}{3}\right) - 2\pi\underline{H}\cdot(\underline{\varepsilon}_{j1}-\underline{\varepsilon}_{j2})\sin\left(\frac{2\pi\ell}{3}\right)] \right.$$
$$\left. - \sin 2\pi(\underline{H}\cdot\underline{r}_j)[2\pi(\underline{H}\cdot\underline{\varepsilon}_{j0})(1 - \cos\left(\frac{2\pi\ell}{3}\right))]\right\} \qquad \text{(V-7)}$$

For those reflections where ℓ=0mod3,

$$F(\underline{H}) = 3\sum_{j=1}^{N/3} f_j(H) \cos 2\pi(\underline{H}.\underline{r}_j) \qquad \text{(V-8)}$$

Thus, if the displacements $\underline{\varepsilon}_{jn}$ are small enough, the average positions $\underline{r}_j$ can be obtained using only the ℓ=0mod3 data.

The practical restrictions on the magnitudes of $\underline{\varepsilon}_{jn}$ are not as severe as the analysis would indicate. As $|\underline{H}|$ becomes large, and the approximations leading to Eqn. (V-7) become more difficult to justify, the scattering factor, $f_j(H)$, decreases, and reflections with large values of $|\underline{H}|$ do not contribute heavily to the Patterson function. Thus the errors in the approximation will not as seriously affect the interpretation of the Patterson function.

The average intensity of the $\ell\neq$0mod3 reflections, compared to the ℓ=0mod3 reflections, was higher for $\beta^1 Mn_3(PO_4)_2$ than for β^1-$Cd_3(PO_4)_2$. This suggests that the displacements were smaller for the cations than for the other atoms in the structure, as the Cd^{++} ions make up a considerably greater fraction of the total scattering in $Cd_3(PO_4)_2$ than do the Mn^{++} ions in $Mn_3(PO_4)_2$. The $\ell\neq$0mod3 reflections were also much stronger in the h0ℓ layer, than in the 0kℓ, which suggests that the displacements $\underline{\varepsilon}_{jn}$ are predominantly in the $\underline{a}$ direction.

The solution of the β^1 structures was undertaken in two stages. First the "average" structure was determined using only the ℓ=0mod3 reflections, which were re-indexed with $\ell' = \ell/3$, and all calculations were performed in the sub-cell, referred to as the "small cell", with $\underline{c}'=\underline{c}/3$. The second stage was the determination of the displacements $\underline{\varepsilon}_{jn}$, and the refinement of the structure in the true unit cell (large cell), with all the data. These two stages are described in the following sections.

F. Solution of the Small Cell Structures

Patterson projections calculated in the small cell using the hk0 and h0ℓ' data of β^1-$Cd_3(PO_4)_2$ were successfully interpreted to yield a consistent set of coordinates for the three cations. The positions of the two phosphorus atoms and the eight oxygen atoms were determined by means of repeated electron density and difference syntheses, and least squares refinements of the atomic coordinates, in these two projections. The 0kℓ' and hk1 (hk3 in the large cell) data were then added to the refinement. The temperature factors (isotropic) of the oxygen atoms were unreasonably large, and, if physically meaningful, would imply thermal vibrations whose rms amplitudes were greater than 0.25 Å ($B_j > 5.0$). The effect of temperature factors of this magnitude is to sharply decrease the atoms' contributions to the scattering of all but the lowest angle reflections, essentially eliminating these atoms from the trial structure. The value of the least squares residual R_2 under these conditions, and with unit weights, was 0.20 .

The 0kℓ' Patterson of β^1-$Mn_3(PO_4)_2$ was also interpreted, yielding y and z coordinates for the cations which essentially agreed with those found for the Cd^{++} ions. All the atoms were than successfully located in this projection. Taking the x coordinates from β^1-$Cd_3(PO_4)_2$, the β^1-$Mn_3(PO_4)_2$ refinement was continued in the small cell. As before, the temperature factors on the oxygen atoms did not correspond to physically meaningful thermal vibrations.

The inability to obtain reasonable thermal parameters for the oxygen atoms in both structures by means of the least squares procedure was attributed to the approximations inherent in using the ℓ=0mod3 data only. This was further emphasized by the gross irregularity of the PO_4 tetrahedra, especially in β^1-$Mn_3(PO_4)_2$. It was now necessary to determine the displacements $\underline{\epsilon}_{jn}$ for the atoms, and continue the refinement of the structure in the large cell.

G. Solution and Refinement of the Large Cell Structures

As the $\ell\neq$0mod3 reflections were stronger for β^1-$Mn_3(PO_4)_2$ than for β^1-$Cd_3(PO_4)_2$, the solution of the large cell structure was undertaken with the β^1-$Mn_3(PO_4)_2$ data. There were a few h0ℓ reflections with $\ell\neq$0mod3 that were fairly strong, and for the larger values of $|\underline{H}|$, their average intensity approached that of the ℓ=0mod3 reflections. Using the absolute scaling provided by the small cell refinement, unitary structure factors were calculated for all the h0ℓ reflections, using Eqn. (II-11). The thermal correction term, $\exp(-\underline{H}.\underline{\underline{\beta}}_j.\underline{H})$, in that equation was calculated using the isotropic temperature factors from the small cell refinement, although these temperature factors were too large, as they were trying to correct for the actual atom displacements. The effects of thermal vibrations and positional disorder are similar, especially when the displacements are small and in random directions. The effect of using too large a thermal correction was to erroneously increase the values of the unitary structure factors calculated for the high angle reflections.

As a result, some of the conclusions regarding the phases were not absolutely correct, but only had a fairly high probability of being so(16).

The reflections were listed in order of decreasing values of $|U_{\underline{H}}|$, in two groups, ℓ=0mod3 and $\ell\neq$0mod3. The signs for the reflections in the first group had already been determined by the solution of the small cell structure. The inequality relationships of Eqn. (II-12) were used with $U_{\underline{H}}$ taken from the first group of reflections, and $U_{\underline{H}'}$ from the second group, starting with the largest values of $|U_{\underline{H}}|$ and $|U_{\underline{H}'}|$. The signs of 13 of the larger $U_{\underline{H}'}$ were related by this procedure, in terms of a parameter "p", which could be ±1. Two additional signs were determined, irrespective of the choice for p.

In order to determine p, the electron density was calculated around the average cation positions, using these 15 reflections, first with p=+1 and then with p=-1. This electron density was treated as though it were a difference synthesis, where a slightly incorrect atomic position is indicated by an electron density gradient. It was thereby possible to shift the nine cations away from their corresponding small cell positions. The new positions determined in this manner for both choices of p were then used to calculate structure factors for all the h0ℓ data. The calculation for p=+1 yielded an R_2 value of 0.55, while p=-1 gave a value of 0.59. The number of the 15 original reflections whose structure factors were calculated to have a sign opposite to the sign predicted from the inequality relationships were 1 and 3, for p=+1 and p=-1 respectively. On these bases, it was assumed that p=+1 was more likely correct, and the large cell refinement continued with this assumption.

The phosphorus and oxygen atoms were introduced into the structure by being placed near their small cell positions, and their coordinates were refined by least squares. During these refinements, the temperature factors of the oxygen atoms were not varied, and only a fraction, usually 1/2 or 1/4, of the calculated shifts of the coordinates were actually applied. After each cycle of refinement, the geometries of the PO_4 tetrahedra were inspected, and the oxygen atom positions readjusted if the irregularities were excessive. At several stages, the temperature factors of the oxygen atoms were allowed to vary, in order to determine if the orientations of the PO_4 tetrahedra were correct. If a tetrahedron was incorrectly oriented, the temperature factors of all its oxygen atoms would increase sharply, effectively eliminating these atoms from the trial structure in an attempt to provide better agreement with the measured data. When this happened, the offending atoms were removed, and a difference synthesis calculated. The atoms were replaced as indicated by this synthesis, and further cycles of least squares refinements undertaken.

Eventually, all the atoms were more or less correctly located by this procedure, but the geometries of the PO_4 groups were still highly irregular. It was noted that, on the average, the $|F_c|$ values for the $\ell \neq 0 \bmod 3$ reflections were too small, which indicated that the displacements $\underline{\varepsilon}_{jn}$ were too small in magnitude. The weighting scheme was then changed from unit weights on all reflections to a scheme whereby the $\ell\neq0$mod3 reflections received unit weights and the $\ell=0$mod3 reflections received a lower weight. This weight was lowered progressively to 0.75 over several least squares cycles. The desired effect, that of emphasizing the displacements from the average positions, was realized, and the atoms (particularly the oxygen atoms) underwent significant shifts in position. The geometry of the PO_4 groups was now more regular, and the reliability indices which had formerly been 0.10 and 0.23 for the $\ell=0$mod3 and $\ell\neq0$mod3 reflections respectively, became 0.09 and 0.13.

At this stage it seemed desirable to further test the original choice of signs for the $\ell\neq0$mod3 reflections (p=+1). The displacements $\underline{\varepsilon}_{jn}$ were reversed, which, by Eqn. (V-7), reverses the signs of these reflections while leaving the $|F_c|$ values of the $\ell=0$mod3 reflections unchanged. Also, the intensities of the $hl\ell$ reflections were measured from a Weissenberg photograph, using the diffractometer-measured β-$Zn_3(PO_4)_2$ $hl\ell$ intensities as an intensity standard, and Lorentz and polarization corrections applied. It was felt that the $\ell\neq0$mod3 reflections in the $hl\ell$ data should provide a reliable check on the validity of the $\underline{\varepsilon}_{jn}$ found for the p=+1 solution.

Structure factors were calculated for all of the data, for both the determined displacements and for the reversed displacements. The R-factors for these two calculations are summarized in Table(V-3). From the agreements shown in this table, the conclusion can be drawn that the initial choice of signs (p=+1) and the resulting displacements $\underline{e}_{jn}$ are indeed correct.

TABLE (V-3)

Residuals for the cases where p=+1 and p=-1 in $\beta\overset{1}{-}Mn_3(PO_4)_2$

Class of reflections	R_2 (p=+1)	R_2 (p=-1)
ℓ = 0mod3	0.09	0.13
$\ell \neq$ 0mod3	0.15	0.43
all reflections	0.11	0.21

TABLE (V-4)

Residuals for $\beta\overset{1}{-}Mn_3(PO_4)_2$ and $\beta\overset{1}{-}Cd_3(PO_4)_2$

		$\beta\overset{1}{-}Mn_3(PO_4)_2$		$\beta\overset{1}{-}Cd_3(PO_4)_2$	
Residual	Conditions	# refl.	Residual value	# refl.	Residual value
R_2	all reflections	1289	0.125	1065	0.109
R_1	all reflections	1289	0.089	1065	0.104
R_2	obs. refl. only	878	0.119	728	0.107
R_1	obs. refl. only	878	0.085	728	0.079

The weighting scheme was again changed to the "Cruickshank" method, and the weights were calculated according to the equation

$$w_i^{-1} = 30.0 - 0.25|F_o|_i + 0.0075|F_o|_i^2 \qquad \text{(V-9)}$$

A final three cycles with this weighting brought the value of R_2 for all the data to 0.125.

The final values for the atomic parameters of β^1-$Mn_3(PO_4)_2$ are listed with their esd's in Table (V-5), and the reliability indices are summarized in Table (V-4). The observed and calculated structure factors are listed in Table (V-6), where the unobserved reflections are marked with an asterisk (*), and the unreliable reflections with the symbol Ø.

The atomic positions of β^1-$Mn_3(PO_4)_2$ were used with the β^1-$Cd_3(PO_4)_2$ data. Least squares refinement of the parameters was carried out in the same general manner as for β^1-$Mn_3(PO_4)_2$.[†] The final weighting scheme was

$$w_i^{-1} = 25.0 + |F_o|_i + 0.005|F_o|_i^2 \qquad \text{(V-10)}$$

and the final value of R_2 for all the data was 0.109 .

The final values for the atomic parameters of β^1-$Cd_3(PO_4)_2$ are also listed in Table (V-5), and the reliability indices in Table (V-4), together with those of β^1-$Mn_3(PO_4)_2$. Table (V-7) contains the list of observed and calculated structure factors, where the unobserved and unreliable reflections are marked as indicated above.

[†] Individual temperature factors were not determined for the atoms by least squares refinement, but were set to the isotropic values determined for the corresponding atoms in β^1-$Mn_3(PO_4)_2$.

TABLE (V-5)

Atomic parameters for β^1-$Mn_3(PO_4)_2$ and β^1-$Cd_3(PO_4)_2$

	β^1-$Mn_3(PO_4)_2$				β^1-$Cd_3(PO_4)_2$		
Atom	x	y	z	B(Å^2)	x	y	z
M(1A)	-.0041(6)	0.0944(7)	0.0599(2)	0.73(8)	-.0001(6)	0.0931(5)	0.0610(2)
M(1B)	0.0085(6)	0.0853(8)	0.7164(2)	0.75(8)	0.0098(6)	0.0894(5)	0.6194(2)
M(1C)	-.0064(6)	0.1058(7)	0.3932(2)	0.78(8)	-.0032(7)	0.1029(4)	0.3918(2)
M(2A)	0.2981(6)	0.3858(6)	0.0758(2)	0.77(7)	0.2956(7)	0.3949(5)	0.0771(2)
M(2B)	0.2875(6)	0.3891(7)	0.7435(2)	0.80(7)	0.3008(7)	0.3961(5)	0.7477(2)
M(2C)	0.3109(6)	0.3881(7)	0.4167(2)	0.81(8)	0.3136(6)	0.3952(5)	0.4159(2)
M(3A)	0.4033(6)	-.2194(7)	0.1407(2)	0.70(8)	0.3890(6)	-.2120(5)	0.1368(2)
M(3B)	0.3975(6)	-.2032(9)	0.7966(2)	0.72(7)	0.3910(6)	-.2023(6)	0.7956(2)
M(3C)	0.4121(6)	-.2172(8)	0.4573(2)	0.82(8)	0.4061(6)	-.2122(6)	0.4569(2)
P(1A)	0.3608(10)	0.0561(12)	0.0609(3)	0.78(13)	0.3615(26)	0.0648(20)	0.0584(8)
P(1B)	0.3704(9)	0.0661(12)	0.7188(3)	0.40(12)	0.3676(24)	0.0724(20)	0.7214(8)
P(1C)	0.3614(10)	0.0767(12)	0.3944(3)	0.90(13)	0.3635(27)	0.0803(20)	0.3941(9)
P(2A)	0.1264(10)	-.3539(10)	-.0009(3)	0.74(11)	0.1261(27)	-.3523(17)	0.0022(9)
P(2B)	0.1205(10)	-.3689(10)	0.6718(3)	0.73(11)	0.1272(28)	-.3635(19)	0.6737(8)
P(2C)	0.1392(10)	-.3551(10)	0.3310(3)	0.86(12)	0.1309(27)	-.3591(20)	0.3330(8)
O(1A)	0.1662(28)	0.0203(29)	0.0209(9)	1.03(33)	0.1664(72)	0.0313(50)	0.0234(23)
O(1B)	0.1713(24)	0.0347(28)	0.6751(8)	0.83(29)	0.1825(64)	0.0425(52)	0.6800(21)
O(1C)	0.1711(28)	0.0304(31)	0.3615(9)	1.30(36)	0.1765(72)	0.0355(54)	0.3619(23)
O(2A)	0.1881(33)	-.3492(34)	0.0714(11)	1.83(46)	0.1776(68)	-.3461(60)	0.0725(25)
O(2B)	0.1344(28)	-.4222(32)	0.7339(9)	1.38(38)	0.1477(73)	-.4096(52)	0.7525(23)
O(2C)	0.1628(28)	-.4329(32)	0.3891(9)	0.79(37)	0.1525(66)	-.4267(40)	0.3915(22)
O(3A)	0.4734(26)	-.0688(28)	0.0968(8)	0.81(30)	0.4563(57)	-.0564(41)	0.0958(21)
O(3B)	0.4773(24)	-.0523(28)	0.7561(7)	0.63(29)	0.4870(54)	-.0429(48)	0.7608(19)
O(3C)	0.4847(27)	-.0424(29)	0.4288(9)	0.89(34)	0.4781(61)	-.0364(50)	0.4276(21)

(continued)

TABLE (V-5) concluded

	$\beta\overset{1}{-}Mn_3(PO_4)_2$				$\beta\overset{1}{-}Cd_3(PO_4)_2$		
Atom	x	y	z	B($\mathring{A}^2$)	x	y	z
O(4A)	0.2373(33)	-.2635(36)	-.0149(10)	1.38(42)	0.2493(67)	-.2550(48)	-.0045(23)
O(4B)	0.2621(28)	-.2581(31)	0.6902(9)	1.09(35)	0.2649(66)	-.2526(45)	0.6887(23)
O(4C)	0.2755(29)	-.2451(34)	0.3542(9)	1.33(35)	0.2520(71)	-.2450(47)	0.3478(23)
O(5A)	0.4290(31)	0.1072(32)	0.0169(9)	1.32(40)	0.4245(66)	0.1109(54)	0.0196(24)
O(5B)	0.4443(27)	0.1161(28)	0.6771(8)	1.03(31)	0.4511(60)	0.1103(50)	0.6824(22)
O(5C)	0.3982(28)	0.1366(30)	0.3446(9)	1.33(36)	0.4075(65)	0.1330(52)	0.3491(24)
O(6A)	0.1359(23)	-.5028(26)	-.0192(8)	0.84(28)	0.1449(54)	-.4912(47)	-.0172(19)
O(6B)	0.1660(29)	-.4840(34)	0.6423(10)	1.44(41)	0.1740(67)	-.4669(53)	0.6368(24)
O(6C)	0.1735(31)	-.4392(33)	0.2862(10)	1.51(42)	0.1705(66)	-.4448(52)	0.2944(24)
O(7A)	0.3880(27)	0.1761(28)	0.1083(8)	0.91(32)	0.3946(68)	0.1780(43)	0.1042(23)
O(7B)	0.3841(31)	0.1857(31)	0.7634(9)	1.34(38)	0.3903(71)	0.1816(56)	0.7606(23)
O(7C)	0.3873(31)	0.1886(31)	0.4418(10)	0.75(38)	0.3739(60)	0.1864(45)	0.4443(22)
O(8A)	0.0619(28)	0.2982(38)	0.0433(9)	0.95(36)	0.0471(70)	0.3037(64)	0.0403(23)
O(8B)	0.0505(27)	0.3023(30)	0.6249(9)	1.30(33)	0.0631(65)	0.3108(51)	0.6248(24)
O(8C)	0.0465(33)	0.2917(46)	0.2947(10)	1.07(43)	0.0448(70)	0.2983(66)	0.2973(24)

TABLE V-6 $\beta'-Mn_3(PO_4)_2$ OBSERVED AND CALCULATED STRUCTURE FACTORS (x10)

UNOBSERVED REFLECTIONS ARE MARKED WITH AN ASTERISK (•), AND UNRELIABLE REFLECTIONS WITH THE SYMBOL (@).

			|FOBS|	FCALC
K	L			H=0
2	0		247	229
4	0		2791	-2625
6	0		3011	-2902
8	0		318	360
10	0		1598	1431
12	0		986	-837
14	0		153	272
2	1		431	-300
3	1		617	564
4	1		328	378
5	1		429	-360
6	1		384	330
7	1		357	-375
8	1		479	-419
9	1		224	-232
10	1	•	146	150
11	1	•	146	165
12	1		347	-399
2	2	•	100	-52
3	2		158	-206
4	2		162	133
5	2		633	-596
6	2		493	425
7	2		586	-549
8	2		686	735
9	2		250	302
10	2		146	64
11	2		361	322
12	2	•	140	10
1	3	•	110	12
2	3		430	-378
3	3		2947	2728
4	3		2155	-2117
5	3		3216	-2914
6	3	•	217	122
7	3	•	231	101
8	3		494	-476
9	3		729	-681
10	3		2161	1956
11	3		1174	1033
12	3	•	242	254
13	3		213	-240
0	4	•	83	-12
1	4	•	91	-53
2	4		273	229
3	4		874	823
4	4		286	253
5	4		574	-542
6	4	•	126	28
7	4		219	297
8	4		584	-521
9	4		602	-601
10	4	•	146	20
11	4		252	-230
12	4		241	192
13	4		210	92
1	5	•	99	-90
2	5		184	-165
3	5		872	-817
4	5		324	-337
5	5		300	173
6	5	•	127	-189
7	5		290	291
8	5	•	140	71
9	5		637	569
10	5		227	-241
11	5	•	162	-39
12	5	•	163	-225
13	5		619	-697
0	6		2219	-2205
1	6		4479	-4331
2	6		2167	-2041
3	6		1833	-1879
4	6		2967	2650
5	6		1965	-1901
6	6		2104	2224
7	6		701	699
8	6		773	688
9	6		1455	1384
10	6		1318	-1249
11	6		886	-900
12	6	•	237	-115
13	6		434	449
2	7		893	800
3	7	•	103	42
4	7		397	344
5	7		188	174
6	7		223	-217
7	7		455	-293
8	7		658	-613
9	7	•	162	169
10	7		578	568
11	7	•	161	-111
12	7	•	151	38
13	7		364	368
0	8		858	-762
1	8	•	93	-17
2	8		458	421
3	8		106	179
4	8		629	548
5	8		389	333
6	8		297	235
7	8		637	599
8	8	•	167	155
9	8		424	-380
10	8	•	163	-174
11	8	•	169	-68
12	8		473	472
13	8		344	-390
1	9		1097	-1152
2	9		1033	-1064
3	9		433	-437
4	9		2837	-2597
5	9		2706	2477
6	9		2858	2525
7	9	•	239	-241
8	9		563	-587
9	9	•	252	257
10	9	•	253	-289
11	9	•	247	-246
12	9		740	-748
13	9		821	-810
0	10		219	-185
1	10		598	-512
2	10		657	550
3	10		176	95
4	10		868	-871
5	10	•	142	-119
6	10	•	149	-129
7	10		335	256
8	10		346	-318
9	10		227	242
10	10	•	163	110
11	10		244	257
12	10		406	451
1	11		490	-398
2	11		466	-439
3	11		253	-164
4	11		676	553
5	11		279	194
6	11	•	151	-180
7	11		230	-181
8	11		357	351
9	11	•	163	-166
10	11		754	-659
11	11	•	173	-61
12	11		575	-574
0	12		255	259
1	12		231	238
2	12		1232	1217
3	12		2920	2736
4	12		2734	-2647
5	12		648	626
6	12		572	603
7	12		1424	-1433
8	12		2081	1983
9	12		627	-577
10	12		751	-700
11	12		369	-303
12	12		315	-298
1	13		334	317
2	13		489	-456
3	13	•	139	-47
4	13		388	-326
5	13		342	-334
6	13	•	155	126
7	13		535	-533
8	13		515	499
9	13		825	848
10	13	•	160	-25
11	13		186	84
0	14		1094	1006
1	14		636	647
2	14	•	139	31
3	14		309	272
4	14		356	326
5	14		190	163
6	14		379	-331
7	14	•	161	-30
8	14		372	-352
9	14		679	-675
10	14	•	159	-17
11	14		225	304
1	15	•	220	73
2	15		2121	2182
3	15	•	228	141
4	15		1791	1797
5	15		724	767
6	15		875	-893
7	15		1978	-1898
8	15		1031	-1067
9	15		776	718
10	15		430	-333
11	15		290	293
0	16	•	146	137
1	16	•	146	64
2	16	•	148	-148
3	16		703	-639
4	16		352	-304
5	16	•	167	145
6	16		368	369
7	16	•	193	265
8	16		284	286
9	16		457	434
10	16	•	169	-123
1	17		405	455
2	17		237	182
3	17		268	350
4	17		186	-212
5	17		1099	-1096
6	17		662	-754
7	17	•	174	98
8	17	•	182	100
9	17		451	-423
10	17		267	309
0	18		720	693
1	18		384	377
2	18		958	892
3	18		1548	-1639
4	18		1130	-1179
5	18	•	253	160
6	18		365	-357
7	18		616	700
8	18		677	-796
9	18		580	-559
10	18		556	-564
1	19		740	-754
2	19	•	169	-14
3	19		485	555
4	19		352	405
5	19		651	691
6	19		329	-380
7	19		205	220
8	19		248	265
9	19		380	-425
10	19		178	-168
0	20		461	432
1	20		756	-790
2	20		896	-895
3	20		581	-642
4	20		554	577
5	20		693	-747
6	20	•	195	-185
7	20	•	172	-120
8	20		420	-471
9	20		377	355
10	20		212	330
1	21		524	589
2	21		2380	-2713
3	21		359	376
4	21		607	-618
5	21		542	-623
6	21	•	256	17
7	21		467	-602
8	21		1173	1349
9	21		259	306
0	22		361	-386
1	22		342	408
2	22		503	-538
3	22	•	177	157
4	22		438	528
5	22		339	429
6	22	•	171	106
7	22	•	163	118
8	22	•	154	105
9	22		243	-328
1	23		565	-595
2	23		222	-208
3	23	•	187	-36
4	23		865	-795
5	23		227	-247
6	23		588	722
7	23		865	956
8	23	•	127	-8
0	24	•	188	197
1	24	•	222	206
2	24		739	-695
3	24		557	-486
4	24		548	-535
5	24		233	-250
6	24		511	524
7	24	•	149	43
1	25	•	258	282
2	25		444	376
3	25	•	276	121
4	25		322	337
5	25		340	-401
6	25		163	-151
0	26		796	-684
1	26		570	-594
2	26		628	-526
3	26		719	660
4	26	•	163	-30
5	26	•	145	70
6	26		219	290
1	27		1514	-1506
2	27		440	642
3	27		719	856
4	27	•	142	150
0	28		1113	1191
1	28	•	143	57
2	28	•	183	160
3	28		239	360
H	L			K=0
2	0		1271	1209
3	0		3030	2814
4	0		1249	-1309
5	0		2290	2098
6	0		1250	1168
7	0		2614	2671
8	0		1424	1458
9	0		608	-517
10	0		1495	1393
2	2	•	170	-127
3	2	•	203	-139
4	2	•	233	9
5	2		667	-673
6	2	•	330	269
7	2	•	362	8
8	2		539	-438
9	2		594	546
3	-2	•	170	92
4	-2	•	201	15
5	-2		306	366
6	-2	•	256	245
7	-2	•	297	-102
8	-2		412	-457
9	-2		852	762
10	-2	•	435	-110
11	-2	•	467	12
12	-2		621	649
13	-2	•	527	-66
1	4		498	476
2	4		313	-301
3	4	•	220	165
4	4	•	282	135
5	4	•	314	-10
6	4		680	-568
7	4	•	377	113
8	4	•	409	289
9	4	•	442	43
3	-4		1100	-1175
4	-4	•	195	39
5	-4		853	-857
6	-4		407	-508
7	-4	•	288	254
8	-4	•	316	298
9	-4	•	392	-124
10	-4		658	-667
11	-4	•	457	-2
12	-4	•	489	-529
13	-4	•	518	-463
0	6		2601	-2205
1	6		489	505
2	6		1660	-1498
3	6		2203	-2037
4	6		3758	-3608
5	6		797	756
6	6		1305	-1253
7	6		865	-852
8	6		969	857
9	6		685	-619
1	-6		1829	1871
2	-6		1860	1698
3	-6		7241	-6019
4	-6		285	-239
5	-6		517	378
6	-6		2129	-2263
7	-6		1124	1281
8	-6		610	-580
9	-6		924	1005
10	-6		1640	-1625
11	-6		1419	-1238
12	-6		1016	922
13	-6		1740	-1607
0	8		769	-762
1	8		400	363
2	8	•	231	-131
3	8		1104	-1173
4	8	•	320	313
5	8	•	349	277
6	8	•	380	-333
7	8	•	411	-20
8	8	•	443	399
9	8	•	474	196
1	-8		274	253
2	-8		715	-755
3	-8		685	-723
4	-8		821	-798
5	-8		1301	-1227
6	-8	•	242	-139
7	-8	•	279	-3
8	-8		367	-380
9	-8		893	-984
10	-8		558	-572
11	-8	•	440	-289
12	-8	•	472	-493
13	-8	•	502	62
0	10	•	202	-185
1	10		1456	1378
2	10		567	682
3	10	•	312	-12
4	10	•	340	-186
5	10	•	369	77
6	10	•	399	360
7	10	•	429	-373
8	10	•	461	95
9	10	•	491	252
1	-10		450	500
2	-10		275	-251
3	-10		867	832
4	-10		877	894
5	-10	•	223	81
6	-10		1296	1315
7	-10	•	278	-211
8	-10		961	930
9	-10		933	963
10	-10	•	403	-18
11	-10	•	434	367
12	-10	•	465	-341
13	-10	•	496	536
0	12	•	224	239
1	12		974	997
2	12		2938	-2858
3	12		790	-708
4	12		475	508
5	12		2971	-3196
6	12		887	814
7	12	•	449	130
8	12	•	479	-198
9	12	•	508	198
1	-12		2428	-1477
2	-12		2234	-1949
3	-12		1412	-1455
4	-12		288	-248
5	-12		3105	-3067
6	-12		554	537
7	-12		1539	1421
8	-12		815	-801
9	-12		517	524
10	-12	•	401	65
11	-12	•	430	-454
12	-12		994	-965
13	-12	•	490	490
0	14		939	1006
1	14	•	273	-307
2	14	•	332	95
3	14	•	357	303
4	14	•	383	317
5	14	•	411	124
6	14	•	439	170
7	14	•	468	186
8	14	•	497	-329
9	14	•	524	94
1	-14	•	243	40
2	-14		479	-499
3	-14		1849	1967
4	-14		904	-976
5	-14		1112	1136
6	-14		512	498
7	-14	•	323	-223
8	-14		968	942
9	-14		789	-701
10	-14		587	708
11	-14	•	428	231
12	-14	•	457	175
13	-14	•	487	625
0	16	•	283	137
1	16	•	334	186
2	16	•	355	177
3	16		547	-559
4	16		812	713
5	16	•	432	-446
6	16	•	460	-339
7	16	•	488	163
8	16	•	515	-190
9	16	•	539	79
1	-16	•	265	84
2	-16		1137	-1167
3	-16		439	478
4	-16		360	-378
5	-16		965	-997
6	-16		589	518
7	-16	•	331	25
8	-16		719	634
9	-16	•	376	-367
10	-16	•	401	-88
11	-16	•	428	-244
12	-16	•	456	-394
13	-16	•	484	-251
0	18		774	693
1	18		555	540
2	18		2453	2281
3	18	•	428	162
4	18	•	428	-110
5	18		1035	1118
6	18		1097	1077
7	18	•	508	280
8	18		856	704
9	18		1483	1171
1	-18		3205	3318
2	-18		608	685
3	-18		496	415
4	-18		971	-941
5	-18		1229	1289
6	-18		926	870
7	-18		777	-721
8	-18		3746	3427
9	-18	•	381	402
10	-18		782	-692
11	-18		980	1185
12	-18	•	456	236
13	-18	•	483	-87
0	20		344	432
1	20	•	382	-305
2	20		901	928
3	20	•	453	276
4	20	•	451	-336
5	20		904	732
6	20		660	-632
1	-20		840	-851
2	-20		320	332
3	-20		755	847
4	-20		348	307
5	-20		1363	1259
6	-20		608	-516
7	-20		721	643
8	-20	•	369	183
9	-20		625	-494
10	-20		837	821
11	-20	•	433	156
12	-20		699	841
13	-20	•	484	-47
0	22		457	-386
1	22	•	406	-273
2	22	•	427	104
3	22	•	478	-345
6	22	•	521	-130
1	-22	•	353	-104
2	-22	•	342	-116
3	-22		836	-850
4	-22		813	-848
5	-22	•	332	-67
6	-22		1310	-1291
7	-22	•	367	265
8	-22	•	381	-9
9	-22	•	397	-292
10	-22	•	417	-59
11	-22		947	-1068
12	-22	•	462	-307
13	-22	•	487	-259
0	24	•	594	197
1	24	•	430	-85
2	24	•	451	-4
3	24		1643	-1175
6	24		883	-777
1	-24	•	376	-200
2	-24		1197	-1091
3	-24		842	933
4	-24		1466	-1366
5	-24		1726	-1754
6	-24	•	354	204
7	-24	•	382	37
8	-24		1319	-1417
9	-24	•	409	215
10	-24	•	426	242
11	-24		1115	-1334
12	-24		687	-749
13	-24	•	491	289
0	26		564	-684
1	26	•	455	215
2	26		1620	-1149
3	26	•	496	647
1	-26		1071	-1083
2	-26	•	387	242
3	-26		1015	-1064
4	-26		578	570
5	-26		756	-767
6	-26		1391	-1304
7	-26	•	399	283
8	-26		1613	-1685
9	-26	•	421	-32
10	-26	•	437	-301
11	-26		1018	-1220
12	-26	•	475	439
13	-26		959	-911
0	28		1032	1191
1	28	•	479	308
1	-28	•	422	-197
2	-28	•	409	387
3	-28		732	474
4	-28	•	393	-118
5	-28	•	390	364
6	-28		1090	1018
7	-28		602	552
8	-28		448	507
9	-28	•	435	436
10	-28	•	449	346
11	-28		635	659
0	30	•	459	-39
1	-30	•	444	283
2	-30		635	569
3	-30		963	-853
4	-30	•	415	-93
5	-30		561	594
6	-30		711	-694
7	-30	•	436	145
8	-30		1375	1355
9	-30		593	-585
10	-30	•	463	99
11	-30	•	477	343
0	32		746	-716
1	-32	•	467	317
2	-32	•	454	299
3	-32	•	444	23
4	-32		1052	1017
6	-32		507	496
7	-32	•	455	-398
9	-32	•	467	432
10	-32	•	477	-429
11	-32		1136	1271
0	34	•	500	-83
1	-34	•	488	405
2	-34	•	476	-85
3	-34		648	-607
6	-34	•	450	-209
7	-34	•	475	350
9	-34	•	484	345
0	36	•	517	482
1	-36	•	506	22
2	-36	•	496	124
3	-36		715	692
6	-36		729	821
7	-36	•	495	347
9	-36	•	501	593
1	-38	•	521	340
2	-38		782	-680
3	-38		813	799
6	-38		1176	1083
7	-38		798	-770
9	-38	•	517	286
9	-40	•	533	16
9	-42	•	547	-479
9	-44		966	-796
H	K			L=0
1	0		465	-473
2	0		1349	1209
3	0		2879	2814
4	0		1246	-1309
5	0		2064	2098
6	0		1176	1168
7	0		2594	2671
8	0		1415	1458
9	0		564	-517
10	0		1389	1393
1	1		495	508
2	1		1384	1280
3	1		1444	1332

TABLE V-6 (CONCLUDED)

			|FOBS|	FCALC
4	1		3213	-2799
5	1	•	196	-69
6	1	•	215	-68
7	1		1421	-1504
8	1		527	614
9	1	•	247	106
10	1		754	676
0	2		209	229
1	2		2208	1904
2	2	•	142	-207
3	2		989	-899
4	2		1109	1045
5	2		790	-823
6	2		3044	2880
7	2	•	234	-194
8	2	•	245	288
9	2		626	603
10	2		559	-441
1	3		4301	-3663
2	3		5697	5095
3	3	•	174	160
4	3		602	-629
5	3	•	206	-33
6	3	•	222	-275
7	3		568	654
8	3		867	-934
9	3		862	904
10	3	•	209	275
0	4		3112	-2625
1	4		1770	-1695
2	4	•	178	-162
3	4		2772	-2249
4	4		1099	-1167
5	4		1346	1282
6	4		1641	-1690
7	4		1545	-1582
8	4		474	-422
9	4		1114	-1069
10	4		701	-708
1	5		568	507
2	5		2174	-1874
3	5		485	-518
4	5	•	211	-276
5	5		1601	1591
6	5		403	-461
7	5		685	105
8	5		527	601
9	5		1137	-1031
0	6		3546	-2902
1	6	•	205	39
2	6		822	-769
3	6		3517	-2639
4	6		2157	-1712
5	6		687	-778
6	6		839	-835
7	6		812	-671
8	6		491	-518
9	6	•	216	-424
1	7		619	633
2	7		998	-946
3	7		793	-823
4	7		768	750
5	7	•	235	240
6	7		1471	-1284
7	7		581	652
8	7	•	232	184
9	7		752	-724
0	8		395	360
1	8		854	909
2	8		1489	-1292
3	8	•	233	-148
4	8		858	911
5	8		1386	-1534
6	8	•	240	38
7	8		1445	1513
8	8		486	-533
1	9		456	503
2	9		637	581
3	9	•	238	210
4	9		643	626
5	9	•	240	-258
6	9	•	236	-94
7	9	•	222	-186
8	9		330	-319
0	10		1470	1431
1	10	•	240	220
2	10		848	832
3	10		1828	1914
4	10		940	920
5	10		701	823
6	10	•	222	29
7	10		1016	1058
1	11		716	-743
2	11		1046	-930
3	11		1219	1199
4	11		651	-723
5	11	•	217	-292
6	11		1415	1448
0	12		813	-837
1	12		855	948
2	12	•	226	234
3	12	•	219	108
4	12		581	638
5	12		291	316
1	13		332	-594
3	13		547	-598
H	L			K=1
2	0		1035	1280
3	0		1106	1332
4	0		2458	-2799
5	0	•	226	-69
6	0	•	252	-68
7	0		1415	-1504
8	0		606	614
9	0	•	329	106
10	0		710	676
11	0	•	381	-9
12	0	•	405	-264
13	0		853	666
14	0		685	-674
2	1	•	206	-107
2	1	•	160	-107
3	1		194	263
4	1		224	-240
5	1	•	253	166
6	1		608	621

			|FOBS|	FCALC
7	1		505	492
8	1	•	338	9
3	-1	•	209	-138
4	-1	•	213	-93
5	-1	•	242	86
6	-1	•	271	-223
7	-1		572	-597
8	-1		353	-320
9	-1	•	410	-22
10	-1	•	443	-256
11	-1	•	476	-138
3	2	•	184	2
4	2		353	-377
5	2		519	566
6	2	•	288	119
7	2	•	315	-184
8	2	•	343	138
4	-2	•	208	7
5	-2		495	-494
6	-2	•	266	-54
7	-2		360	-416
8	-2	•	322	-49
9	-2	•	404	64
10	-2	•	437	-42
11	-2	•	470	-104
2	3		1493	1770
3	3		382	-471
4	3		2174	2765
5	3		1537	1735
6	3		679	-709
7	3		322	369
8	3		639	667
9	3		618	-619
10	3		498	495
11	3		970	902
3	-3		3869	4053
4	-3		748	-797
5	-3		715	730
6	-3		1997	2347
7	-3		870	-898
8	-3		608	-663
9	-3		1263	1315
10	-3		483	-447
11	-3		520	596
12	-3		527	544
2	4	•	172	57
3	4	•	198	147
4	4	•	246	-138
5	4	•	273	-150
6	4		521	574
7	4	•	328	-226
8	4	•	356	-307
3	-4	•	158	-77
4	-4	•	203	64
5	-4		566	518
6	-4		762	774
7	-4	•	286	-233
8	-4		513	484
9	-4	•	395	-71
10	-4		427	-380
11	-4	•	460	238
0	5	•	133	-90
2	5		472	-517
3	5		226	-196
4	5		274	245
5	5	•	280	-77
6	5	•	308	38
7	5	•	335	210
8	5	•	363	-114
9	5		423	-348
4	-5	•	201	-219
5	-5	•	229	-27
6	-5		627	-636
7	-5	•	283	-185
8	-5	•	310	-48
9	-5	•	390	-30
10	-5	•	423	-42
11	-5	•	455	-323
0	6		4338	-4331
1	6		2832	3059
2	6		3023	-3016
3	6		1449	-1603
4	6		1067	1243
5	6		1822	-2252
6	6		446	-440
7	6		1046	-1138
8	6	•	370	237
11	6		582	613
1	-6		2498	-2867
2	-6		1554	-1489
3	-6		1759	-1767
4	-6		1121	-1195
5	-6		1609	-1652
6	-6		1304	1372
7	-6	•	281	-85
8	-6		972	-1037
9	-6	•	386	320
10	-6		936	-979
11	-6	•	451	-320
0	7	•	158	-156
1	7	•	178	-117
2	7	•	200	98
3	7		244	-298
4	7		330	302
5	7	•	296	282
6	7	•	323	-164
7	7	•	350	-60
8	7	•	378	65
1	-7		323	-237
2	-7		614	642
3	-7		615	509
4	-7		468	439
5	-7	•	227	137
6	-7	•	253	-8
7	-7	•	279	58
8	-7	•	305	-69
9	-7	•	383	-287
10	-7		549	512
11	-7	•	447	220
0	8	•	170	-17
1	8		394	-411
2	8		264	333
3	8	•	231	77
4	8	•	278	-54
5	8	•	304	252
6	8	•	382	-391
7	8	•	358	232
8	8	•	385	27

			|FOBS|	FCALC
1	-8	•	201	-210
2	-8	•	158	81
3	-8		829	696
4	-8		1296	-1215
5	-8		617	658
6	-8	•	252	-67
7	-8		506	-566
8	-8		606	716
9	-8		538	-583
10	-8	•	412	313
11	-8	•	443	-0
0	9		1227	-1152
1	9		4115	-4177
2	9		827	-982
3	9		1103	-1262
4	9	•	287	-281
5	9		541	-592
6	9		415	-387
7	9	•	558	-504
8	9		1924	-2081
9	9	•	420	-279
1	-9		625	469
2	-9		1894	-1775
3	-9		3325	-3106
4	-9	•	208	-27
5	-9		1726	-1828
6	-9		2271	-2321
7	-9	•	277	103
8	-9		674	-748
9	-9		1794	-2244
10	-9	•	409	45
11	-9	•	440	-443
0	10		499	-512
1	10		246	355
2	10		746	825
3	10		496	-450
4	10	•	296	323
5	10	•	321	-50
6	10	•	347	105
1	-10	•	180	53
2	-10	•	177	-20
3	-10		709	697
4	-10		369	-359
5	-10	•	232	86
6	-10		507	523
7	-10		319	341
8	-10	•	301	201
9	-10		421	-408
10	-10	•	407	280
11	-10	•	438	-191
0	11		404	-398
1	11		275	-296
3	11	•	281	290
4	11	•	305	-162
5	11	•	330	11
6	11	•	355	309
1	-11		241	-256
2	-11		220	266
3	-11	•	189	-111
4	-11		252	-217
5	-11	•	235	-147
6	-11		833	-889
7	-11		299	254
8	-11		388	-381
9	-11	•	375	-210
10	-11	•	405	279
11	-11		487	-495
0	12		268	298
1	12		249	287
2	12		2082	2416
3	12		1034	1041
4	12		1256	1310
5	12		757	-758
6	12		786	821
9	12		1275	1271
1	-12		2973	2545
2	-12		3128	-3015
3	-12		1304	1319
4	-12		1738	1723
5	-12		585	-604
6	-12		1216	1264
7	-12	•	278	164
8	-12		1665	1690
9	-12		937	-926
10	-12	•	404	-90
11	-12		1147	1213
12	-12		519	-406
0	13		297	317
1	13		259	-280
2	13	•	279	128
3	13		300	317
4	13	•	349	-137
5	13	•	376	-28
6	13	•	403	163
1	-13		421	506
2	-13	•	204	130
3	-13		765	753
4	-13		566	597
5	-13	•	263	288
6	-13	•	281	221
7	-13	•	280	-173
8	-13		326	253
9	-13		593	581
10	-13	•	403	-56
11	-13		529	582
0	14		638	647
1	14	•	246	-140
2	14	•	289	324
3	14		669	583
4	14		744	-740
5	14		412	460
6	14	•	413	215
1	-14		539	-557
2	-14		1280	1288
3	-14		446	341
4	-14	•	238	-167
5	-14		761	768
6	-14		458	-428
7	-14		799	778
8	-14	•	303	-70
9	-14		398	313
10	-14		1104	1052
11	-14	•	432	-278
12	-14		515	372
0	15	•	241	73
1	15		1023	988
2	15	•	299	-330
3	15		904	819

			|FOBS|	FCALC
4	15		1046	1045
5	15		945	878
6	15	•	422	146
8	15		568	278
1	-15		795	-821
2	-15		2633	2576
3	-15		2250	2348
4	-15		1453	-1473
5	-15		2461	2445
6	-15		336	299
7	-15		350	-289
8	-15		352	347
9	-15		705	683
10	-15	•	403	127
11	-15	•	431	18
0	16	•	250	64
1	16		604	-614
2	16	•	309	216
3	16	•	330	-239
4	16	•	380	-219
6	16	•	432	-158
1	-16		524	-568
2	-16		528	-554
3	-16		502	-510
4	-16		594	-642
5	-16		426	407
6	-16		590	-541
7	-16		312	272
8	-16		561	-512
9	-16		757	-718
10	-16	•	404	-282
11	-16		506	-569
0	17		507	455
1	17		368	374
2	17		319	-297
3	17	•	340	248
4	17		391	379
6	17	•	442	-17
7	17		707	143
1	-17		770	763
2	-17		987	1059
3	-17		765	794
4	-17	•	261	-189
5	-17	•	268	-65
6	-17		580	648
8	-17		1445	1473
9	-17		762	814
10	-17	•	406	-78
11	-17	•	432	312
0	18		381	377
1	18	•	311	161
2	18		1317	1433
3	18		571	-572
6	18		1255	-1292
1	-18		447	-361
2	-18		806	-838
3	-18		695	788
4	-18		2030	-1933
5	-18		1209	1286
6	-18		821	881
7	-18		1153	-1181
8	-18	•	314	41
9	-18		576	-485
10	-18		594	-565
11	-18		719	-657
0	19		749	-754
1	19	•	321	140
2	19	•	340	-170
3	19		689	-703
1	-19		535	-566
2	-19		449	-376
3	-19		755	-714
4	-19	•	321	151
5	-19		346	-358
6	-19		336	-348
7	-19		761	-728
8	-19		1360	-1374
9	-19		411	-302
10	-19	•	410	27
11	-19	•	435	-219
0	20		753	-790
1	20		606	446
2	20		700	-807
3	20	•	370	140
1	-20		525	-519
2	-20		865	885
3	-20		881	-864
4	-20		586	519
5	-20		976	-978
6	-20		343	-320
7	-20	•	308	20
8	-20		1315	-1215
9	-20		618	565
11	-20	•	437	-125
13	-20		845	-864
0	21		680	589
1	21		1135	-1170
2	21		806	799
3	21		621	641
1	-21		627	600
2	-21		912	-909
3	-21		824	714
4	-21		1620	1693
5	-21		632	-620
6	-21	•	304	267
7	-21		513	449
8	-21	•	327	20
9	-21		396	-304
11	-21		466	471
0	22		435	408
1	22	•	381	186
2	22	•	401	78
3	22	•	422	328
2	-22		831	802
3	-22		308	-257
4	-22		320	-272
5	-22		829	774
6	-22		440	404
7	-22		826	768
8	-22	•	332	-131
9	-22	•	401	13
11	-22	•	442	-92
0	23		751	-595
1	23		696	-540
3	23	•	433	-307
1	-23		723	706
1	-23		819	706
2	-23		621	-490

			|FOBS|	FCALC
3	-23	•	290	-88
4	-23		329	-176
5	-23		1204	-1220
6	-23	•	319	-227
7	-23	•	327	-20
8	-23	•	365	-154
9	-23		406	191
11	-23		546	-575
0	24	•	358	206
1	24		404	-445
3	24		750	633
4	24		786	-766
5	24		822	-626
1	-24		745	-636
2	-24	•	334	-291
3	-24		1117	-1016
4	-24		619	636
5	-24	•	349	288
6	-24		800	-713
7	-24		1186	1168
8	-24	•	371	-255
9	-24		920	-1016
11	-24		477	-452
0	25	•	369	282
1	25	•	415	-27
3	25		454	460
1	-25	•	324	-143
3	-25	•	308	137
4	-25		384	316
5	-25		358	318
6	-25	•	334	-175
7	-25	•	341	-57
8	-25	•	404	261
9	-25		443	-488
11	-25	•	454	350
0	26		759	-594
3	26	•	465	52
1	-26		539	456
3	-26	•	317	-38
4	-26		684	646
5	-26		901	-869
6	-26		685	546
7	-26	•	348	-353
8	-26	•	411	-186
9	-26	•	424	263
11	-26		760	714
12	-26		829	-753
0	27		1511	-1506
1	27	•	468	295
3	27		804	-648
1	-27		615	-492
3	-27		744	-645
4	-27		674	-666
5	-27	•	378	234
6	-27		453	-317
7	-27		740	-703
8	-27		663	-571
9	-27	•	431	88
11	-27		492	-512
12	-27		539	544
1	28	•	480	195
1	-28	•	387	32
3	-28	•	367	-246
4	-28		693	619
5	-28	•	388	-99
6	-28		441	408
7	-28	•	393	362
8	-28	•	400	-219
9	-28	•	438	147
11	-28	•	469	79
12	-28	•	487	136
1	29	•	492	216
1	-29		629	-519
3	-29	•	378	-214
4	-29		568	-566
5	-29	•	398	158
6	-29		499	-481
7	-29		567	-433
8	-29		487	413
9	-29		669	-595
11	-29	•	474	-360
12	-29		521	-464
1	30		796	740
3	-30		388	-324
4	-30	•	412	-48
5	-30		756	756
6	-30		1089	936
7	-30	•	410	-137
8	-30	•	416	231
9	-30		752	799
11	-30	•	480	-54
12	-30		608	600
3	-31		563	543
4	-31	•	423	294
6	-31		590	500
7	-31	•	419	-130
8	-31	•	424	19
9	-31		730	699
11	-31		486	497
3	-32		866	799
4	-32	•	433	-86
6	-32		854	759
7	-32		724	-691
8	-32		895	865
9	-32	•	470	34
11	-32		954	861
3	-33		512	483
4	-33		557	579
8	-33	•	441	53
9	-33		507	-428
11	-33		585	568
3	-34		494	-503
8	-34	•	481	-282
9	-34		499	-350
11	-34		536	-485
8	-35	•	490	423
9	-35		495	418
10	-35	8	665	434
1	36	•	522	-127
8	-36	•	499	-390
9	-36		534	-402
8	-37		843	-705
9	-37		789	-620
9	-38		637	-616

TABLE (V-7) β'-$Co_3(PO_4)_2$ OBSERVED AND CALCULATED STRUCTURE FACTORS (x 10)

UNOBSERVED REFLECTIONS ARE MARKED WITH AN ASTERISK (*), AND UNRELIABLE REFLECTIONS WITH THE SYMBOL (Ø).

		|FOBS|	FCALC
H	K		L=0
2	0	1991	2103
3	0	Ø6170	8116
4	0	1197	-982
5	0	4300	4119
6	0	3206	2956
7	0	5260	5041
8	0	2511	2677
9	0	581	-537
10	0	Ø4318	4362
11	0	Ø 464	132
12	0	* 428	-51
13	0	2901	2686
14	0	* 471	240
15	0	529	732
16	0	1188	1051
17	0	1238	806
2	1	* 152	-22
3	1	3193	3613
4	1	Ø6201	-4725
5	1	834	-700
6	1	2065	2065
7	1	4079	-4106
8	1	995	1221
9	1	660	723
10	1	* 375	-321
11	1	Ø 441	324
12	1	664	-827
13	1	1069	940
14	1	1154	-964
15	1	* 483	-337
16	1	1105	902
1	2	3405	3985
2	2	Ø 362	-201
3	2	555	-477
4	2	3499	3681
5	2	2215	-2198
6	2	4337	4537
7	2	Ø1263	929
8	2	710	-755
9	2	2137	2144
10	2	* 378	-469
11	2	1918	1512
12	2	* 430	379
13	2	Ø 453	131
14	2	1266	1258
15	2	749	-647
16	2	* 485	466
1	3	Ø5345	-7034
2	3	Ø6141	7919
3	3	* 205	-212
4	3	2320	-2401
5	3	452	417
6	3	393	-343
7	3	383	360
8	3	1948	-2144
9	3	1669	1808
10	3	* 382	301
11	3	1906	-1952
12	3	988	958
13	3	* 456	-285
14	3	1271	-1052
16	3	* 484	53
0	4	4955	-5417
1	4	3328	-3557
2	4	Ø 492	-350
3	4	4352	-4745
4	4	2897	-3150
5	4	2249	2139
6	4	3856	-4059
7	4	3512	-3654
8	4	* 335	103
9	4	2736	-2514
10	4	1756	-1797
11	4	522	-621
12	4	* 437	150
13	4	1361	-1156
14	4	1504	-1289
16	4	1144	-986
1	5	813	694
2	5	2345	-2261
3	5	* 235	-79
4	5	454	-417
5	5	1685	1413
6	5	* 296	-37
7	5	* 319	-222
8	5	614	682
9	5	932	-1042
10	5	* 394	-391
11	5	* 418	100
12	5	685	-802
13	5	507	537
14	5	* 478	11
16	5	* 482	96
0	6	5947	-6299
1	6	1382	-1318
2	6	801	-754
3	6	5187	-5713
4	6	3448	-3500
5	6	890	-927
6	6	2870	-3001
7	6	2363	-2613
8	6	706	-745
9	6	1431	-1362
10	6	1986	-2014
11	6	1615	-1282
12	6	567	-651
13	6	1645	-1471
14	6	1008	-941
16	6	607	-699
1	7	2832	3028
2	7	2918	-2997
3	7	724	-725
4	7	2283	2216
5	7	* 302	-228
6	7	2049	-1995
7	7	1633	1363
8	7	830	980
9	7	1747	-1614
10	7	* 411	299
11	7	1736	1498
12	7	813	-918
13	7	* 472	-101
14	7	916	823
0	8	* 269	-203
1	8	1859	1467
2	8	1827	-1725
3	8	* 288	-12
4	8	2096	1997
5	8	2714	-2852
6	8	734	871
7	8	1895	1822
8	8	1116	-1092
9	8	1380	1203
10	8	* 421	301
11	8	484	-372
12	8	* 461	-18
13	8	* 476	18
1	9	Ø1965	1046
2	9	1099	1181
3	9	929	-1154
4	9	2093	2158
5	9	* 333	-53
6	9	1486	-1439
7	9	1320	1389
8	9	427	-585
9	9	899	812
10	9	472	606
11	9	* 451	131
12	9	* 468	614
13	9	607	-659
0	10	5614	6032
1	10	* 312	-297
2	10	1201	1297
3	10	5290	5567
4	10	1115	1174
5	10	1887	1876
6	10	1135	1213
7	10	2533	2636
8	10	* 403	393
9	10	* 423	-90
10	10	3311	3156
11	10	* 459	14
12	10	* 474	257
13	10	2263	2005
1	11	697	-622
2	11	1906	-1666
3	11	2840	2900
4	11	2147	-2197
5	11	736	-550
6	11	3057	3034
7	11	2393	-2387
8	11	* 417	339
9	11	871	850
10	11	701	-676
11	11	* 468	302
12	11	* 479	-94
13	11	614	647
0	12	801	-821
1	12	2531	2570
2	12	357	409
3	12	922	920
4	12	2255	2384
5	12	* 386	-387
6	12	1772	1866
7	12	* 415	508
8	12	473	489
9	12	1854	1710
10	12	507	-503
11	12	1410	1198
12	12	* 483	518
13	12	* 485	52
1	13	2745	-2541
2	13	1986	2102
3	13	1191	-1179
4	13	* 393	-368
5	13	404	440
6	13	* 417	342
7	13	431	454
8	13	1544	-1497
9	13	1126	1028
10	13	* 472	-170
11	13	Ø1925	-1441
12	13	1149	1064
13	13	* 483	-291
0	14	Ø 351	-597
1	14	1087	-1089
2	14	796	874
3	14	1533	-1381
4	14	3110	-2884
4	14	3110	-2884
5	14	1731	1799
6	14	1736	-1717
7	14	1324	-1223
8	14	1589	1334
9	14	841	-876
10	14	959	-731
13	14	523	-542
1	15	1416	1359
1	15	1387	1359
2	15	1152	-1033
3	15	847	808
4	15	* 431	-169
5	15	482	-478
6	15	* 450	-224
7	15	582	-636
8	15	841	814
9	15	741	-832
10	15	* 484	-28
13	15	* 468	-17
0	16	2181	-2244
1	16	672	-596
2	16	874	-860
3	16	1722	-1513
4	16	896	-803
5	16	998	-958
6	16	973	-913
7	16	1550	-1423
8	16	* 479	-466
9	16	* 484	-365
10	16	1624	-1461
13	16	644	-735
1	17	903	913
2	17	* 454	64
3	17	1295	-1158
4	17	1015	1081
5	17	* 469	-77
6	17	1520	-1457
7	17	744	805
8	17	* 484	258
9	17	Ø1121	-701
0	18	* 466	234
1	18	886	-790
2	18	726	-733
3	18	* 472	467
4	18	* 475	145
5	18	Ø 606	-767
6	18	* 483	-18
7	18	* 485	283
8	18	Ø1302	-890
1	19	* 478	-232
2	19	* 479	232
3	19	* 481	-248
4	19	* 483	184
6	19	* 485	12
7	19	* 484	471
0	20	1777	1612
1	20	* 485	237
2	20	* 485	73
3	20	1018	1058
4	20	614	561
6	20	* 482	488
7	20	1090	923
1	21	* 485	-301
2	21	* 484	20
3	21	683	746
4	21	861	-812
6	21	1196	942
7	21	Ø1018	-685
1	22	1130	946
2	22	Ø 738	534
3	22	* 474	-90
4	22	786	700
2	23	651	714
H	K		L=3
1	1	2866	2890
2	1	1726	1765
3	1	1255	-1253
4	1	5065	5625
5	1	1732	1645
6	1	1640	-1635
7	1	1831	1859
8	1	928	1011
1	2	Ø6383	-8826
2	2	Ø4563	-5248
3	2	2653	-2665
5	2	3853	-4178
6	2	2145	-2343
7	2	1190	1128
8	2	4199	-4478
9	2	2633	-2687
11	2	2878	-2880
0	3	3722	3740
1	3	2044	-1983
2	3	1910	-1894
3	3	2447	2595
4	3	4507	-4815
6	3	752	758
7	3	2063	-2109
8	3	1341	1357
0	4	3393	-3281
1	4	1690	-1427
2	4	Ø5593	-6391
3	4	732	-681
5	4	4790	-5248
7	4	2115	-2322
8	4	1748	-1863
12	4	1843	-1777
0	5	5013	-5458
1	5	4113	-4107
2	5	1023	1015
3	5	2705	-2775
5	5	2791	-3026
6	5	1938	1993
8	5	3401	-3652
9	5	2795	2797
11	5	1895	-1760
12	5	1238	1343
0	6	1628	1412
1	6	1153	-1123
2	6	Ø6378	7203
3	6	1685	-1808
4	6	956	845
5	6	4320	4674
6	6	2505	-2626
7	6	Ø 767	1176
10	6	1420	1338
12	6	1470	1567
1	7	1648	-1573
2	7	2465	-2374
3	7	2664	2765
4	7	2189	-2378
5	7	829	1013
7	7	1843	-1872
9	7	1353	-1408
1	8	4485	4792
2	8	1246	1298
3	8	1177	1405
4	8	2127	2073
5	8	2575	2819
6	8	3448	3663
8	8	3005	3270
9	8	1865	1888
11	8	2509	2449
1	9	3696	3928
3	9	2077	-2167
4	9	4119	4382
7	9	2250	2345
0	10	3033	2974
1	10	1651	-1598
0	11	1835	1740
1	11	2170	2191
7	11	1344	1394
8	11	1449	1512
2	12	2640	-2756
5	12	2983	-3091
8	12	1627	-1654
3	13	1413	1391
4	13	Ø3118	-1515
2	14	2264	-2203
5	14	1686	-1803
1	15	2107	-2146
2	16	1750	1831
3	16	1465	-1463
5	16	2013	2110
1	18	2101	2155
H	K		L=-3
3	1	Ø5309	6035
4	1	1428	-1282
5	1	1891	1686
6	1	4995	4948
9	1	3432	3333
12	1	1829	1749
2	2	6268	-6969
3	2	3084	2978
4	2	3795	-3731
5	2	6924	-7446
6	2	1998	-1971
7	2	1426	-1430
8	2	3508	-3406
9	2	1995	-1899
11	2	2068	-1989
12	2	2117	-2080
14	2	1429	-1374
2	3	2138	2031
3	3	2556	-2317
5	3	Ø1794	1154
6	3	3352	-3353
7	3	2719	2573
9	3	1553	-1444
1	4	3151	-2849
2	4	1910	-1822
3	4	4282	-4175
4	4	1640	1556
5	4	5060	-5242
7	4	2123	1881
8	4	4343	-4334
11	4	2053	-1982
1	5	5875	6169
2	5	6814	-7548
3	5	3718	-3526
4	5	2255	2298
5	5	5044	-5115
6	5	1736	-1594
9	5	2180	-2087
10	5	1775	-1693
11	5	1858	1528
12	5	2551	-2471
1	6	2471	2301
2	6	1692	1643
4	6	1701	-1739
5	6	4014	4046
6	6	Ø1414	970
7	6	1113	-1142
8	6	3637	3759
1	7	4539	-4574
2	7	2929	2687
3	7	1732	-1784
5	7	2405	2296
6	7	3961	-4039
8	7	1271	-1213
9	7	2531	-2283
10	7	1372	1291
11	7	1842	-1516
1	8	3943	3844
2	8	Ø6626	7233
3	8	1921	-1899
4	8	3450	3603
5	8	2527	2554
7	8	1575	1501
8	8	2125	1966
9	8	2879	2717
11	8	1550	1555
12	8	2024	1971
2	9	1712	1615
3	9	1831	1898
6	9	3208	3327
7	9	1377	-1488
9	9	2371	2168
3	10	2980	2930
4	10	1599	-1385
8	10	1521	1355
2	11	2092	2034
3	11	1178	1227
6	11	1726	1674
9	11	1869	1730
1	12	2583	-2546
2	12	3143	-3127
2	12	3143	-3127
4	12	1006	-1164
5	12	2449	-2558
8	12	2120	-2038
4	13	1647	1585
3	14	1076	-1325
5	14	1392	-1502
2	15	2457	-2547
4	15	1396	1264
5	15	1416	-1495
8	16	1433	1484
1	18	1823	1303
2	18	1648	1631
K	L		H=0
2	0	Ø 355	-172
4	0	Ø4560	-5417
6	0	Ø5061	-6299
8	0	* 526	-203
10	0	Ø4235	6032
12	0	752	-821
14	0	* 646	-597
2	1	263	-269
3	1	522	553
4	1	388	429
5	1	435	-353
6	1	505	482
7	1	548	-596
8	1	527	-510
9	1	623	-560
10	1	* 586	64
11	1	* 606	149
12	1	750	-731
13	1	* 725	39
14	1	* 609	569
0	2	* 206	-153
2	2	* 260	-36
3	2	* 329	-286
4	2	* 374	235
5	2	1004	-764
6	2	* 456	251
7	2	551	-460
8	2	799	835
9	2	661	758
10	2	* 587	-108
11	2	605	530
12	2	* 749	-31
13	2	* 722	-70
14	2	* 602	-168
1	3	Ø 417	319
2	3	586	462
3	3	4072	3740
4	3	3461	-3281
5	3	Ø4500	-5458
6	3	1386	1412
7	3	711	824
8	3	1245	-1282
9	3	857	-833
10	3	2608	2974
11	3	1941	1740
12	3	1160	972
13	3	* 719	302
14	3	1975	-1459
0	4	* 290	-59
1	4	* 302	-160
2	4	337	267
3	4	920	794
4	4	397	336
5	4	673	-643
6	4	* 469	55
7	4	* 503	367
8	4	649	-643
9	4	564	-451
10	4	* 722	-49
11	4	* 743	-182
12	4	832	639
13	4	* 714	252
14	4	* 572	281
1	5	* 333	-255
2	5	* 318	-132
3	5	969	-997
4	5	* 412	-131
5	5	618	564
6	5	477	-466
7	5	568	544

TABLE (V —7) CONCLUDED

		|FOBS|	FCALC
8	5	• 540	-64
9	5	584	546
10	5	• 724	44
11	5	• 743	-179
12	5	• 744	-26
13	5	1292	-1264
14	5	• 545	71
0	6	5093	-5709
1	6	05962	-7824
2	6	3402	-3699
3	6	2895	-2668
5	6	2798	-2672
6	6	4261	4777
7	6	1244	1308
8	6	• 545	-241
9	6	3538	3875
10	6	3360	-3752
11	6	3184	-2685
12	6	1354	-1295
13	6	• 698	368
14	6	3006	2385
1	7	• 388	-78
2	7	1022	925
3	7	• 420	-231
4	7	• 443	256
5	7	• 469	265
6	7	497	-469
7	7	601	-651
8	7	832	-919
9	7	705	541
10	7	933	831
11	7	• 743	-356
12	7	• 736	356
13	7	• 686	461
0	8	1329	-1152
1	8	• 413	332
2	8	424	373
3	8	• 440	-27
4	8	460	531
5	8	• 483	384
6	8	551	484
7	8	898	912
8	8	• 557	507
9	8	1132	-989
10	8	• 731	-525
11	8	• 742	-182
12	8	• 731	163
13	8	• 669	-349
1	9	2527	-2511
2	9	1857	-1890
3	9	795	-691
4	9	04406	-5115
6	9	04298	5141
7	9	• 541	-323
8	9	• 563	-291
9	9	• 583	-61
10	9	• 733	-135
11	9	1831	-1539
12	9	2168	-1670
13	9	1944	-1393
0	10	• 453	-275
1	10	• 457	71
2	10	806	853
3	10	• 477	253
4	10	853	-994
5	10	• 510	-136
6	10	• 529	77
7	10	• 549	-273
8	10	• 569	8
9	10	• 587	164
10	10	• 735	-47
11	10	• 737	561
12	10	713	592
13	10	• 619	123
1	11	• 477	-111
2	11	711	-663
3	11	• 494	-299
4	11	1221	1221
5	11	• 523	-138
6	11	• 540	-582
7	11	• 558	-216
8	11	608	421
9	11	• 724	-98
10	11	766	-819
11	11	• 733	85
12	11	920	-781
13	11	• 577	256
0	12	• 492	-327
1	12	1011	1058
2	12	2752	2922
3	12	4467	4886
4	12	3769	-4218
5	12	01023	718
6	12	• 550	-497
7	12	3808	-3358
8	12	3700	3363
9	12	1330	-1454
10	12	863	-919
11	12	• 726	-417
12	12	1097	868
13	12	2180	1846
1	13	• 512	303
2	13	1246	-1040
3	13	• 525	-418
4	13	• 535	-209
6	13	• 560	128
6	13	• 560	128
7	13	704	-669
8	13	1243	1305
9	13	1196	1276
10	13	• 732	-521
11	13	• 716	-29
12	13	• 656	-3
13	13	431	-344
0	14	1492	1724
1	14	1108	1089
2	14	• 532	-152
3	14	• 539	255
4	14	• 547	210
5	14	• 558	22
6	14	697	-698
7	14	• 711	-102
8	14	784	-803
9	14	1103	-1130
10	14	• 728	642
11	14	805	597
12	14	• 759	306
1	15	1202	1164
2	15	3946	4563
3	15	1307	-1248
4	15	4555	4403
5	15	1420	1317
6	15	3380	-2883
7	15	4048	-3694
8	15	3670	-3308
9	15	1573	1672
10	15	856	-785
11	15	1150	786
12	15	2353	2202
0	16	553	603
1	16	• 555	330
2	16	• 684	-107
3	16	1262	-1396
4	16	• 697	-345
5	16	• 706	634
6	16	• 715	77
7	16	763	642
8	16	• 728	426
9	16	• 725	276
10	16	• 708	31
11	16	• 655	-201
1	17	• 694	49
2	17	• 697	91
3	17	874	942
4	17	• 708	-213
5	17	1541	-1614
6	17	804	-732
7	17	767	590
8	17	• 726	303
9	17	704	-651
10	17	690	654
11	17	• 614	288
0	18	• 574	-146
1	18	1523	1512
2	18	1296	1330
3	18	3699	-3357
4	18	1240	-1146
5	18	• 721	70
6	18	• 725	-688
7	18	1566	1667
8	18	851	-705
9	18	787	-635
10	18	1151	-1098
2	19	• 718	7
3	19	825	861
4	19	806	882
5	19	• 725	541
6	19	• 726	-632
7	19	• 723	517
8	19	• 713	438
9	19	904	-1064
10	19	627	-574
0	20	742	862
1	20	1559	-1539
2	20	1478	-1599
3	20	831	-810
4	20	856	951
5	20	832	-830
6	20	• 724	270
7	20	• 716	294
8	20	697	-723
9	20	868	1046
10	20	646	499
1	21	966	1076
3	21	• 727	446
4	21	1223	-1291
5	21	1360	-1547
6	21	• 717	359
7	21	743	-723
8	21	05919	4415
9	21	• 618	535
10	21	• 433	-269
0	22	• 728	-277
1	22	728	679
2	22	905	-1092
3	22	• 726	400
4	22	1221	1450
5	22	• 716	108
6	22	• 705	376
7	22	• 684	-312
8	22	• 642	-347
9	22	545	-450
1	23	725	-666
2	23	• 723	182
3	23	• 720	56
4	23	1235	-1289
5	23	• 703	-290
6	23	1186	1363
7	23	1261	1394
8	23	• 587	-362
9	23	• 363	341
0	24	0 758	1295
1	24	799	841
2	24	1305	-1558
3	24	1043	-1247
4	24	• 698	-243
5	24	• 682	-237
6	24	691	588
7	24	711	568
8	24	• 480	399
1	25	• 702	275
2	25	• 697	397
3	25	• 688	475
4	25	0 711	145
5	25	765	-851
6	25	• 605	50
7	25	• 514	208
0	26	779	-945
1	26	801	-882
2	26	• 631	-219
3	26	1208	1677
4	26	• 634	-77
5	26	• 595	59
6	26	• 517	221
1	27	3323	-3181
2	27	1834	1964
3	27	1924	1791
4	27	884	1088
5	27	1189	1368
0	28	1703	2008
H	L		K=0
2	0	2066	2103
3	0	06767	8116
4	0	987	-982
6	0	3067	2956
8	0	2391	2677
9	0	•1168	-537
1	2	• 410	-17
2	2	• 514	-151
3	2	• 608	114
4	2	• 693	14
5	2	943	-710
6	2	•1029	-304
7	2	•1136	456
8	2	1156	-1107
9	2	•1161	178
1	-2	• 328	230
2	-2	496	516
3	-2	• 536	-438
4	-2	• 627	364
5	-2	• 711	651
6	-2	• 788	95
7	-2	•1047	602
8	-2	•1117	41
9	-2	1264	1414
10	-2	•1151	-794
0	4	• 438	-59
1	4	• 502	32
2	4	630	-607
3	4	• 661	503
4	4	• 737	167
5	4	• 988	-582
6	4	•1067	-194
7	4	1131	874
8	4	•1165	-421
9	4	•1132	-158
1	-4	• 421	-433
2	-4	530	375
3	-4	1290	-1501
4	-4	• 617	143
5	-4	695	-800
6	-4	881	-729
7	-4	•1024	34
8	-4	•1097	-145
9	-4	•1151	-183
10	-4	1336	-1128
0	6	04813	-5709
1	6	01160	986
2	6	3180	-3479
3	6	2977	-3243
4	6	5196	-5856
5	6	0 917	888
6	6	1911	-1780
7	6	3985	-4407
8	6	2393	2240
9	6	1881	-1720
1	-6	• 513	44
2	-6	03889	4466
3	-6	07679	-10873
4	-6	969	-888
5	-6	1758	2229
6	-6	04522	-5919
7	-6	1008	864
8	-6	•1081	-320
9	-6	•1138	347
10	-6	1857	-2224
11	-6	1692	-1896
0	8	1292	-1152
1	8	• 657	27
2	8	• 709	336
3	8	1095	-1164
4	8	• 826	-200
5	8	930	926
6	8	•1132	-513
7	8	•1160	-214
8	8	1157	789
1	-8	679	585
2	-8	1547	-1642
3	-8	721	-727
4	-8	• 652	-595
5	-8	1993	-2560
6	-8	• 760	453
7	-8	•1001	-850
8	-8	1058	-1112
9	-8	•1127	-714
10	-8	•1159	-1231
11	-8	•1134	-195
0	10	• 686	-275
1	10	1734	1785
2	10	902	908
3	10	861	-633
4	10	• 866	-68
5	10	•1113	472
6	10	•1151	-25
7	10	•1147	-616
8	10	•1022	594
1	-10	1431	1470
2	-10	• 657	4
3	-10	1003	858
4	-10	1368	1531
5	-10	• 725	-536
6	-10	2069	2403
7	-10	•1003	506
8	-10	•1064	521
9	-10	2105	1929
10	-10	•1153	131
11	-10	•1142	1056
12	-10	•1139	-19
0	12	• 747	-327
1	12	1542	1579
2	12	04352	-5988
3	12	• 858	-234
4	12	2186	2137
5	12	05764	-6681
6	12	1787	2104
7	12	01089	588
8	12	1349	-1604
1	-12	1813	-1803
2	-12	3615	-3927
3	-12	1505	-1422
4	-12	731	675
5	-12	05304	-6829
6	-12	930	881
7	-12	2130	2054
8	-12	4574	-4348
9	-12	1211	1162
10	-12	•1147	342
11	-12	1929	-2191
12	-12	1532	-1366
0	14	1850	1724
1	14	• 827	-302
2	14	• 859	357
3	14	• 894	462
4	14	•1129	640
5	14	•1147	369
6	14	•1116	17
7	14	• 915	396
1	-14	• 780	210
2	-14	881	-622
3	-14	2637	3040
4	-14	1339	-1350
5	-14	1798	1721
6	-14	958	1194
7	-14	1185	-1215
8	-14	2255	2713
9	-14	1314	-1167
10	-14	•1143	450
11	-14	1239	1294
12	-14	•1236	-264
0	16	• 845	603
1	16	• 868	-314
2	16	• 894	37
3	16	• 919	-493
4	16	•1142	790
5	16	1189	-980
6	16	•1003	5
1	-16	• 827	524
2	-16	1822	-1938
3	-16	• 812	808
4	-16	• 815	-312
5	-16	893	-874
6	-16	•1026	419
7	-16	1085	-1101
8	-16	1392	1208
9	-16	1215	-1041
10	-16	•1139	-196
11	-16	•1134	736
0	18	• 882	-146
1	18	1582	1571
2	18	04512	5816
3	18	01065	-818
4	18	1482	1713
5	18	2793	3013
1	-18	06253	7563
2	-18	2004	2158
3	-18	1644	1437
4	-18	0 923	978
5	-18	2711	3103
6	-18	2133	2279
7	-18	1111	-958
8	-18	05564	7167
9	-18	2231	2140
10	-18	1305	-1408
11	-18	3876	3800
0	20	986	862
1	20	944	-698
2	20	•1132	469
3	20	•1120	689
4	20	1173	-1234
5	20	1041	816
1	-20	2065	-1806
2	-20	•1086	586
3	-20	•1080	463
4	-20	•1079	-302
5	-20	2401	2409
6	-20	1787	-1786
7	-20	1662	1297
8	-20	•1114	470
9	-20	1367	-1418
10	-20	2379	2507
11	-20	•1112	-899
0	22	• 923	-277
1	22	1129	-978
2	22	•1111	330
3	22	1045	-958
4	22	971	-1119
1	-22	1289	-1120
2	-22	•1115	-340
3	-22	1208	-820
4	-22	2330	-1927
5	-22	•1109	302
6	-22	1928	-1923
7	-22	•1118	-896
8	-22	•1124	-670
9	-22	•1129	-1129
10	-22	•1124	-94
11	-22	1651	-1638
0	24	1219	1295
1	24	2066	-2245
2	24	1282	-1375
3	24	1596	-1488
1	-24	1904	-1960
2	-24	3209	-3316
3	-24	2243	2444
4	-24	3778	-3516
5	-24	3518	-3796
6	-24	•1128	275
7	-24	1129	-977
8	-24	2648	-2851
9	-24	•1125	-232
10	-24	•1109	867
11	-24	2935	-2724
12	-24	2143	-1768
0	26	1135	-945
1	26	1082	1144
2	26	1686	-1897
1	-26	1868	-1833
2	-26	•1121	804
3	-26	2504	-2285
4	-26	1230	1054
5	-26	1373	-1266
6	-26	2377	-2090
7	-26	•1128	784
8	-26	2938	-2997
9	-26	•1109	235
10	-26	•1080	-829
11	-26	01010	-2335
0	28	2446	2008
1	28	582	732
1	-28	•1034	127
2	-28	1309	1216
3	-28	1197	895
4	-28	1349	1088
5	-28	1150	904
6	-28	1214	856
7	-28	1782	1961
8	-28	1201	925
9	-28	1456	1160
10	-28	•1028	1183
11	-28	1388	1337
1	-30	• 815	226
2	-30	1715	1739
3	-30	2754	-2661
4	-30	•1054	-58
5	-30	1904	1917
6	-30	2883	-2722
6	-30	2883	-2722
7	-30	•1065	-86
8	-30	1970	2238
9	-30	1582	-1627
10	-30	• 930	-443
3	-32	• 809	232
4	-32	2453	2522
5	-32	1160	-862
6	-32	1551	1523
7	-32	• 966	76
8	-32	• 937	180
9	-32	2400	1891

H. Description of the Structures

The large cell comprises three sub-cells, which are labelled A, B and C respectively. The nomenclature used to identify the atoms is the same as that used for β-$Zn_3(PO_4)_2$ except that the sub-cell designation has been appended.

The phosphorus atom environments are shown in Table (V-8) for both the β^1 structures. The esd's of the P-O bond distances are much higher than those in β-$Zn_3(PO_4)_2$. This is due to the higher values of the residuals, R_2, and to the considerably lower degree of overdeterminacy[†] in the β^1 structures. In β^1-$Cd_3(PO_4)_2$ the PO_4 groups appear highly irregular, and this is due to the incomplete refinement of this structure. The average P-O bond distances in β^1-$Mn_3(PO_4)_2$ and β^1-$Cd_3(PO_4)_2$ are 1.542±0.024 Å and 1.544±0.056 Å respectively. The average O-P-O angles are 109.5° and 109.2°.

The major differences between the β-$Zn_3(PO_4)_2$ structure and the two β^1 structures becomes apparent upon considering the cation environments. In Table (V-9), the cation-oxygen bond distances are listed for all three structures. As can be seen from this table, there

---

[†] The overdeterminacy is usually defined as the ratio of the number of independent observations to the number of independent parameters. If projection data only is used, the effective overdeterminacy is reduced, as each parameter does not contribute to each observation, (hk0 data cannot be used to determine z coordinates, for example). It is necessary to have a large overdeterminacy in a crystal structure analysis because there exists no mathematically unique solution for the electron density, and because each measured intensity is inexact.

TABLE (V-8)

(a) Bond distances in PO_4 tetrahedra in β^1-$Mn_3(PO_4)_2$ and β^1-$Cd_3(PO_4)_2$

Bonded atoms	β^1-$Mn_3(PO_4)_2$ Distance (Å)	β^1-$Cd_3(PO_4)_2$ Distance (Å)	Bonded atoms	β^1-$Mn_3(PO_4)_2$ Distance (Å)	β^1-$Cd_3(PO_4)_2$ Distance (Å)
P(1A)-O(1A)	1.54(2)	1.59(6)	P(2A)-O(2A)	1.54(3)	1.57(7)
P(1A)-O(3A)	1.56(3)	1.54(5)	P(2A)-O(4A)	1.51(4)	1.59(7)
P(1A)-O(5A)	1.56(3)	1.44(8)	P(2A)-O(6A)	1.57(3)	1.55(5)
P(1A)-O(7A)	1.59(3)	1.55(6)	P(2A)-O(8A)	1.56(3)	1.48(6)
P(1B)-O(1B)	1.57(2)	1.51(5)	P(2B)-O(2B)	1.54(3)	1.46(7)
P(1B)-O(3B)	1.50(3)	1.58(5)	P(2B)-O(4B)	1.57(3)	1.61(6)
P(1B)-O(5B)	1.54(3)	1.57(7)	P(2B)-O(6B)	1.52(3)	1.60(7)
P(1B)-O(7B)	1.57(3)	1.44(6)	P(2B)-O(8B)	1.51(2)	1.64(6)
P(1C)-O(1C)	1.54(3)	1.56(6)	P(2C)-O(2C)	1.52(3)	1.53(6)
P(1C)-O(3C)	1.55(3)	1.54(5)	P(2C)-O(4C)	1.52(3)	1.53(6)
P(1C)-O(5C)	1.52(3)	1.48(8)	P(2C)-O(6C)	1.52(3)	1.48(7)
P(1C)-O(7C)	1.54(3)	1.63(6)	P(2C)-O(8C)	1.56(3)	1.53(6)

(b) Bond angles in PO_4 tetrahedra in β^1-$Mn_3(PO_4)_2$ and β^1-$Cd_3(PO_4)_2$

Bonded atoms	β^1-$Mn_3(PO_4)_2$ Angle (°)	β^1-$Cd_3(PO_4)_2$ Angle (°)	Bonded atoms	β^1-$Mn_3(PO_4)_2$ Angle (°)	β^1-$Cd_3(PO_4)_2$ Angle (°)
O(1A)-P(1A)-O(3A)	111.	107.	O(2A)-P(2A)-O(4A)	110.	106.
O(1A)-P(1A)-O(5A)	111.	116.	O(2A)-P(2A)-O(6A)	108.	112.
O(1A)-P(1A)-O(7A)	110.	108.	O(2A)-P(2A)-O(8A)	112.	113.
O(3A)-P(1A)-O(5A)	106.	112.	O(4A)-P(2A)-O(6A)	112.	111.
O(3A)-P(1A)-O(7A)	113.	109.	O(4A)-P(2A)-O(8A)	104.	106.
O(5A)-P(1A)-O(7A)	106.	104.	O(6A)-P(2A)-O(8A)	111.	110.
O(1B)-P(1B)-O(3B)	114.	117.	O(2B)-P(2B)-O(4B)	109.	109.
O(1B)-P(1B)-O(5B)	110.	112.	O(2B)-P(2B)-O(6B)	107.	115.
O(1B)-P(1B)-O(7B)	106.	110.	O(2B)-P(2B)-O(8B)	115.	113.
O(3B)-P(1B)-O(5B)	107.	100.	O(4B)-P(2B)-O(6B)	108.	101.
O(3B)-P(1B)-O(7B)	113.	111.	O(4B)-P(2B)-O(8B)	105.	111.
O(5B)-P(1B)-O(7B)	107.	106.	O(6B)-P(2B)-O(8B)	113.	107.
O(1C)-P(1C)-O(3C)	110.	109.	O(2C)-P(2C)-O(4C)	109.	109.
O(1C)-P(1C)-O(5C)	110.	112.	O(2C)-P(2C)-O(6C)	113.	113.
O(1C)-P(1C)-O(7C)	108.	102.	O(2C)-P(2C)-O(8C)	109.	109.
O(3C)-P(1C)-O(5C)	110.	109.	O(4C)-P(2C)-O(6C)	104.	103.
O(3C)-P(1C)-O(7C)	112.	111.	O(4C)-P(2C)-O(8C)	109.	104.
O(5C)-P(1C)-O(7C)	107.	114.	O(6C)-P(2C)-O(8C)	112.	114.

TABLE (V-9)

Cation-oxygen bond lengths in β-$Zn_3(PO_4)_2$, β^{1}-$Mn_3(PO_4)_2$ and β^{1}-$Cd_3(PO_4)_2$

Bonded atoms	Distance (Å)	Bonded atoms	Distance (Å)	Bonded atoms	Distance (Å)	Bonded atoms	Distance (Å)
Mn(1A)-O(1A)	2.08(2)	Mn(1B)-O(1C)	2.09(2)	Mn(1C)-O(1B)	2.10(2)	Zn(1)-O(1)	1.95
Mn(1A)-O(1A)′	2.29(3)	Mn(1B)-O(1B)	2.20(3)	Mn(1C)-O(1C)	2.22(3)	Zn(1)-O(1)′	2.11
Mn(1A)-O(6B)	2.10(3)	Mn(1B)-O(6C)	2.15(3)	Mn(1C)-O(6A)	2.10(2)	Zn(1)-O(6)	1.89
Mn(1A)-O(8A)	2.22(4)	Mn(1B)-O(8C)	2.14(5)	Mn(1C)-O(8B)	2.14(3)	Zn(1)-O(8)	1.96
Mn(1A)-O(4A)	2.47(3)	Mn(1B)-O(4C)	2.74(3)	Mn(1C)-O(4B)	2.63(2)	Zn(1)-O(4)	2.55
Mn(1A)-O(2C)	2.32(3)	Mn(1B)-O(2B)	2.16(3)	Mn(1C)-O(2A)	2.24(4)	Zn(1)-O(2)	----
< Mn(1A)-O >	2.20	< Mn(1B)-O >	2.15	< Mn(1C)-O >	2.16	< Zn(1)-O >	1.98
Mn(2A)-O(2A)	2.82(4)	Mn(2B)-O(2B)	2.28(3)	Mn(2C)-O(2C)	2.13(3)	Zn(2)-O(2)	1.99
Mn(2A)-O(7A)	2.25(3)	Mn(2B)-O(7B)	2.17(3)	Mn(2C)-O(7C)	2.10(3)	Zn(2)-O(7)	2.02
Mn(2A)-O(8A)	2.04(3)	Mn(2B)-O(8C)	2.10(3)	Mn(2C)-O(8B)	2.19(3)	Zn(2)-O(8)	2.05
Mn(2A)-O(5B)	2.10(2)	Mn(2B)-O(5C)	2.13(2)	Mn(2C)-O(5A)	2.09(2)	Zn(2)-O(5)	2.09
Mn(2A)-O(3C)	2.13(3)	Mn(2B)-O(3B)	2.18(3)	Mn(2C)-O(3A)	2.16(3)	Zn(2)-O(3)	2.28
Mn(2A)-O(6A)	2.28(2)	Mn(2B)-O(2)	2.46(3)	Mn(2C)-O(6C)	-------	Zn(2)-O(6)	2.51
< Mn(2A)-O >	2.16	< Mn(2B)-O >	2.17	< Mn(2C)-O >	2.13	< Zn(2)-O >	2.09
Mn(3A)-O(4B)	2.15(3)	Mn(3B)-O(4C)	2.23(3)	Mn(3C)-O(4A)	2.00(3)	Zn(3)-O(4)	1.92
Mn(3A)-O(3A)	2.12(3)	Mn(3B)-O(3B)	2.12(3)	Mn(3C)-O(3C)	2.11(3)	Zn(3)-O(3)	2.00
Mn(3A)-O(5C)	2.17(3)	Mn(3B)-O(5B)	2.19(3)	Mn(3C)-O(5A)	2.15(2)	Zn(3)-O(5)	2.01
Mn(3A)-O(2A)	2.21(3)	Mn(3B)-O(2B)	-------	Mn(3C)-O(2C)	-------	Zn(3)-O(2)	2.17
Mn(3A)-O(7B)	2.14(2)	Mn(3B)-O(7A)	2.12(2)	Mn(3C)-O(7C)	2.18(2)	Zn(3)-O(7)	2.26
Mn(3A)-O(6B)	-------	Mn(3B)-O(6C)	2.37(3)	Mn(3C)-O(6A)	-------	Zn(3)-O(6)	----
Mn(3A)-O(4A)	-------	Mn(3B)-O(4B)	2.28(2)	Mn(3C)-O(4C)	2.16(2)	Zn(3)-O(4)	----
< Mn(3A)-O >	2.16	< Mn(3B)-O >	2.22	< Mn(3C)-O >	2.12	< Zn(3)-O >	2.08

(continued)

Table (V-9) continued

Bonded atoms	Distance (Å)	Bonded atoms	Distance (Å)	Bonded atoms	Distance (Å)
Cd(1A)-O(1A)	2.26(5)	Cd(1B)-O(1C)	2.27(5)	Cd(1C)-O(1B)	2.27(5)
Cd(1A)-O(1A)'	2.26(8)	Cd(1B)-O(1B)	2.31(7)	Cd(1C)-O(1C)	2.25(7)
Cd(1A)-O(6B)	2.18(5)	Cd(1B)-O(6C)	2.26(5)	Cd(1C)-O(6A)	2.27(4)
Cd(1A)-O(8A)	2.33(7)	Cd(1B)-O(8C)	2.25(7)	Cd(1C)-O(8B)	2.33(6)
Cd(1A)-O(4A)	2.60(5)	Cd(1B)-O(4C)	2.66(6)	Cd(1C)-O(4B)	2.70(5)
Cd(1A)-O(2C)	2.26(7)	Cd(1B)-O(2B)	2.31(7)	Cd(1C)-O(2A)	2.26(8)
< Cd(1A)-O >	2.26	< Cd(1B)-O >	2.28	< Cd(1C)-O >	2.28
Cd(2A)-O(2A)	2.87(6)	Cd(2B)-O(2B)	2.37(6)	Cd(2C)-O(2C)	2.25(5)
Cd(2A)-O(7A)	2.38(5)	Cd(2B)-O(7B)	2.33(6)	Cd(2C)-O(7C)	2.25(5)
Cd(2A)-O(8A)	2.20(6)	Cd(2B)-O(8C)	2.27(6)	Cd(2C)-O(9B)	2.18(5)
Cd(2A)-O(5B)	2.26(5)	Cd(2B)-O(5C)	2.21(6)	Cd(2C)-O(5A)	2.24(6)
Cd(2A)-O(3C)	2.26(6)	Cd(2B)-O(3B)	2.17(6)	Cd(2C)-O(3A)	2.34(6)
Cd(2A)-O(6A)	2.35(5)	Cd(2B)-O(6B)	2.77(6)	Cd(2C)-O(6C)	-------
< Cd(2A)-O >	2.29	< Cd(2B)-O >	2.27	< Cd(2C)-O >	2.25
Cd(3A)-O(4B)	2.15(7)	Cd(3B)-O(4C)	2.31(8)	Cd(3C)-O(4A)	2.13(7)
Cd(3A)-O(3A)	2.16(5)	Cd(3B)-O(3B)	2.24(6)	Cd(3C)-O(3C)	2.19(6)
Cd(3A)-O(5C)	2.35(6)	Cd(3B)-O(5B)	2.31(5)	Cd(3C)-O(5A)	2.28(6)
Cd(3A)-O(2A)	2.26(5)	Cd(3B)-O(2B)	-------	Cd(3C)-O(2C)	-------
Cd(3A)-O(7B)	2.34(5)	Cd(3B)-O(7A)	2.27(4)	Cd(3C)-O(7C)	2.27(4)
Cd(3A)-O(6B)	2.71(6)	Cd(3B)-O(6C)	2.53(6)	Cd(3C)-O(6A)	-------
Cd(3A)-O(4A)	-------	Cd(3B)-O(4B)	2.35(5)	Cd(3C)-O(4C)	2.36(5)
< Cd(3A)-O >	2.25	< Cd(3B)-O >	2.30	< Cd(3C)-O >	2.25

are considerable differences in bonding. Mn(1A), Mn(1B) and Mn(1C) have all gained a ligand, O(2), and retain the "long" bond found to exist between Zn(1) and O(4) in β-$Zn_3(PO_4)_2$ thereby having 5-fold coordination with a sixth oxygen atom more weakly bonded. Mn(2C) has lost its analogue of the weak Zn(2)-O(6) bond, and remains 5-coordinate. Mn(2B) remains weakly bonded to its sixth ligand, O(6B). The analogous bond to Mn(2A) has decreased in length, giving a Mn(2A)-O(6A) distance of 2.28 Å. This cation remains strongly bonded to only five oxygen atoms however, as its analogue of the short Zn(2)-O(2) bond has lengthened greatly to 2.82 Å. Mn(3A) retains the 5-fold coordination of Zn(2). Mn(3B) and Mn(3C) lose O(2B) and O(2C) respectively, but gain the new ligands O(4B) and O(4C). In addition, Mn(3B) acquires a sixth ligand, O(6C), at a distance of 2.37 Å. The average bond distances in each of these cation polyhedra are also given in Table (V-9). These averages include only M-O bonds below 2.45 Å in length, thereby neglecting the weakly bonded oxygen atoms.

The differences in the linkages between the cation polyhedra can be seen from Fig. (V-1) and Fig. (V-2). These figures are the β^1-$Mn_3(PO_4)_2$ analogues of Fig. (IV-1) and Fig. (IV-2) respectively. The closed ring of two $Zn(2)O_5$ and two $Zn(3)O_5$ polyhedra shown in Fig. (IV-1) is not complete in β^1-$Mn_3(PO_4)_2$. The spiral chains of polyhedra still exist around the 2_1 axes, as in β-$Zn_3(PO_4)_2$, but their connectivity is now higher. The new linkages occur between adjacent Mn(3) sites, creating three-membered rings with neighbouring Mn(2) sites.

Fig. (V-1) Cation polyhedra linkages in β^1-$Mn_3(PO_4)_2$. This figure is the analogue of Fig. (IV-1) for β-$Zn_3(PO_4)_2$. The solid bonds denote M-O distances that are significantly shorter here than in β-$Zn_3(PO_4)_2$, and the bonds represented by broken lines are significantly longer than the analogous β-$Zn_3(PO_4)_2$ bonds. The rings of MO_5 polyhedra are not closed here and the infinite chains do not exist as they do in β-$Zn_3(PO_4)_2$.

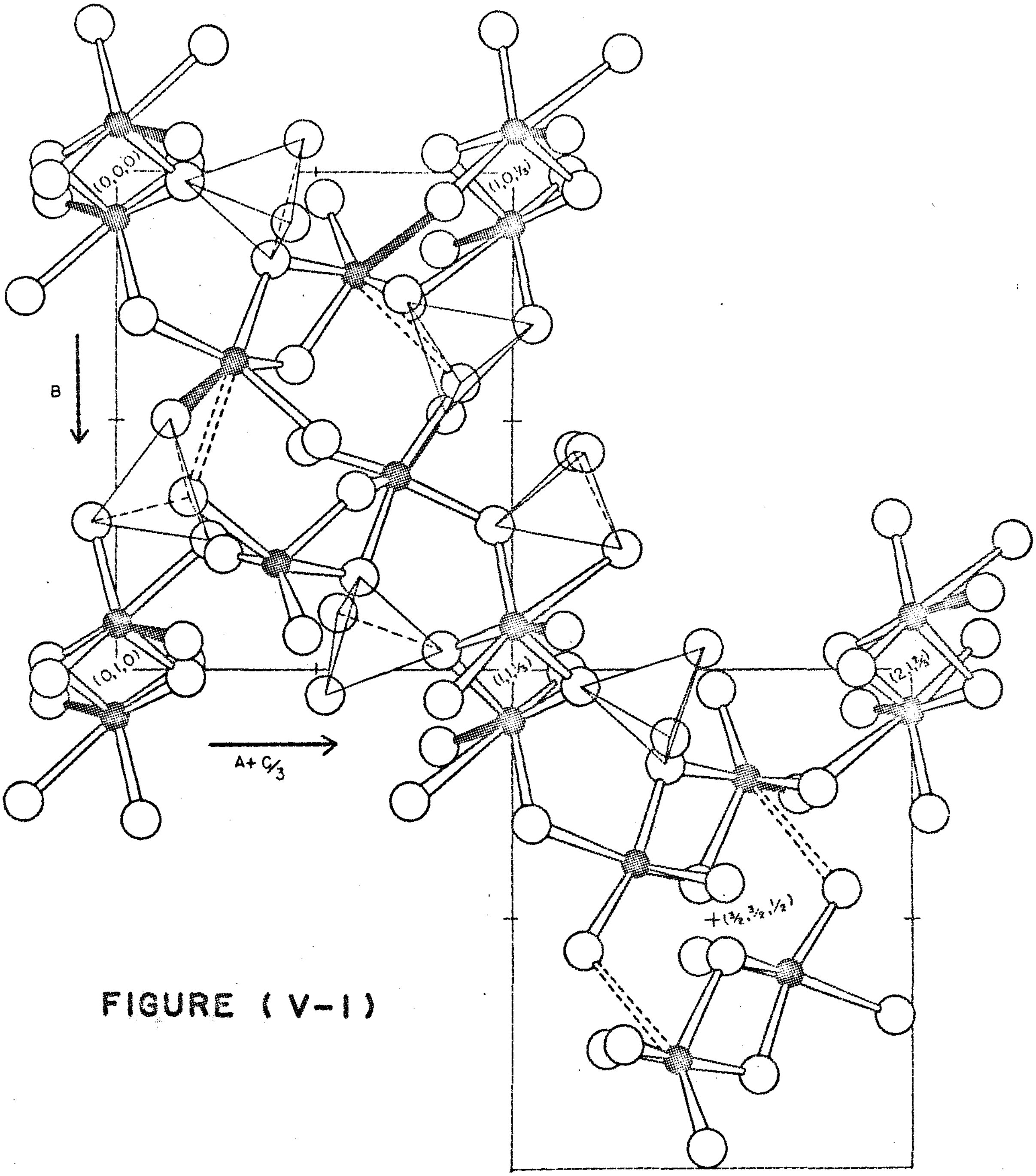
(0,0,0)
(1,0,1/3)
B
(0,1,0)
(1,1,1/3)
(2,1,2/3)
A+C/3
+(3/2,3/2,1/2)

FIGURE (V-1)

Fig. (V-2) Spiral cation polyhedra chains in β^1-$Mn_3(PO_4)_2$. This figure is the analogue of Fig. (IV-2) for β-$Zn_3(PO_4)_2$ except that only 1/2 of each spiral is shown here. The solid bonds denote M-O distances that are significantly shorter than the corresponding ones in Fig. (IV-2), and the dashed bonds denote those that are significantly longer in the β^1 structure.

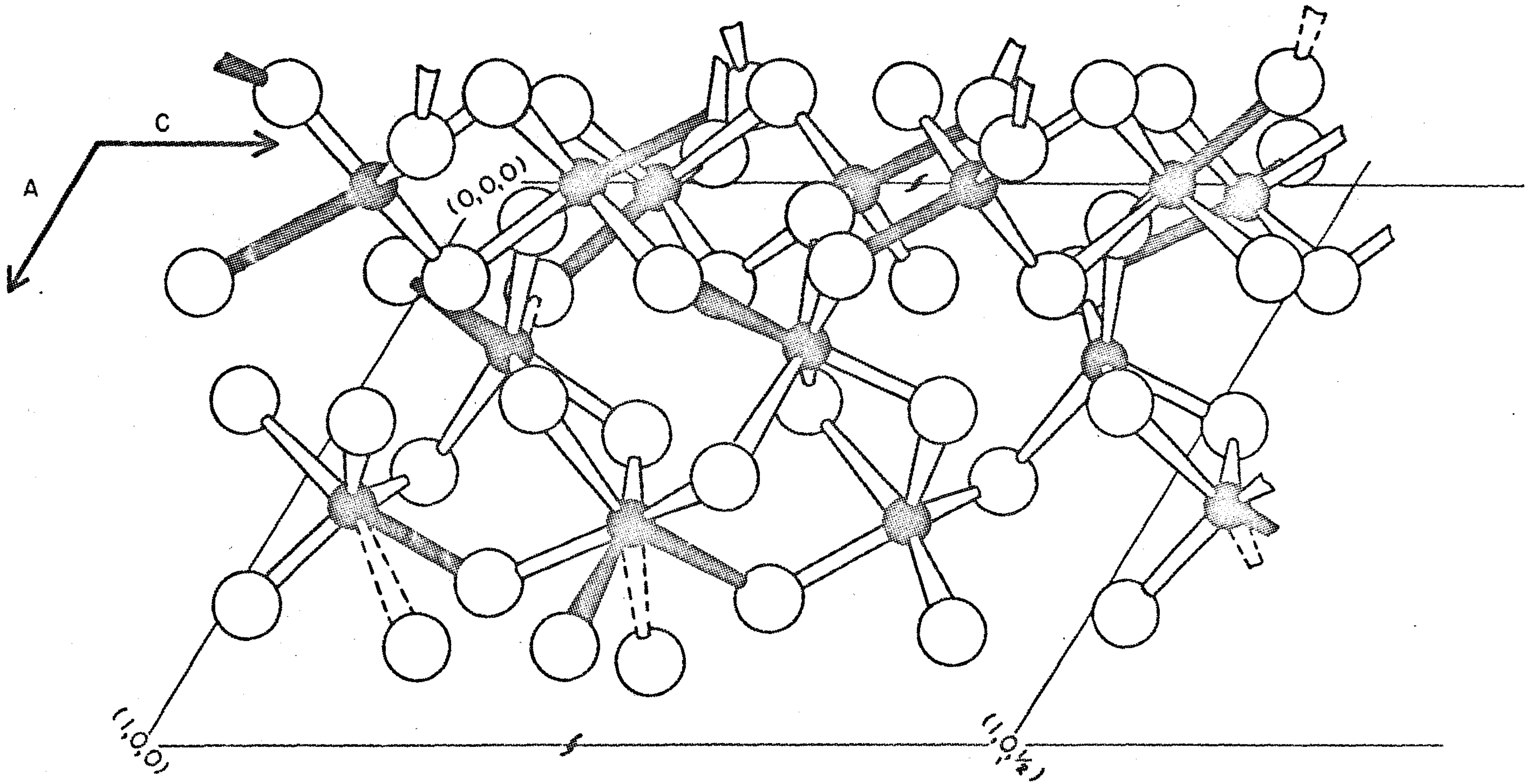
C
A
(0,0,0)
(1,0,0)
(1,0,½)

FIGURE (V-2)

There are also more linkages between Mn(1) and Mn(2) sites. In Fig. (V-1) and Fig. (V-2) these new linkages, which do not correspond to strong Zn-O bonds in β-$Zn_3(PO_4)_2$, are shown in black, while the weak Mn-O bonds which are analogues of stronger Zn-O bonds are shown with broken lines. As with the averages in Table (V-9) the dividing point between a "weak" and a "strong" bond has been arbitrarily set at 2.45 Å.

β^1-$Cd_3(PO_4)_2$ can be considered, within the limits of its incomplete refinement, to be isostructural with β^1-$Mn_3(PO_4)_2$. The cation coordination is the same, with the average Cd-O bond distance being approximately 5% larger.

TABLE (V-10)

Bond angles subtended at oxygen atoms in β^1-$Mn_3(PO_4)_2$

Bonded atoms	Angle (°)	Sum of angles (°)	Bonded atoms	Angle (°)	Sum of angles (°)
Mn(1A)-O(1A)-Mn(1A)'	106.0	359.9	Mn(2B)-O(5C)-Mn(3A)	97.4	353.5
Mn(1A)-O(1A)-P(1A)	116.4		Mn(2B)-O(5C)-P(1C)	127.5	
Mn(1A)'-O(1A)-P(1A)	137.5		Mn(3A)-O(5C)-P(1C)	128.6	
Mn(1B)-O(1B)-Mn(1C)	98.6	354.2	Mn(2A)-O(7A)-Mn(3B)	102.7	353.4
Mn(1B)-O(1B)-P(1B)	115.8		Mn(2A)-O(7A)-P(1A)	124.2	
Mn(1C)-O(1B)-P(1B)	139.8		Mn(3B)-O(7A)-P(1A)	126.5	
Mn(1B)-O(1C)-Mn(1C)	98.3	359.9	Mn(2B)-O(7B)-Mn(3A)	97.0	355.2
Mn(1B)-O(1C)-P(1C)	140.4		Mn(2B)-O(7B)-P(1B)	133.1	
Mn(1C)-O(1C)-P(1C)	121.2		Mn(3A)-O(7B)-P(1B)	125.1	
Mn(3A)-O(3A)-Mn(2C)	116.7	358.8	Mn(2C)-O(7C)-Mn(3C)	99.0	355.3
Mn(3A)-O(3A)-P(1A)	125.4		Mn(2C)-O(7C)-P(1C)	125.5	
Mn(2C)-O(3A)-P(1A)	116.7		Mn(3C)-O(7C)-P(1C)	130.8	
Mn(3B)-O(3B)-Mn(2B)	111.0	358.8	Mn(1C)-O(2A)-Mn(3A)	110.5	354.7
Mn(3B)-O(3B)-P(1B)	125.6		Mn(1C)-O(2A)-P(2A)	121.3	
Mn(2B)-O(3B)-P(1B)	122.2		Mn(3A)-O(2A)-P(2A)	122.9	
Mn(3C)-O(3C)-Mn(2A)	100.2	355.3	Mn(1B)-O(2B)-Mn(2B)	118.0	354.8
Mn(3C)-O(3C)-P(1C)	124.4		Mn(1B)-O(2B)-P(2B)	139.1	
Mn(2A)-O(3C)-P(1C)	130.7		Mn(2B)-O(2B)-P(2B)	97.7	
Mn(2C)-O(5A)-Mn(3C)	100.6	352.0	Mn(1A)-O(2C)-Mn(2C)	112.6	358.6
Mn(2C)-O(5A)-P(1A)	131.0		Mn(1A)-O(2C)-P(2C)	126.5	
Mn(3C)-O(5A)-P(1A)	120.4		Mn(2C)-O(2C)-P(2C)	119.5	
Mn(2A)-O(5B)-Mn(3B)	105.6	348.8	Mn(3C)-O(4A)-Mn(1A)	123.3	351.1
Mn(2A)-O(5B)-P(1B)	122.5		Mn(3C)-O(4A)-P(2A)	137.3	
Mn(3B)-O(5B)-P(1B)	120.7		Mn(1A)-O(4A)-P(2A)	90.5	
Mn(3A)-O(4B)-Mn(3B)	121.9	346.8	Mn(1B)-O(6C)-Mn(3B)	134.4	356.6
Mn(3A)-O(4B)-P(2B)	112.8		Mn(1B)-O(6C)-P(2C)	128.9	
Mn(3B)-O(4B)-P(2B)	112.1		Mn(3B)-O(6C)-P(2C)	93.3	
Mn(3B)-O(4C)-Mn(3C)	125.6	337.7	Mn(1A)-O(8A)-Mn(2A)	130.3	360.0
Mn(3B)-O(4C)-P(2C)	99.0		Mn(1A)-O(8A)-P(2A)	98.7	
Mn(3C)-O(4C)-P(2C)	113.1		Mn(2A)-O(8A)-P(2A)	131.0	
Mn(1C)-O(6A)-Mn(2A)	121.1	358.7	Mn(1C)-O(8B)-Mn(2C)	125.4	360.0
Mn(1C)-O(6A)-P(2A)	131.3		Mn(1C)-O(8B)-P(2B)	107.8	
Mn(2A)-O(6A)-P(2A)	106.3		Mn(2C)-O(8B)-P(2B)	126.8	
Mn(1A)-O(6B)-Mn(2B)	113.9	332.4	Mn(1B)-O(8C)-Mn(2B)	126.1	359.8
Mn(1A)-O(6B)-P(2B)	127.5		Mn(1B)-O(8C)-P(2C)	105.9	
Mn(2B)-O(6B)-P(2B)	91.0		Mn(2B)-O(8C)-P(2C)	127.8	

CHAPTER VI

THE GRAFTONITE STRUCTURE

A. Occurrence of the Graftonite Structure

The mineral "graftonite" is an anhydrous orthophosphate of Fe^{++}, Mn^{++} and Ca^{++}.(11) It occurs in nature in close association with the mineral "sarcopside",(11) whose structure is said to be similar to that of lithiophilite,(35) although the details of this investigation have not been made available. The unit cell parameters and space group have been determined for the mineral(33) and these are listed in Table (VI-1), together with the lattice parameters of other compounds which have the graftonite structure.

It was noted in Ch. V that $Mn_3(PO_4)_2$ could be prepared with the graftonite structure, and the lattice parameters of this compound, which will be referred to as Mn-graftonite, are included in Table (VI-1). Single-crystal X-ray photographs of Mn-graftonite and a sample of the mineral confirmed the similarity of the two structures.

The phase diagram of the $(Zn, Cd)_3(PO_4)_2$ system which is reproduced in Fig. (I-1), shows the existence of the two solid solution regions, "B" and "C", the former having compositions near $Zn_2Cd(PO_4)_2$ and the latter near $ZnCd_2(PO_4)_2$. The powder patterns quoted for the B and C solid solution structures(4) bear a striking similarity to the pattern of the mineral graftonite.

TABLE (VI-1)

Lattice parameters of graftonite-like compounds

Parameter	Mineral(33)	Mn-graftonite	B-graftonite	C-graftonite
a (Å)	8.87	8.81	9.032(4)	9.056
b (Å)	11.57	11.45	11.417(5)	11.75
c (Å)	6.17	6.27	5.952(6)	6.190
β (°)	99.2	99.	98.8(2)	100.25
V (Å^3)	625.	625.	606.(1)	648.
Z	4	4	4	4
space group	$P\text{-}2_1/c$	$P\text{-}2_1/c$	$P\text{-}2_1/c$	$P\text{-}2_1/c$

Single crystals with compositions which lay within the B and C regions of the phase diagram were prepared, and preliminary photographs showed that both these solid solutions had the graftonite structure. There were small differences in lattice parameters between the B and C region crystals, and also some changes in the intensities of the reflections. The differences between these solid solution structures will be discussed later.

The determination of the graftonite structure was undertaken with a single crystal of approximate composition $(Zn_{0.75}Cd_{0.25})_3(PO_4)_2$ which lies in the B region of the phase diagram. It was felt that the presence of the heavy Cd^{++} ions in the sample would simplify the solution of the Patterson functions, and, at that time, single crystals in the C region had not been prepared. This structure determination is reported in the following sections.

B. Preparation

A sample of composition $(Zn_{1-x}Cd_x)_3(PO_4)_2$ was prepared by reacting stoichiometric proportions of $Zn_3(PO_4)_2$, $CdCO_3$ and H_3PO_4, according to the equation

$$(1-x)Zn_3(PO_4)_2 + 3xCdCO_3 + 2xH_3PO_4 \longrightarrow (Zn_{1-x}Cd_x)_3(PO_4)_2 + 3xH_2O + 3xCO_2 \qquad \text{(VI-1)}$$

where x=0.20 . The initial reaction was carried out in an aqueous slurry, and the mixture was then evaporated to dryness, ground finely with mortar and pestle, and heated to about 600°C. in a covered silica crucible to carry the reaction to completion. The sample was then transferred to a vycor tube, and fused at a temperature slightly above 1000°C.

From the phase diagram in Fig. (I-1), it is seen that the sample corresponded to a eutectic composition, and therefore the crystallization of a β-$Zn_3(PO_4)_2$ solid solution and B solid solution should take place simultaneously. According to the phase diagram, the B-type crystals should correspond to a composition of $(Zn_{0.75}Cd_{0.25})_3(PO_4)_2$.

After cooling the sample slowly through the freezing point(4) and then quenching more rapidly from about 950°C. down to room temperature, the vycor tube and sample were broken apart. The sample contained the characteristic cylindrical crystals found to occur in Mn-graftonite. These crystals were intergrown with a second phase which consisted of flat crystalline plates. The cylindrical crystals were found to have lattice parameters comparable to those of the other graftonite-like compounds, with the c axis being the axis of the cylinder. The flat crystalline plates were examined and found to have the β-$Zn_3(PO_4)_2$ structure.

A small single-crystal of the graftonite-like phase, which will be referred to as B-graftonite, was selected and mounted so that it could be rotated around its long axis. The dimensions of this crystal were found to be approximately 0.05 mm in diameter, and 0.5 mm in length. This crystal was used in the determination of accurate lattice parameters and in the collection of all the intensity data reported here.

C. Lattice Parameters

An hk0 Weissenberg photograph was taken with Cu-Kα radiation, and powder lines from Al_2O_3 (corundum) were superimposed near each edge of the film. The values of a* and b* were determined by least squares refinement of the corrected θ values of the high angle reflections, following the procedure outlined in Ch. IV. Precession photographs of the h0ℓ and 0kℓ planes were taken with Mo-Kα radiation. The β angle was measured directly from the h0ℓ photograph, with the assumption that any film shrinkage was isotropic and that the angle would not be distorted. The spacings between the rows of reflections were measured in the b* and c* directions on the 0kℓ photograph, and the average inter-row spacings determined. Again assuming isotropic film shrinkage, the value of c* was determined using the value for b*, obtained from the hk0 Weissenberg photograph, as a calibration standard. The corresponding real lattice parameters are listed in Table (VI-1) with their esd's in parentheses.

D. Intensity Data

Mo-Kα radiation was employed in all intensity measurements in order to minimize absorption by the crystal. Integrated precession photographs were taken of the h0ℓ and 0kℓ planes, and the intensities measured with a Leeds & Northrup microdensitometer. The intensities of the reflections in the planes hkL, with L=0,1,..5, were measured on the diffractometer and dead-time corrections calculated, according to the methods outlined in Ch. III.

The linear absorption coefficient for the crystals of B-graftonite with this composition, for Mo-Kα radiation, is 121 cm^{-1}. For a cylindrical crystal of 0.05 mm diameter, the maximum correction factor between any two reflections within a layer-line is approximately 1.7%. The errors due to absorption were therefore negligible. Lorentz and polarization corrections were applied to all measured intensity data.

E. The Trial Solution

The positions of the three cations were deduced with the aid of generalized Patterson projections, down the short c axis of the unit cell, which were prepared using the hk0, hk1,..hk5 data.

Generalized Patterson projections can be defined as(36)

$$P_L(uv) = P'_L(uv) + iP''_L(uv) = c\int_0^1 P(uvw)\exp(2\pi iLw)\,dw \qquad \text{(VI-2)}$$

which reduces to

$$P'_L(uv) = \frac{1}{2A}\sum_{hk}\left[\left|F_{hkL}\right|^2 + \left|F_{\bar{h}\bar{k}L}\right|^2\right]\cos 2\pi(hu + kv)$$

and (VI-3)

$$P''_L(uv) = \frac{1}{2A}\sum_{hk}\left[\left|F_{\bar{h}\bar{k}L}\right|^2 - \left|F_{hkL}\right|^2\right]\sin 2\pi(hu + kv)$$

in the cases where Friedel's Law(37) holds, as it does for all centro-symmetric structures. In these cases a generalized projection can be calculated from the data contained within one layer-line.

When L=0, $P_L(uv)$ is the usual Patterson projection down the c axis defined in Eqn. (II-10).

The usefulness of generalized projections is that they yield information concerning the third coordinate, w, of the Patterson peaks, without the necessity of calculating the full three dimensional synthesis. For a projection where all the peaks are resolved,

$$P'_L(uv) = P_0(uv)\cos 2\pi Lw$$

and (VI-4)

$$P''_L(uv) = P_0(uv)\sin 2\pi Lw$$

Even if the Patterson peaks are not all resolved in $P_0(uv)$, the use of several of these generalized projections will usually enable them to be resolved, and their individual w coordinates determined.

A trial solution for the coordinates of the three cations in the structure was obtained through a systematic inspection of the $P'_L(uv)$ diagrams. As $|F_{hk\ell}| \neq |F_{hk\bar{\ell}}|$ in the space group $P\text{-}2_1/c$, it would have been possible to use the $P''_L(uv)$ as well, but the extra resolution that they would have afforded was not necessary to obtain the correct trial solution. A single cycle of least squares refinement using these trial cation coordinates resulted in a value of 0.42 for R_2, supporting the validity of these positions. Difference syntheses for each of the axial projections were calculated at this point, but were inconsistent in their indications of possible phosphorus and oxygen atom positions.

The rather short c axis length of 5.95 Å, together with the c glide operation, places severe steric restrictions on the possible locations of the phosphorus atoms. These atoms cannot approach the cations too closely due to the tetrahedral arrangement of oxygen atoms around each phosphorus atom. In addition, their high nominal positive charges would tend to keep them apart. In the structures of β-$Zn_3(PO_4)_2$ and β^1-$Mn_3(PO_4)_2$ the closest approach of a cation and a phosphorus atom is 2.80 Å. In the majority of cases, this distance is greater than 3.0 Å. The possible positions for the two phosphorus atoms were determined geometrically, using the proposed cation positions, and the criterion that no cation or other phosphorus atom could lie within 3.0 Å. Only two locations in the asymmetric unit were consistent with this criterion; (0.14,0.13,0.45) and (0.62,0.31,0.27). Phosphorus atoms were then placed at these positions.

Further difference syntheses failed to indicate the positions of the oxygen atoms with any degree of certainty. Again, a geometric criterion was used to locate these atoms. The structures of β-$Zn_3(PO_4)_2$ and β^1-$Mn_3(PO_4)_2$ had shown that the environment around each oxygen atom was very nearly planar, and that this planarity seemed to be a general feature of the anhydrous orthophosphates of divalent cations such as Zn^{++}, Mn^{++} and Cd^{++}. The probable oxygen atom locations were determined by requiring them to have this planar environment, and to make bonds of 1.5 Å and 2.0 Å in length to a phosphorus atom and two cations respectively. The number of possible positions was reduced by requiring the oxygen atoms to be approximately tetrahedrally arrayed about each phosphorus atom.

Subsequent cycles of least squares refinement showed that all the oxygen atom positions around P(1) were essentially correct, but two of the atoms surrounding P(2) developed abnormally high temperature factors. The positions of these two atoms were redetermined, assuming the PO_4 group to be an ideal tetrahedron whose orientation was fixed by the phosphorus atom and the two well-behaved oxygen atoms. Further least squares refinement indicated that these new positions were correct.

F. The Refinement

As there were the two different cations, Zn^{++} and Cd^{++} in the crystal, the cation scattering factors had to be adjusted to correspond to their relative abundances. This was accomplished by calculating the cation contribution to the structure factors using the equation,

$$F_{cation} = \sum_{j=1}^{3} [k_j f_{Zn}(H) + (1-k_j) f_{Cd}(H)] \exp 2\pi i(\underline{H}.\underline{r}_j) \cdot \exp(-\underline{H}.\underline{\underline{\beta}}_j.\underline{H}) \qquad \text{(VI-5)}$$

where an overall Zn^{++} concentration of 75 mole per cent would require $k_1+k_2+k_3 = 2.25$.

The refinement of the trial structure was undertaken with unit weights, isotropic temperature factors on all the atoms, and with the cations randomly distributed; k_j equal to 0.75 for all three sites. The molecular geometry was calculated after each least squares cycle and deviations from regularity of the PO_4 tetrahedra were noted. If a P-O bond length deviated from the accepted average value(31) of 1.54 Å by more than 0.05 Å, the oxygen atom was shifted radially to a position exactly 1.54 Å from the phosphorus atom. After a number of cycles of refinement, the magnitude of the shifts in the coordinates had diminished to a point where this readjustment was no longer necessary. The reliability index had remained at a relatively high value, approximately 0.2, until this stage. This unusually high dependence of the reliability index on the exact oxygen atom coordinates was probably responsible for the difficulties encountered in the interpretation of the earlier difference syntheses which had been calculated without contributions from these atoms.

The isotropic temperature factors for the three cations were 0.46, 3.00 and 1.14 $Å^2$ for M(1), M(2) and M(3) respectively. This indicated that the Zn^{++} and Cd^{++} were not randomly distributed among the three sites, but that Cd^{++} was selectively entering the M(1) site in preference to the other two cation sites. All of the Cd^{++} ions were assigned to the M(1) site, with M(2) and M(3) restricted to Zn^{++}. The values of k_j in Eqn. (VI-5) which correspond to this cation distribution are, k_1=0.25, and k_2=k_3=1.0 . The temperature factors on all the atoms were converted to anisotropic form and the refinement continued with unit weights. The best value of R_2 that could be obtained under these conditions was 0.101 .

The discrepancies between the observed and calculated structure factors were, on the average, considerably larger than the differences between the $|F_o|$ values for the reflections which had been measured more than once. This suggested that further refinement was necessary.

In addition, the anisotropic temperature factors of about half of the atoms were non-positive-definite†, possibly indicating some disorder in the structure. The values of k_j in Eqn. (VI-5) were allowed to vary in succeeding cycles of refinement. The weighting scheme was also changed; the weights were calculated by the equation

$$w_i^{-1} = 5.0 + 0.35|F_o|_i \qquad \text{(VI-6)}$$

where these co-efficients were determined in accordance with Cruickshank's criterion.(20) The reliability index was lowered to 0.079 in three cycles of refinement. Before the third cycle, the multiply-measured reflections were averaged in the manner stated in Ch. IV.

The values for the parameters k_j were 0.35(4), 1.07(3) and 0.94(3) for j=1, 2 and 3 respectively. Unless some of the cation sites are unoccupied, $0 \leqq k_j \leqq 1$, and the values of k_2 and k_3 probably are not meaningfully different from unity. k_2 and k_3 were reset to 1.0 and a final cycle of least squares refinement carried out in which k_1 was still allowed to vary. The value of k_1 became 0.38(4), and the least squares residual R_2 assumed the value 0.089 . During this final cycle, all parameter changes were smaller than the esd's of the parameters.

---

† An anisotropic temperature factor is non-positive-definite when any of the diagonal elements of the temperature factor matrix $\underline{\beta}$, the co-factors of any diagonal element, or the determinant of the matrix, are negative or zero. This corresponds to a concavity in the surface of the vibrational ellipsoid, so that it no longer corresponds to a physically meaningful thermal motion about a single fixed point.

The final atomic parameters and their esd's are listed in Table (VI-2). The reliability indices, R_1 and R_2, are summarized in Table (VI-3). Table (VI-4) shows the agreement between the observed and calculated structure factors for the 1999 independent reflections. 888 of these reflections were too weak to be observed (marked by an asterisk (*) in the table), and only 30 of these reflections have $|F_c| > |F_{min}|$. For these 30 reflections, the fraction of $|F_{min}|$ used to calculate the discrepancy was 0.85 . The $|F_o|$ values of 20 reflections were classed as unreliable, and these reflections are marked with the symbol Ø in Table (VI-4).

G. Description of the Structure

The refinement indicates that Cd^{++} exhibits a strong preference for the first cation site, M(1). The final value of k_1=0.38 corresponds to a total Cd^{++} content in the crystal of 21 mole per cent, which is slightly lower than the 25 mole per cent predicted from the phase diagram. The site which contains the Cd^{++} is seven-fold coordinate, with an average M-O distance of 2.33±0.18 Å. The shortest distance is 2.09 Å and the longest is 2.60 Å. The cation M(2), which is entirely Zn^{++}, is bonded to four oxygen atoms at the corners of a irregular tetrahedron, at an average distance of 1.98±0.09 Å. M(3) also consists primarily of Zn^{++} and is bonded to five oxygen atoms. These atoms are arranged at the corners of an irregular trigonal bipyramid, where the two axial bonds average 2.15±0.04 Å in length. The three equatorial oxygen atoms have an average M-O bond distance of

TABLE (VI-2)

Atomic parameters in B-graftonite

Atom	x=X/a	y=Y/b	z=Z/c	U_{11}(Å^2)	U_{22}(Å^2)	U_{33}(Å^2)	U_{12}(Å^2)	U_{13}(Å^2)	U_{23}(Å^2)
M(1)	0.9445(2)	0.3787(1)	0.3321(3)	0.0139(7)	0.0100(6)	0.0267(16)	-.0008(5)	-.0028(5)	-.0059(5)
M(2)	0.6960(3)	0.0560(2)	0.3243(4)	0.0445(14)	0.0383(13)	0.0052(16)	0.0221(11)	0.0053(9)	0.0026(8)
M(3)	0.3694(2)	0.1942(1)	0.1234(3)	0.0095(8)	0.0086(7)	0.0009(15)	0.0016(6)	0.0004(6)	-.0008(6)
P(1)	0.1049(4)	0.1363(3)	0.3970(7)	0.0046(14)	0.0098(14)	0.0044(22)	-.0013(10)	0.0028(12)	-.0017(11)
O(1)	0.0844(10)	0.0658(9)	0.1760(21)	0.0034(39)	0.0092(42)	0.0168(66)	0.0026(29)	0.0012(35)	-.0046(35)
O(3)	0.9617(14)	0.2033(11)	0.4301(24)	0.0156(60)	0.0269(62)	0.0211(80)	0.0075(44)	0.0147(49)	-.0009(46)
O(5)	0.2354(11)	0.2231(10)	0.3777(21)	0.0056(42)	0.0202(50)	0.0134(73)	-.0081(35)	0.0055(38)	-.0014(42)
O(7)	0.1441(13)	0.0598(10)	0.6063(21)	0.0175(51)	0.0185(51)	0.0146(72)	-.0051(41)	0.0027(42)	0.0068(42)
P(2)	0.6074(4)	0.3089(3)	0.3059(7)	0.0033(14)	0.0066(13)	0.0046(24)	0.0009(10)	0.0025(11)	0.0002(11)
O(2)	0.4776(12)	0.3244(10)	0.3199(19)	0.0093(46)	0.0207(52)	0.0035(60)	0.0044(35)	0.0016(38)	0.0057(39)
O(4)	0.6957(11)	0.3722(10)	0.1128(20)	0.0055(40)	0.0167(45)	0.0123(64)	-.0026(35)	0.0074(34)	0.0018(39)
O(6)	0.7230(11)	0.0969(9)	0.0206(18)	0.0061(37)	0.0170(47)	0.0009(61)	-.0005(32)	0.0016(34)	0.0007(36)
O(8)	0.4590(11)	0.0353(8)	0.2353(21)	0.0082(41)	0.0074(42)	0.0164(69)	0.0014(31)	0.0017(37)	-.0063(35)

TABLE (VI-3)

Residuals for B-graftonite

Residual	Conditions	# of refl.	Value of residual
R_2	all reflections	1999	0.089
R_1	all reflections	1999	0.074
R_2	obs. refl. only	1111	0.087
R_1	obs. refl. only	1111	0.068

TABLE VI-4 B-GRAFTONITE OBSERVED AND CALCULATED STRUCTURE FACTORS (x10)

UNOBSERVED REFLECTIONS ARE MARKED WITH AN ASTERISK (*), AND UNRELIABLE REFLECTIONS WITH THE SYMBOL (#).

H	K		|FOBS|	FCALC
H	K			L=0
0	4		1869	-1764
0	6		631	-527
0	8		312	-291
0	10		509	413
0	12		977	-1041
0	14	*	302	-92
0	16		649	644
0	18	*	362	-195
1	3		2011	1939
1	4		1446	-1378
1	5		340	364
1	6		362	-306
1	7		865	-730
1	8		1554	1534
1	9	*	226	292
1	10		344	-343
1	11	*	256	-124
1	12		609	-633
1	13	*	287	83
1	14	*	303	204
1	15	*	318	-73
1	16		424	461
1	17	*	348	-222
2	0		555	555
2	1		726	559
2	2		391	-356
2	3		1462	-1549
2	4		883	-899
2	5		1078	-1080
2	6		520	466
2	7		200	249
2	8		863	844
2	9		355	-323
2	10		268	279
2	11		1011	982
2	12		395	-396
2	13	*	290	-18
2	14	*	305	-197
2	15		480	-510
2	16	*	336	222
2	17		206	266
2	18	*	364	8
3	0		1947	2043
3	1		167	-162
3	2		155	-90
3	3	*	159	-34
3	4		548	-560
3	5		607	-581
3	6		253	-245
3	7		1304	-1303
3	8		278	-280
3	9		371	374
3	10		492	519
3	11		480	502
3	12		483	-489
3	13	*	295	211
3	14	*	310	-146
3	15	*	325	-104
3	16		333	342
3	17	*	354	-191
4	0		712	-700
4	1		1278	1253
4	2		314	270
4	3		1289	1325
4	4		144	146
4	5	*	196	43
4	6		300	-278
4	7		305	-303
4	8		489	495
4	9		612	562
4	10		325	-363
4	11		514	520
4	12	*	287	66
4	13		404	-377
4	14	*	316	-82
4	15		619	-563
4	16	*	345	-133
5	0		856	-884
5	1		1323	1273
5	2		859	-873
5	3		497	471
5	4		574	567
5	5		807	-849
5	6	*	221	96
5	7		483	-470
5	8		338	-263
5	9		263	-215
5	10		828	829
5	11		751	718
5	12		346	319
5	13	*	309	-344
5	14	*	323	-174
5	15		465	-493
5	16	*	351	-269
5	17		343	416
5	18	*	376	-165
6	0		695	-573
6	1	*	205	90
6	2	*	208	7
6	3		888	847
6	4		855	802
6	5		651	-682
6	6		464	390
6	7		997	-952
6	8		681	-637
6	9		682	771
6	10		193	-163
6	11	*	293	267
7	0		912	-858
7	1		923	959
7	2		741	738
7	3	*	232	207
7	4		428	374
7	5		277	-383
7	6		296	-413
7	7	*	261	5
7	8	*	271	-222
7	9		386	393
7	10		486	-455
7	11		346	420
7	12		380	446
7	13		698	-691
7	14	*	342	165
7	15		396	-368
7	16	*	366	-362
8	0	*	243	-163
8	1		896	978
8	2		734	-695
8	3	#	465	641
8	4		453	490
8	5	*	261	-144
8	6		203	244
8	7	*	277	-239
8	8		666	-699
8	9	*	296	-135
8	10		495	457
8	11	*	318	148
8	12		445	413
8	13	*	341	-79
9	0		831	-937
9	1		601	-563
9	2	*	266	6
9	3	*	269	-34
9	4		586	686
9	5	*	279	-156
9	6		308	369
9	7		440	-421
9	8	*	302	-78
9	9	*	311	288
9	10		592	-598
9	11	*	332	-160
10	0	*	283	-145
10	1	*	284	168
10	2	*	285	258
10	3		335	-416
10	4	*	292	20
10	5	*	298	107
10	6	*	304	-201
10	7		710	697
10	8	*	319	-224
10	9		305	-266
10	10	*	336	-229
11	0	*	128	-75
11	1	*	303	-252
11	2	*	305	-209
11	3	*	308	91
11	4	*	311	263
11	5		532	511
11	6	*	322	273
12	0		588	-668
12	1		531	-500
12	2	*	325	147
12	3		624	-537
12	4	*	330	229
13	0	*	342	260
H	K			L=1
0	1		228	173
0	2		265	332
0	3		851	-774
0	4	*	106	49
0	5	*	116	-63
0	6		2171	-2278
0	7	*	135	-86
0	8		370	-408
0	9		486	480
0	10		595	570
0	11		602	630
0	12		317	293
0	13		527	-523
0	14		180	137
0	15	*	308	9
1	2		897	869
1	3		1865	1912
1	4		435	418
1	5		1116	-968
1	6		926	-910
1	7	*	191	121
1	8	*	206	-47
1	9		484	-496
1	10		1024	1002
1	11		463	-488
1	12	*	264	160
1	13	*	279	205
1	14		524	-470
1	15	*	309	-249
2	1	#	290	175
2	2		2436	2545
2	3		267	-274
2	4		235	-229
2	5		514	535
2	6		265	-214
2	7		718	-668
2	8	*	211	-86
2	9	*	225	26
2	10		497	523
2	11		601	583
2	12	*	268	120
2	13	*	282	-118
2	14		911	-919
2	15	*	312	-80
3	1		1515	-1514
3	2		579	501
3	3	*	158	31
3	4		980	873
3	5		884	874
3	6		2295	-2364
3	7	*	205	23
3	8	*	218	70
3	9	*	232	-4
3	10		1013	1051
3	11		273	277
3	12	*	273	-212
3	13		219	183
3	14	*	302	4
4	1		250	-148
4	2		538	563
4	3		1476	1523
4	4		1137	-1150
4	5	*	194	-118
4	6		788	-843
4	7	*	216	-202
4	8	*	228	218
4	9		736	-703
4	10		532	553
4	11		218	-151
4	12		284	339
4	13		490	513
4	14		590	-573
4	15	#	322	-426
5	1		191	-223
5	2		943	1032
5	3		445	-461
5	4		710	786
5	5		921	879
5	6	*	218	-71
5	7		492	-574
5	8	*	239	-185
5	9		500	-514
5	10	*	263	108
5	11		556	572
5	12	*	289	26
6	1		1327	-1371
6	2		319	-297
6	3		443	481
6	4		422	451
6	5		624	697
6	6		412	-366
6	7		456	487
6	8	*	252	123
6	9		262	-274
6	10	*	275	50
6	11	*	287	-151
6	12	#	299	-390
6	13		531	470
6	14	*	324	211
7	1	*	223	-221
7	2		460	-501
7	3		364	354
7	4		625	-633
7	5	*	241	255
7	6		613	629
7	7		427	-409
7	8	*	266	-146
7	9		393	-324
7	10		396	-350
7	11	*	298	237
7	12	*	310	299
7	13		500	524
7	14	*	334	-64
8	1	*	242	40
8	2		412	-440
8	3	*	247	81
8	4		850	824
8	5		848	785
8	6		640	583
8	7		532	-607
8	8	*	281	21
8	9		506	-525
8	10		635	-632
8	11	*	311	143
9	1		659	-591
9	2		946	-891
9	3		412	484
9	4	*	270	182
9	5	*	275	-82
9	6		489	531
9	7	*	289	90
10	1	*	280	47
10	2		369	-308
10	3	*	284	190
10	4		535	-472
10	5	*	293	232
10	6		607	722
10	7		468	-467
10	8	*	313	-153
10	9	*	321	-77
10	10		464	-459
10	11	*	338	253
11	1	*	299	70
11	2	#	592	-763
11	3	*	303	-51
12	1	*	318	86
H	K			L=-1
1	3		888	-813
1	4		290	257
1	5		866	-850
1	6		746	-729
1	7		794	756
1	8		181	-222
1	9		1030	968
1	10		336	-337
1	11	*	248	-97
1	12		436	-419
1	13		403	-336
1	14		926	939
1	15	*	308	39
2	2	*	120	80
2	3	*	134	107
2	4		813	-733
2	5		1367	-1273
2	6		400	422
2	7		786	760
2	8		423	373
2	9		119	102
2	10	*	237	85
2	11		1097	-1118
2	12	*	266	46
2	13	*	281	-170
2	14		298	-301
2	15	*	310	213
3	1		2212	2147
3	2		630	557
3	3		1256	-1235
3	4		487	494
3	5		1000	-901
3	6		341	375
3	7	*	201	-75
3	8		369	378
3	9		644	598
3	10		203	-217
3	11	*	256	48
3	12		243	-239
3	13		691	-684
3	14		304	-273
3	15		450	476
3	16	*	328	-7
4	1		234	204
4	2	*	160	-167
4	3		882	-878
4	4		1006	874
4	5		1405	-1354
4	6		998	-923
4	7		1535	1567
4	8		355	-295
4	9		674	681
4	10		286	267
4	11		534	-570
4	12	*	277	-55
4	13	*	291	-207
4	14		412	386
4	15	*	319	227
5	1		1103	1214
5	2		374	268
5	3	*	185	-71
5	4		1540	-1570
5	5		746	-797
5	6		265	-252
5	7		505	498
5	8		309	-246
5	9	*	246	270
5	10		446	504
5	11		797	-757
5	12		614	632
5	13		329	-351
5	14		510	-495
5	15	*	326	213
6	1		688	730
6	2		331	390
6	3		843	-903
6	4		899	935
6	5	*	217	79
6	6		651	-675
6	7		375	-375
6	8	*	246	-72
6	9	*	257	147
6	10		422	414
6	11	*	281	205
7	1		836	-854
7	2	*	216	173
7	3		479	497
7	4		335	349
7	5		446	-384
7	6		620	-612
7	7		698	720
7	8	*	260	-65
7	9		350	321
7	10	*	281	294
8	1	*	233	-68
8	2		701	694
8	3	*	238	-154
8	4		612	-592
8	5	*	250	233
8	6		540	-498
8	7	#	355	-226
8	8		389	-285
8	9	*	284	34
8	10	*	294	365
8	11		487	521
8	12		439	466
8	13	*	328	-166
8	14		403	-459
8	15	*	351	-148
9	1		370	-383
9	2		630	671
9	3		540	496
9	4		862	815
9	5		681	613
9	6		695	-769
9	7		400	-412
9	8	*	289	9
9	9		418	-392
9	10		516	557
9	11	*	318	110
10	1		726	-659
10	2	#	302	447
10	3		414	482
10	4	*	280	-151
10	5	*	284	118
10	6	*	291	-125
10	7	*	298	-139
10	8		220	159
10	9	*	314	-163
11	1	*	290	23
11	2	#	378	544
11	3	*	294	-42
11	4	*	298	59
11	5		363	427
11	6		394	-345
11	7		489	-441
11	8	*	322	-61
12	1	*	309	-281
12	2	*	311	23
12	3		373	314
12	4	*	317	214
12	5	*	321	317
12	6		421	-463
12	7	*	331	-1
12	8	*	338	157
12	9		489	-502
12	10	*	352	154
13	1	*	328	-93
13	2	*	329	-15
13	3	*	331	197
13	4	*	334	-232
13	5	*	338	-59
13	6		442	438
13	7	*	348	-154
14	1	*	346	51
14	2	*	347	-226
15	1	*	362	-99
15	2		446	-486
15	3	*	365	168
16	1	*	376	48
H	K			L=2
0	0		1475	-1490
0	1		831	756
0	2		854	-825
0	3		1512	1455
0	4		392	401
0	5		237	-193
0	6		368	327
0	7		1149	-1071
0	8	*	198	21
0	9		876	933
0	10	*	165	140
0	11	*	170	83
0	12	*	173	206
0	13		245	-239
1	0		1483	-1229
1	2		340	-305
1	3		558	-586
1	4		472	454
1	5		1413	-1399
1	6		336	273
1	7		451	-434
1	8		440	408
1	9		238	228
1	10		386	-325
1	11		995	933
1	12		476	461
1	13		235	-267
1	14	*	295	115
1	15		365	-351
1	16		579	-597
1	17		362	310
1	18	*	340	-62
2	0	*	279	191
2	1		590	586
2	2		614	-526
2	3		407	407
2	4		1101	1089
2	5		605	-532
2	6		383	331
2	7		408	-391
2	8		1364	-1367
2	9	*	220	-196
2	10	*	233	81
2	11		301	323
2	12	*	261	181
2	13	*	275	145
2	14	*	289	234
2	15	*	303	-92
2	16	*	317	-130
2	17	*	330	46
2	18		418	-435
2	19	*	353	-7
2	20		468	437
2	21	*	369	-0
3	0		1915	-1944
3	1		695	-688
3	2	*	150	106
3	3		688	688
3	4		717	737
3	5		1204	1227
3	6		467	466
3	7		314	311
3	8	*	214	-220
3	9		322	286
3	10		608	-632
3	11		558	-463
3	12		546	540
3	13	*	280	-134
4	0		1348	-1315
4	1		619	529
4	2	*	168	-134
4	3		931	-1036
4	4		362	308
4	5		345	277
4	6	*	202	-49
4	7		527	578
4	8	*	224	-85
4	9		1175	-1133
4	10	*	248	188
4	11	*	261	80
4	12		666	647
4	13	*	287	130
5	0	*	183	185
5	1		641	-661
5	2		358	-299
5	3	*	192	-183
5	4		1224	1190
5	5		605	597
5	6		481	415
5	7	*	225	-59
5	8		1295	-1270
5	9		279	-261
5	10	*	258	-122
5	11		305	-273
5	12	*	282	88
5	13		496	517
5	14	*	308	35
5	15		390	370
5	16	*	332	5
6	0		1327	-1197
6	1		904	-881
6	2		739	740
6	3		635	-585
6	4		688	649
6	5		754	756
6	6		490	-561
6	7		877	809
6	8	*	248	-247
6	9	*	258	-176
6	10		570	-551
6	11		574	-575
6	12		448	495
6	13	*	304	-17
6	14	*	316	208
6	15	*	328	111
6	16		350	-283
6	17	*	350	-141
7	0	*	220	-93
7	1	*	220	57
7	2		284	-263
7	3		603	-527
7	4	*	231	-10
7	5		377	386
7	6	*	245	12
7	7		740	722
7	8		292	-290
7	9		752	-810
7	10		538	468
7	11	*	292	-224
7	12		306	310
7	13	*	314	234
7	14	*	326	-95
7	15		311	298
7	16	*	347	-35
8	0	*	238	-108
8	1		747	-753
8	2	*	241	89
8	3		388	-453
8	4	*	248	193
8	5	*	254	-22
8	6	*	260	185
8	7	*	268	-148
8	8	*	276	-59
8	9	*	285	228
8	10	*	295	-95
8	11		476	-402
8	12	*	315	-270
8	13	*	325	167
8	14	*	335	-102
8	15		502	478
8	16	*	354	183
9	0	*	257	130
9	1	*	257	32
9	2		401	385
9	3	#	309	-431
9	4		327	-378
9	5		229	171
9	6		324	-418
9	7		606	590
9	8		336	302
9	9	*	300	12
10	0		567	680
10	1	*	275	15
10	2		417	-339
10	3	*	280	-52
10	4		365	-360
10	5	*	288	125
10	6	*	293	193
10	7	*	300	215
10	8		342	288
10	9	*	314	-250
10	10	*	322	202
10	11	*	331	-242
10	12		483	-445
10	13	*	347	29
11	0		445	402
11	1		488	-472
11	2	*	295	56
11	3	*	298	-144
11	4		668	-652
11	5	*	305	-151
11	6	*	310	52
11	7	*	316	-17
11	8		545	621
11	9		348	389
11	10	*	336	-98
12	0		601	509
12	1		300	265
12	2		380	313
12	3	*	316	-47
12	4		518	-541
12	5	*	322	22
12	6	*	327	-180
12	7	*	332	81
12	8		389	425
12	9	*	343	-229
13	0		316	376
13	1	*	330	-54
13	2		393	-338
13	3	*	333	0
14	0	*	345	148
14	1	*	345	-185
14	2	*	346	168
14	3	*	348	14
14	4	*	350	-293
14	5	*	352	-18
14	6	*	355	-188
14	7	*	358	-147
14	8		420	433
14	9	*	365	208
H	K			L=-2
1	0		1910	1880
1	3		505	-453
1	4		494	589
1	5		967	952
1	6		284	-234
1	7		443	384
1	8		1450	-1493
1	9		300	-346
1	10		312	265
1	11		861	-877
1	12	*	255	76
1	13		545	573
1	14	*	284	-196
1	15		485	482

TABLE VI- 4 (CONTINUED)

			|FOBS|	FCALC
1	16	•	313	-29
1	17		374	-393
1	18	•	339	-172
2	0		1463	-1446
2	3		180	-219
2	4	•	143	90
2	5		1810	1849
2	6		466	-393
2	7		784	844
2	8		473	452
2	9		732	-703
2	10		418	-454
2	11		764	-830
2	12	•	257	98
2	13	•	272	187
2	14	•	286	85
2	15		482	430
2	16	•	314	31
2	17	•	328	-259
2	18		402	453
2	19	•	352	-248
3	0		1302	1184
3	1	•	124	-50
3	2		930	-942
3	3		1548	-1668
3	4		189	-174
3	5	•	167	-104
3	6	•	180	80
3	7		1131	1164
3	8	•	207	51
3	9		499	-483
3	10		905	913
3	11	•	247	-160
3	12		277	-244
3	13	•	275	57
3	14		264	-294
3	15	•	303	115
4	0		1391	1406
4	1		1331	-1358
4	2	Ø	131	235
4	3	•	159	37
4	4		365	-350
4	5		272	-208
4	6		507	-539
4	7		791	-743
4	8	•	215	-49
4	9		237	252
4	10	Ø	522	310
4	11		433	-443
4	12		306	-254
4	13		403	414
4	14	•	294	-201
4	15		566	567
4	16		269	209
4	17	•	334	-278
5	0		219	161
5	1		584	575
5	2		634	610
5	3	•	176	-1
5	4		647	-635
5	5		269	307
5	6		225	-203
5	7		957	985
5	8		816	761
5	9	•	237	-118
5	10		486	-478
5	11	•	261	-8
5	12		451	-465
5	13	•	287	-176
5	14	•	301	13
5	15	•	314	-94
5	16		354	349
5	17	•	339	70
6	0		1633	1608
6	1		362	318
6	2		802	-826
6	3	•	193	-147
6	4		1206	-1205
6	5		228	-197
6	6		176	248
6	7	•	226	-57
6	8		469	520
6	9	•	247	36
6	10		877	870
6	11	•	271	-19
6	12		454	-500
6	13	•	295	-309
6	14	•	308	-119
6	15	•	321	4
6	16		377	397
6	17	•	344	163
7	0		699	738
7	1	•	203	33
7	2		188	186
7	3		391	323
7	4		608	-662
7	5		396	-398
7	6	•	230	-32
7	7		759	-698
7	8		806	876
7	9	Ø	326	454
7	10		333	-310
7	11	•	281	143
7	12		581	-603
7	13	•	305	174
8	0		933	1076
8	1		534	497
8	2		203	216
8	3	•	228	-186
8	4		456	-577
8	5	•	239	-201
8	6	•	246	-188
8	7		298	246
8	8		436	403
8	9	•	272	-128
8	10		286	-263
8	11		433	508
8	12		457	-400
8	13	•	315	-221
8	14	•	326	113
8	15		465	-418
8	16	•	347	211
9	0		607	708
9	1	•	240	183
9	2		466	-438
9	3		569	660
9	4		505	-564
9	5	•	255	18
9	6	•	262	167
9	7		305	-372
9	8	•	277	195
9	9	•	286	-22
9	10		405	387
9	11	•	305	131
10	0		555	-612
10	1	•	258	7
10	2		243	207
10	3	•	263	-44
10	4	•	267	-0
10	5		378	-316
10	6	•	278	198
10	7		554	-526
10	8		390	461
10	9	•	301	168
10	10		382	-342
10	11		376	358
10	12	•	328	-93
11	0	•	404	106
11	1	Ø	791	567
11	2	•	278	-9
11	3	•	281	-96
11	4	•	285	137
11	5	•	289	-114
11	6		227	-255
11	7	•	301	94
11	8		310	-294
11	9	•	315	-125
11	10	•	323	293
11	11		440	494
11	12	•	339	149
11	13	•	348	-72
11	14	•	355	-8
11	15		351	-349
11	16	•	367	-150
12	0		320	-284
12	1	•	295	56
12	2		285	-225
12	3		630	656
12	4		377	400
12	5	•	307	98
12	6	•	312	162
12	7	Ø	307	-493
12	8	•	323	-256
13	0		853	-902
13	1	•	313	230
13	2	•	315	146
13	3	•	317	40
13	4	•	320	326
13	5		374	-279
13	6	•	328	-88
13	7	•	333	30
13	8	•	338	57
13	9	•	344	154
13	10	•	349	-162
13	11	•	355	145
13	12		268	288
13	13	•	365	-309
H	K			L=3
0	1		347	-346
0	2		679	-723
0	3		1421	1450
0	4		1164	1126
0	5	•	144	95
0	6	•	149	-71
0	7		333	-309
0	8		374	379
0	9		757	-791
0	10	•	207	33
0	11		378	-406
0	12	•	211	-188
0	13		614	638
0	14	•	295	160
0	15	•	310	-185
0	16		329	-341
0	17	•	338	-152
1	1		698	-784
1	2		524	427
1	3		606	551
1	4		193	132
1	5		505	493
1	6		1240	1329
1	7		529	-491
1	8		305	-220
1	9		476	-462
1	10		867	-843
1	11		771	705
1	12		349	303
1	13		498	488
1	14	•	297	-212
1	15		404	-390
1	16	•	326	-3
1	17		432	-435
1	18	•	352	-85
2	1		1436	-1383
2	2		1332	-1437
2	3		97	107
2	4		491	426
2	5		1484	1440
2	6	•	189	41
2	7		362	-353
2	8		280	-248
2	9		416	-371
2	10		415	-422
2	11		436	460
2	12	•	273	-15
2	13	•	287	-9
2	14		868	821
2	15	•	315	122
2	16	•	329	-62
2	17	•	342	-222
2	18		324	-288
2	19	•	364	49
3	1	•	156	113
3	2		1371	-1367
3	3		1300	1286
3	4		617	-564
3	5	•	189	-168
3	6		527	525
3	7		335	-360
3	8		403	410
3	9		630	-608
3	10		193	-275
3	11		266	-221
3	12		284	-255
3	13		419	438
3	14		295	282
3	15		368	-383
3	16	•	333	14
4	1	•	176	-29
4	2		295	293
4	3		238	-234
4	4		238	238
4	5		291	267
4	6		1135	1130
4	7		745	-732
4	8	•	236	-21
4	9	•	248	70
4	10		672	-715
4	11		479	492
4	12	•	286	-11
4	13	•	300	82
4	14	•	313	91
4	15	•	326	73
4	16		314	313
4	17	•	351	-136
5	1		470	-462
5	2		946	-972
5	3		296	-308
5	4		433	387
5	5		491	523
5	6	•	227	-137
5	7		355	372
5	8		362	363
5	9	•	259	109
5	10		437	-435
5	11	•	283	-62
5	12		412	-495
5	13	•	308	-231
5	14		680	603
5	15	•	333	123
6	1		539	542
6	2		523	-599
6	3	•	222	125
6	4		636	-686
6	5		929	-968
6	6		417	447
6	7		328	386
6	8	•	261	204
6	9	•	272	153
6	10		249	-181
6	11		474	-398
6	12	•	306	-83
6	13	•	318	100
6	14	•	330	79
6	15	•	341	59
6	16		323	321
6	17	•	362	132
7	1		849	937
7	2	•	236	234
7	3		823	-851
7	4	•	245	35
7	5	•	251	48
7	6		626	568
7	7	•	267	-41
7	8	•	275	131
7	9	•	285	155
7	10		297	-270
7	11		278	-219
7	12	•	317	-112
7	13		562	-501
7	14	•	339	112
7	15		480	513
7	16	•	359	103
8	1	•	253	263
8	2	Ø	417	-711
8	3		519	-496
8	4	•	263	255
8	5		612	-582
8	6	•	275	-132
8	7		540	531
8	8	•	291	178
8	9		558	501
8	10	•	309	-30
8	11		269	-341
8	12		361	-373
8	13	•	339	-44
9	1		681	593
9	2	•	274	97
9	3		300	-309
9	4		471	-462
9	5		614	-546
9	6	•	292	224
9	7		298	393
9	8	•	306	-173
9	9		349	375
9	10	•	323	-191
9	11		290	-356
9	12		483	481
9	13	•	350	-248
10	1		359	325
10	2	•	293	-200
10	3		482	-510
10	4	•	299	75
10	5	•	303	100
10	6	•	309	-165
10	7	•	315	133
10	8	•	322	37
10	9	•	329	126
10	10	•	337	187
10	11	•	345	-133
10	12	•	353	-9
10	13		555	-483
10	14	•	367	-53
11	1	•	310	56
11	2	•	311	68
11	3	•	313	46
11	4	•	317	74
11	5		528	-561
11	6	•	326	-70
11	7	•	331	162
11	8	•	337	32
11	9		420	371
11	10	•	350	208
12	1	•	328	-29
12	2		469	507
12	3	•	331	-131
12	4	•	334	-117
12	5	•	338	140
12	6	•	342	-146
12	7	•	347	11
12	8		398	-385
12	9	•	357	217
13	1	•	345	-81
13	2	•	346	179
13	3	•	348	-8
13	4	•	350	163
13	5	•	353	173
13	6		361	-387
13	7	•	360	-104
13	8	•	364	237
13	9	•	368	26
13	10	•	372	353
13	11	Ø	362	39
13	12	•	377	-108
14	1	•	360	-40
14	2		503	452
14	3	•	362	268
H	K			L=-3
1	4		445	436
1	5		1429	1384
1	6		664	656
1	7		506	-482
1	8		568	558
1	9		344	-335
1	10	•	215	-8
1	11		525	512
1	12		322	-336
1	13	•	256	78
1	14		208	-238
1	15	•	283	92
1	16	•	296	88
1	17		426	-445
1	18	•	320	0
2	3		751	725
2	4		367	299
2	5	•	149	-27
2	6		322	-315
2	7		732	667
2	8	•	190	-118
2	9	•	204	9
2	10		494	-438
2	11	•	230	92
2	12		252	-244
2	13		601	609
2	14		627	635
2	15		367	-359
2	16	•	297	123
2	17		338	-378
2	18	•	321	-181
3	2		1025	-957
3	3		330	386
3	4		1291	-1210
3	5		139	196
3	6		1702	1658
3	7	•	182	38
3	8	•	195	8
3	9		590	-600
3	10		626	-641
3	11	•	234	-153
3	12		319	287
3	13	•	260	122
4	1		963	846
4	2		799	-769
4	3		225	-209
4	4		1114	1114
4	5	•	167	-46
4	6		1103	1114
4	7		716	-670
4	8	•	202	50
4	9	•	214	-15
4	10		676	-689
4	11		364	358
4	12		511	-490
4	13	•	265	-110
4	14		424	499
4	15	•	290	67
5	1		1006	-1056
5	2		503	-577
5	3		390	426
5	4		519	453
5	5		344	-288
5	6		755	762
5	7		523	540
5	8		227	-215
5	9	•	223	140
5	10		779	-786
5	11	•	246	-168
5	12	•	258	-53
5	13		355	339
5	14		603	523
5	15	•	295	-256
5	16	•	307	39
5	17	•	318	308
5	18		298	-282
5	19	•	336	115
6	1		509	530
6	2		1197	-1301
6	3	•	180	195
6	4		1070	-1092
6	5	•	194	49
6	6		749	793
6	7		350	-389
6	8	•	222	156
6	9	•	232	-17
6	10		579	-462
6	11	•	255	62
6	12		286	249
6	13		369	-395
6	14	•	290	39
7	1		765	812
7	2		427	-432
7	3	•	196	-180
7	4		708	717
7	5		583	-696
7	6	•	216	-7
7	7		203	-263
7	8		218	172
7	9	•	243	50
7	10	•	254	-183
7	11	•	264	239
7	12		287	-257
7	14		546	551
7	15	•	309	90
8	1		312	-295
8	2		183	243
8	3		198	220
8	4		237	-213
8	5		621	-558
8	6		151	167
8	7		645	607
8	8	•	246	-45
8	9		434	367
8	10	•	265	66
8	11		293	-348
8	12	•	285	-59
9	1		492	458
9	2	•	226	-26
9	3		749	-743
9	4		551	-541
9	5	•	239	32
9	6		309	-288
9	7	•	252	-26
9	8	•	260	101
9	9		389	432
9	10	•	277	96
9	11	•	287	160
9	12	•	296	70
9	13		377	-415
9	14	•	315	-14
10	1		469	434
10	2	•	243	14
10	3	•	246	-126
10	4		615	558
10	5		475	-491
10	6		462	-547
10	7		512	484
10	8	•	274	191
10	9	•	282	166
10	10	•	290	295
10	11		563	-516
10	12	•	307	-117
11	1	•	259	212
11	2		411	481
11	3		347	-333
11	4		303	-325
11	5		477	-502
11	6	•	276	-8
11	7		555	486
11	8	•	288	62
11	9		316	273
11	10	•	303	96
11	11	•	310	-174
11	12	•	318	79
11	13	•	325	-71
11	14		470	-485
11	15	•	338	136
12	1		319	285
12	2	•	277	246
12	3		480	-455
12	4	•	283	327
12	5	•	287	81
12	6		423	-372
12	7	•	297	97
12	8	•	302	-245
12	9	•	309	144
12	10	•	315	176
12	11	•	322	64
12	12	•	328	81
12	13		301	-286
12	14	•	339	114
13	1	•	293	-94
13	2	•	294	-86
13	3	•	296	110
13	4	•	299	59
13	5	•	302	-47
13	6	•	306	-196
13	7	•	311	305
13	8	•	316	-41
13	9	•	321	-37
13	10	•	327	118
13	11		414	-402
13	12	•	336	24
14	1	•	309	155
14	2	•	310	170
15	1	•	323	-199
15	2	•	324	184
15	3	•	325	90
15	4	•	327	332
15	5	•	329	265
15	6		442	-382
15	7	•	335	-117
16	1	•	335	-305
16	2	•	336	-20
16	3		355	317
16	4	•	338	-55
17	1	•	343	68
17	2		210	236
17	3	•	344	1
H	K			L=4
0	0		1909	-1892
0	1		834	-854
0	2		673	640
0	3		1337	-1319
0	4		521	433
0	5	•	192	-148
0	6		212	-223
0	7		359	349
0	8		232	178
0	9	•	169	14
0	10		265	-282
0	11	•	208	-217
0	12		535	552
0	13	•	293	24
0	14	•	308	-72
0	15		286	291
0	16		472	-518
0	17	•	350	-5
1	0		1039	1022
1	1		690	704
1	2	•	131	105
1	3		476	-459
1	4	•	160	109
1	5		357	364
1	6		205	-158
1	7		707	691
1	8		746	-737
1	9		892	-867
1	10	•	251	138
1	11	•	266	-217
1	12	•	281	-21
1	13	•	296	165
1	14	•	310	32
1	15		323	348
1	16	•	339	144
2	0	•	143	-66
2	1		638	-698
2	2		345	-393
2	3		589	537
2	4	•	174	-24
2	5		955	962
2	6		368	383
2	7		231	302
2	8		288	295
2	9		458	466
2	10	•	257	-206
2	11		827	-853
2	12		301	-288
2	13	•	300	-238
2	14	•	315	161
2	15		325	379
2	16	•	342	246
3	0		162	-124
3	1	•	168	-83
3	2		263	298
3	3		894	-975
3	4		736	-786
3	5		287	-299
3	6		303	-323
3	7		591	640
3	8		886	929
3	9		507	-442
3	10	•	265	-162
3	11		258	-250
3	12	•	292	41
4	0		1783	1903
4	1		330	-305
4	2	•	193	56
4	3		400	-396
4	4		612	-636
4	5		236	225
4	6		274	219
4	7		270	268
4	8	•	249	-116
4	9		276	-259
4	10	•	274	-47
4	11	•	287	-63
4	12		767	-687
4	13	•	314	265
4	14	•	327	-5
4	15		290	318
4	16		650	607
4	17	•	363	-82
5	0		562	580
5	1		614	-543
5	2		416	406
5	3	•	218	-76
5	4		913	-916
5	5		390	397
5	6		261	-264
5	7		208	134
5	8		785	751
5	9		303	296
5	10		262	-294
5	11		401	-413
5	12		376	-346
5	13	•	323	-63
6	0		287	274
6	1		315	354
6	2	•	232	-143
6	3		364	-315
6	4		710	-673
6	5	•	249	16
6	6	•	257	-50
6	7	•	266	137
6	8		720	748
6	9		522	-502
6	10	•	298	191
6	11		266	277
6	12	•	321	-161
7	0		722	669
7	1		405	-441
7	2	•	252	-209
7	3		238	-246
7	4	•	260	-90

TABLE VI-4 (CONCLUDED)

			|FOBS|	FCALC
7	5		273	-277
7	6	•	274	204
7	7		274	-216
7	8	•	291	87
7	9	•	300	201
7	10	•	311	203
7	11	•	321	59
7	12		582	-568
7	13	•	343	152
8	0	•	268	60
8	1	•	269	-26
8	2		432	452
8	3		375	357
8	4		505	-542
8	5	•	284	22
8	6		417	-479
8	7	•	298	-128
8	8		459	441
8	9		379	359
8	10	•	324	28
9	0	•	288	-197
9	1		748	823
9	2	•	290	-147
9	3		349	415
9	4	•	297	45
9	5		285	-253
9	6	•	308	104
9	7	•	315	-233
9	8	•	322	90
9	9	•	330	-237
9	10		300	290
9	11		425	345
9	12	•	355	-154
10	0	•	307	-38
10	1	•	307	-73
10	2	•	309	-172
10	3	•	312	219
10	4	•	315	148
10	5		373	-338
10	6	•	325	119
10	7		489	-428
10	8	•	338	-126
10	9		666	654
10	10	•	352	164
11	0	•	326	-40
11	1		509	441
11	2		392	371
11	3		474	400
11	4	•	333	-41
11	5	•	337	-238
11	6		384	-380
11	7	•	347	-196
12	0	•	343	-25
12	1		415	396
12	2		383	-296
12	3		342	379
12	4	•	349	128
H	K			L=-4
1	0		1549	-1519
1	4		1005	983
1	5		566	-583
1	6		848	781
1	7	•	245	-172
1	8		598	-632
1	9	•	211	60
1	10		440	409
1	11		543	534
1	12		311	263
1	13		247	-220
1	14	•	280	-17
1	15		225	-271
1	16	•	307	-32
2	0	•	357	175
2	3		313	375
2	4		894	936
2	5		609	-603
2	6		443	-361
2	7		647	-698
2	8		949	-936
2	9		942	916
2	10	•	226	-146
2	11	•	240	-175
2	12		361	371
2	13	•	268	-81
2	14	•	281	5
2	15	•	295	111
2	16		412	-408
2	17	•	320	-37
3	0	#	986	-1344
3	2		264	217
3	3		819	796
3	4		741	792
3	5	•	162	99
3	6		183	-99
3	7		241	269
3	8		402	-374
3	9	•	216	-81
3	10		387	-480
3	11	•	243	-4
3	12		556	526
3	13		322	-374
3	14	•	284	201
3	15	•	297	-82
3	16		383	-334
3	17		282	327
3	18	•	332	173
4	0		419	-427
4	1	•	135	-87
4	2		776	-822
4	3	•	150	-206
4	4		499	518
4	5		192	-247
4	6		519	556
4	7		309	317
4	8		662	-619
4	9	•	222	150
4	10		564	545
4	11	•	248	-203
4	12		248	243
4	13	•	275	-111
4	14	•	288	15
4	15	•	300	57
4	16	•	313	-195
4	17	•	324	170
4	18		445	-454
4	19	•	342	-36
4	20		360	344
4	21	•	351	-42
5	0		397	-301
5	1		706	-742
5	2		235	273
5	3		161	-214
5	4	•	176	101
5	5	•	185	-75
5	6	•	196	59
5	7		587	-547
5	8	•	218	-56
5	9	•	230	116
5	10		452	-405
5	11		378	-361
5	12		281	268
5	13		250	265
5	14	•	293	166
5	15		464	526
5	16	•	317	-237
6	0	•	174	-11
6	1		264	288
6	2	•	179	50
6	3		585	-562
6	4		371	329
6	5		496	497
6	6	•	208	9
6	7		1112	1106
6	8	•	229	-162
6	9		349	-344
6	10		415	-375
6	11	•	263	-73
7	0		599	654
7	1		832	-867
7	2		656	-656
7	3	•	201	-151
7	4		181	-160
7	5		635	642
7	6	•	222	86
7	7		252	260
7	8		293	-264
7	9		235	-287
7	10		693	670
7	11		584	-648
7	12	#	310	205
7	13	•	296	180
8	0		529	-563
8	1		581	-603
8	2		326	347
8	3		290	-304
8	4	•	223	-15
8	5		395	417
8	6	•	237	-55
8	7	•	245	151
8	8		374	448
8	9		557	-487
8	10		424	-389
8	11		225	-236
8	12	•	294	-114
8	13		607	501
8	14	•	315	9
8	15		315	323
8	16	•	334	-26
9	0		594	672
9	1	•	230	-80
9	2	•	232	79
9	3		712	-807
9	4	•	240	6
9	5		306	234
9	6	•	252	-45
9	7		743	731
9	8		423	-392
9	9		444	-339
9	10	•	285	106
10	0	•	397	273
10	1		413	-344
10	2	•	250	-65
10	3	•	253	143
10	4	•	257	-119
10	5		505	453
10	6	#	205	-331
10	7	•	274	-68
10	8	•	282	-88
10	9	•	290	-0
10	10		401	425
10	11		353	-335
10	12	•	315	29
11	0	•	265	-177
11	1	•	266	8
11	2	•	267	91
11	3		419	-350
11	4	•	273	3
11	5	•	278	-186
11	6	•	283	-32
11	7	•	289	62
11	8		405	409
11	9	•	303	-197
12	0		700	612
12	1	•	281	151
12	2	•	284	-87
12	3	•	287	-63
12	4		258	-247
12	5	•	294	-286
13	0	•	300	-18
13	1	•	300	106
13	2	•	301	39
13	3		365	353
13	4	•	306	-192
13	5	•	310	-96
13	6	•	314	108
13	7	•	318	-286
13	8		300	247
13	9	•	329	236
14	0	•	316	-2
14	1	•	316	301
14	2	•	317	-35
14	3	•	319	-217
14	4		297	-263
14	5	•	324	-144
14	6	•	327	-0
14	7	•	331	101
14	8		444	421
14	9	•	339	-18
15	0		718	658
15	1	•	330	193
H	K			L=5
0	1		490	435
0	2	•	164	-165
0	3		438	-442
0	4	•	146	-129
0	5		898	-948
0	6		962	1004
0	7		594	588
0	8	•	169	82
0	9		493	469
0	10		518	-526
0	11		295	-267
0	12	•	265	-180
1	1		358	443
1	2		456	-490
1	3		1095	-1107
1	4		279	-319
1	5		350	294
1	6	•	185	-51
1	7		253	201
1	8	•	213	-183
1	9		406	426
1	10		278	-313
1	11		274	-215
1	12		262	268
1	13		488	-514
1	14		447	420
1	15		611	560
1	16	•	320	149
2	1		821	878
2	2		1172	-1139
2	3	•	159	141
2	4	•	170	206
2	5		627	-658
2	6	•	194	-104
2	7		244	247
2	8		353	351
2	9	•	233	-83
2	10	•	246	-7
2	11		552	-541
2	12	•	273	-239
3	1		285	254
3	2		431	468
3	3		371	-382
3	4	•	185	-90
3	5		720	-725
3	6		891	897
3	7		238	248
3	8		216	-220
3	9		550	542
3	10		315	-353
3	11	•	267	15
3	12		228	265
3	13	•	292	-150
4	1	•	186	88
4	2		166	-231
4	3		748	-786
4	4	•	202	10
4	5		413	425
4	6		489	-509
4	7	•	230	155
4	8	•	240	-41
4	9		463	466
4	10		275	257
4	11	•	275	112
4	12	•	287	-122
4	13		620	-649
5	1		272	266
5	2	•	208	127
5	3		456	472
5	4	•	218	-97
5	5		717	-777
5	6		523	-538
5	7	•	243	-81
5	8	•	253	69
5	9	•	263	261
5	10		377	432
5	11	•	285	-140
6	1	•	224	170
6	2		992	1064
6	3	•	230	-197
6	4	•	235	-6
6	5	•	241	215
6	6	•	249	-3
6	7	•	257	-175
6	8	•	266	-66
6	9	•	275	15
6	10	•	285	144
6	11	•	296	93
6	12	•	306	213
6	13	•	316	-327
6	14		532	-479
6	15	•	334	87
7	1	•	242	-181
7	2	•	244	152
7	3	•	247	-195
7	4	•	252	125
7	5	•	258	3
7	6		843	-833
7	7	•	272	90
7	8	•	280	188
7	9		261	254
7	10		603	562
7	11	•	307	173
8	1	•	260	99
8	2		770	757
8	3	•	265	292
8	4	•	269	-250
8	5		332	-311
8	6		493	-449
8	7	•	287	61
9	1	•	278	-98
9	2		558	459
9	3	•	283	-173
9	4	•	286	-8
9	5		554	509
9	6	•	296	-168
11	1	•	312	-208
11	2	•	313	243
11	3	•	315	265
11	4	•	318	-117
11	5	•	321	48
11	6	•	325	86
11	7	•	329	33
11	8		346	-335
11	9	•	338	-163
12	1	•	327	-91
12	2	•	328	-144
12	3	•	329	6
12	4	•	332	83
12	5		421	436
12	6	•	337	183
H	K			L=-5
1	3		172	175
1	4		786	-740
1	5	•	147	20
1	6		358	-354
1	7	•	177	53
1	8		546	-611
1	9		349	-337
1	10		195	206
1	11		562	-565
1	12		659	710
1	13	•	257	-79
1	14		451	-427
1	15		375	390
1	16	•	294	60
2	2	•	98	82
2	3		393	-394
2	4		551	562
2	5		380	413
2	6	•	163	-6
2	7		271	-248
2	8		315	308
2	9		173	-204
2	10		440	435
2	11		248	240
2	12	•	245	-136
2	13	•	258	-136
2	14		238	-223
2	15	•	283	220
2	16		365	-399
2	17	•	304	-118
3	1		901	-952
3	2		323	277
3	3		425	451
3	4	•	141	-13
3	5		354	-341
3	6		493	-449
3	7		479	461
3	8		556	-569
3	9		334	299
3	10		262	242
3	11	•	234	51
3	12		228	216
3	13		424	447
3	14	•	272	4
3	15		412	-415
3	16	•	295	-32
4	1		459	-415
4	2		438	441
4	3		162	193
4	4		957	-927
4	5		977	1014
4	6		189	-120
4	7		515	-514
4	8	•	201	-73
4	9		371	-375
4	10		344	280
4	11		195	173
4	12		460	468
4	13	•	263	[illegible]
4	14		439	[illegible]
4	15	•	287	-13
5	1	•	147	-197
5	2	•	151	46
5	3		655	673
5	4		863	907
5	5		289	313
5	6		419	-362
5	7		703	-671
5	8		270	254
5	9		411	-455
5	10		284	216
5	11		492	440
5	12		429	-440
5	13		226	253
5	14	•	280	4
5	15		338	-278
5	16	•	302	-90
6	1		1087	-1172
6	2		809	734
6	3		600	604
6	4	•	182	-164
6	5	•	190	79
6	6		255	305
6	7		230	301
6	8	•	219	-82
6	9	•	230	-177
6	10	•	241	-180
6	11	•	252	103
6	12	•	264	-72
6	13		442	442
6	14	•	286	-209
6	15		349	-262
6	16	•	306	249
7	1	•	184	75
7	2	•	187	-129
7	3	•	191	-20
7	4		544	-603
7	5		654	627
7	6		260	-174
7	7		526	-441
7	8	•	230	138
7	9		314	-250
7	10		255	252
7	11		339	313
7	12	•	271	-191
8	1	•	202	28
8	2	•	204	69
8	3		499	435
8	4		495	480
8	5	•	219	-214
8	6		187	-162
8	7		285	-240
8	8	•	242	91
8	9		358	-322
8	10	•	261	-58
8	11	•	270	-38
8	12		215	-272
8	13		434	458
8	14		301	353
8	15	•	308	-114
9	1		324	-291
9	2	•	221	-120
9	3	•	224	56
9	4		233	-232
9	5	•	234	92
9	6		620	637
9	7		279	298
9	8	•	255	91
9	9	•	263	-131
9	10		283	-329
9	11	•	281	-224
10	2		594	-590
10	3		324	-391
10	4	•	244	-111
10	5	•	249	-90
10	6	•	254	52
10	7	•	261	-0
10	8	•	268	120
10	9	•	275	115
10	10		266	-216
10	11		296	280
10	12	•	299	-113
11	1	•	252	42
11	2		312	-326
11	3		372	314
11	4		341	278
11	5	•	264	-287
11	6		317	252
11	7	•	275	214
11	8	•	281	-147
11	9		229	-165
11	10	•	294	-93
11	11	•	301	-256
11	12	•	308	46
11	13	•	314	102
11	14		377	360
11	15	•	323	-124
12	1	•	268	10
12	2		375	-347
12	3	•	272	-105
12	4	•	275	-265
12	5	•	279	35
12	6		768	644
12	7	•	288	-83
12	8	•	294	16
12	9	•	299	90
12	10		399	-341
12	11	•	311	-1
13	1	•	284	175
13	2		509	-386
13	3	•	287	-162
H	K			L=6
0	0		928	888
0	1		586	597
0	2		463	459
0	3	•	169	0
0	4		420	-418
0	5	•	168	65
0	6		473	-454
0	7		361	403
0	8	•	162	-46
0	9		501	-566
1	0	•	400	26
2	0		473	-362
3	0		711	697
4	0	•	393	157
5	0		617	-587
6	0	•	357	223
7	0	#	278	-182
H	K			L=-6
1	0	•	400	63
2	0		400	336
3	0		593	602
4	0		522	433
5	0	•	399	151
6	0		416	-500
7	0	•	392	-99
8	0	•	379	-380
9	0		1025	-1090
H	K			L=7
0	1	•	163	109
0	2		514	525
0	3		378	-402
0	4		794	-808
0	5		304	237
0	6		434	-388

2.03±0.03 Å, and the cation lies in the equatorial plane (the sum of the bond angles subtended to M(3) by the three equatorial oxygen atoms is 359.4°). The bond distances and angles for these cation polyhedra, and also for the two anion tetrahedra, are listed in Table (VI-5).

Two M(1) polyhedra share an edge across a centre of symmetry. Each M(1) is further linked to the two other M(1) ions related to it by the c glide plane by sharing two corners. This results in a planar network of M(1) ions near the x=0 plane. In Fig. (VI-1), the bonding within this planar network is shown in black. Each M(1) corner-shares its remaining three oxygen atoms with neighbouring M(2) ions as shown in the figure.

The third cation, M(3), shares two edges with the cations related to it by the c glide plane. The bonds forming these linkages are shown in black in Fig. (VI-2), where the resulting infinite chains of M(3) polyhedra can be seen. The fifth oxygen atom in each polyhedron, O(8), which is not involved in the formation of the chain, is bonded to a M(2) ion as shown in Fig. (VI-2). The same $M(2)O_4$ tetrahedra are also shown in Fig. (VI-1) where they complete the linkages between the $M(1)O_7$ and $M(3)O_5$ polyhedra.

These linkages produce corrugated sheets of cation polyhedra which lie perpendicular to the a axis. Adjacent sheets are held together by the PO_4 groups, as shown in Fig. (VI-3), where these groups are shown as solid tetrahedra. In all three figures, the oxygen atoms have been labelled according to their designation in Table (VI-2).

TABLE (VI-5)

Bond distances and angles in B-graftonite

Bonded atoms	Distance (Å)	Bonded atoms	Angle (°)	Bonded atoms	Angle (°)
M(1)-0(3)	2.60(2)	0(3)-M(1)-0(3)'	84.	0(1)-M(1)-0(1)'	78.
M(1)-0(3)'	2.09(1)	0(3)-M(1)-0(1)	144.	0(1)-M(1)-0(7)	93.
M(1)-0(1)	2.32(1)	0(3)-M(1)-0(1)'	111.	0(1)-M(1)-0(4)	145.
M(1)-0(1)'	2.16(1)	0(3)-M(1)-0(7)	57.	0(1)-M(1)-0(6)	86.
M(1)-0(7)	2.51(1)	0(3)-M(1)-0(4)	71.	0(1)'-M(1)-0(7)	79.
M(1)-0(4)	2.42(1)	0(3)-M(1)-0(6)	129.	0(1)'-M(1)-0(4)	85.
M(1)-0(6)	2.55(1)	0(3)'-M(1)-0(1)	91.	0(1)'-M(1)-0(6)	78.
		0(3)'-M(1)-0(1)'	164.	0(7)-M(1)-0(4)	114.
		0(3)'-M(1)-0(7)	113.	0(7)-M(1)-0(6)	156.
		0(3)'-M(1)-0(4)	98.	0(4)-M(1)-0(6)	60.
		0(3)'-M(1)-0(6)	91.		
M(2)-0(8)	2.14(1)	0(8)-M(2)-0(7)	131.	0(7)-M(2)-0(6)	100.
M(2)-0(7)	1.96(1)	0(8)-M(2)-0(6)	93.	0(7)-M(2)-0(4)	102.
M(2)-0(6)	1.92(1)	0(8)-M(2)-0(4)	98.	0(6)-M(2)-0(4)	140.
M(2)-0(4)	1.96(1)				
M(3)-0(5)	2.10(1)	0(5)-M(3)-0(2)	171.	0(2)-M(3)-0(8)	89.
M(3)-0(2)	2.19(1)	0(5)-M(3)-0(5)'	96.	0(2)-M(3)-0(2)'	108.
M(3)-0(5)'	1.99(1)	0(5)-M(3)-0(8)	98.	0(5)'-M(3)-0(8)	145.
M(3)-0(8)	2.06(1)	0(5)-M(3)-0(2)'	76.	0(5)'-M(3)-0(2)'	105.
M(3)-0(2)'	2.05(1)	0(2)-M(3)-0(5)'	75.	0(8)-M(3)-0(2)'	109.
P(1)-0(1)	1.530(13)	0(1)-P(1)-0(3)	112.	0(3)-P(1)-0(5)	111.
P(1)-0(3)	1.541(14)	0(1)-P(1)-0(5)	105.	0(3)-P(1)-0(7)	106.
P(1)-0(5)	1.560(11)	0(1)-P(1)-0(7)	113.	0(5)-P(1)-0(7)	110.
P(1)-0(7)	1.520(13)				
P(2)-0(2)	1.532(12)	0(2)-P(2)-0(4)	111.	0(4)-P(2)-0(6)	104.
P(2)-0(4)	1.554(13)	0(2)-P(2)-0(6)	111.	0(4)-P(2)-0(8)	111.
P(2)-0(6)	1.572(11)	0(2)-P(2)-0(8)	108.	0(6)-P(2)-0(8)	112.
P(2)-0(8)	1.523(10)				

Fig. (VI-1) Infinite sheets of $M(1)O_7$ polyhedra in B-graftonite. The edge and corner-sharing of the $M(1)O_7$ polyhedra are shown with solid bonds. The three remaining bonds are to oxygen atoms which are corner-shared with $M(2)O_4$ tetrahedra. The fourth oxygen atom in each tetrahedron is bonded to a M(3) cation as shown in Fig. (VI-2). The oxygen atoms are labelled according to the positions given in Table (VI-2).

FIGURE VI-1

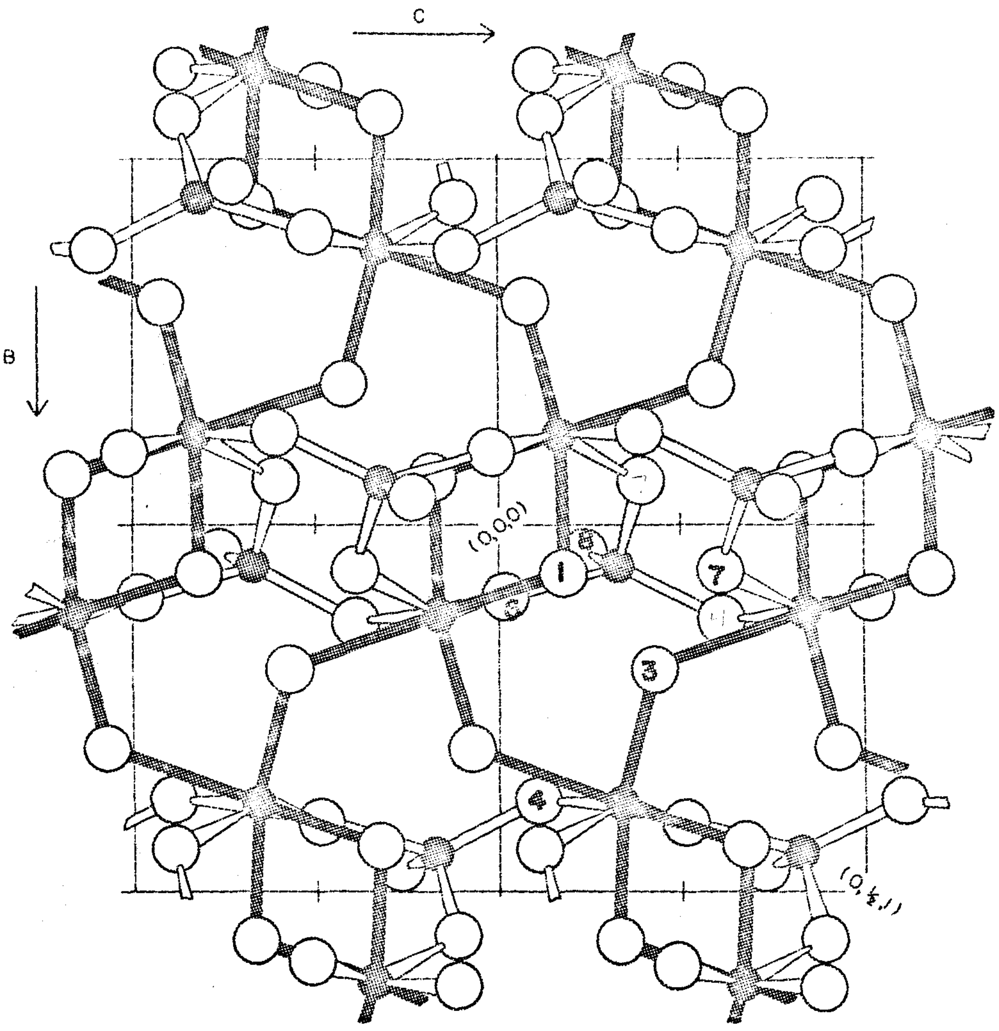
C
B
(0,0,0)
(0,½,1)
1
2
3
4
5
7
8
9

Fig. (VI-2) Infinite chains of $M(3)O_5$ polyhedra in B-graftonite. Each $M(3)O_5$ polyhedron shares two edges with glide-plane-related groups. These linkages are shown with solid bonds. The fifth oxygen atom in each group is corner-shared with a $M(2)O_4$ tetrahedron. The remaining three tetrahedral oxygen atoms are corner-shared with $M(1)O_7$ polyhedra as shown in Fig. (VI-1). The oxygen atoms are again labelled according to the positions given in Table (VI-2).

FIGURE VI-2

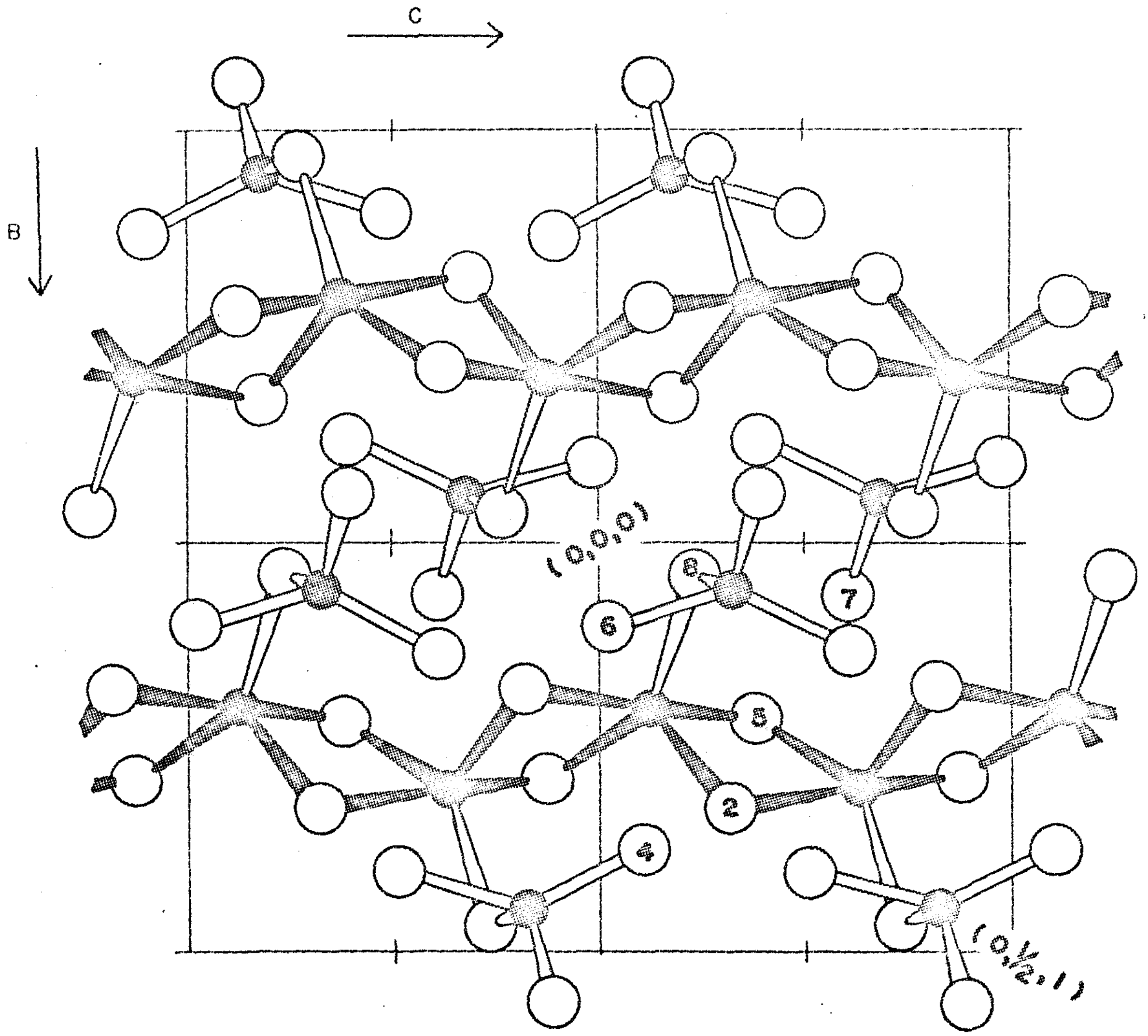
C
B
(0,0,0)
8
7
6
5
2
4
(0,½,1)

Fig. (VI-3) Interlocking sheets of cation polyhedra in B-graftonite. The corrugated sheets of cation polyhedra lie perpendicular to the $\underline{a}$ axis and are joined only through the phosphate tetrahedra which are shown here in outline. The cation-oxygen bonds which are broken in the figure denote bonding to an atom one unit cell away in the $\pm\underline{c}$ direction. As in Fig. (VI-1) and Fig. (VI-2), the oxygen atoms are labelled as in Table (VI-2).

FIGURE VI-3

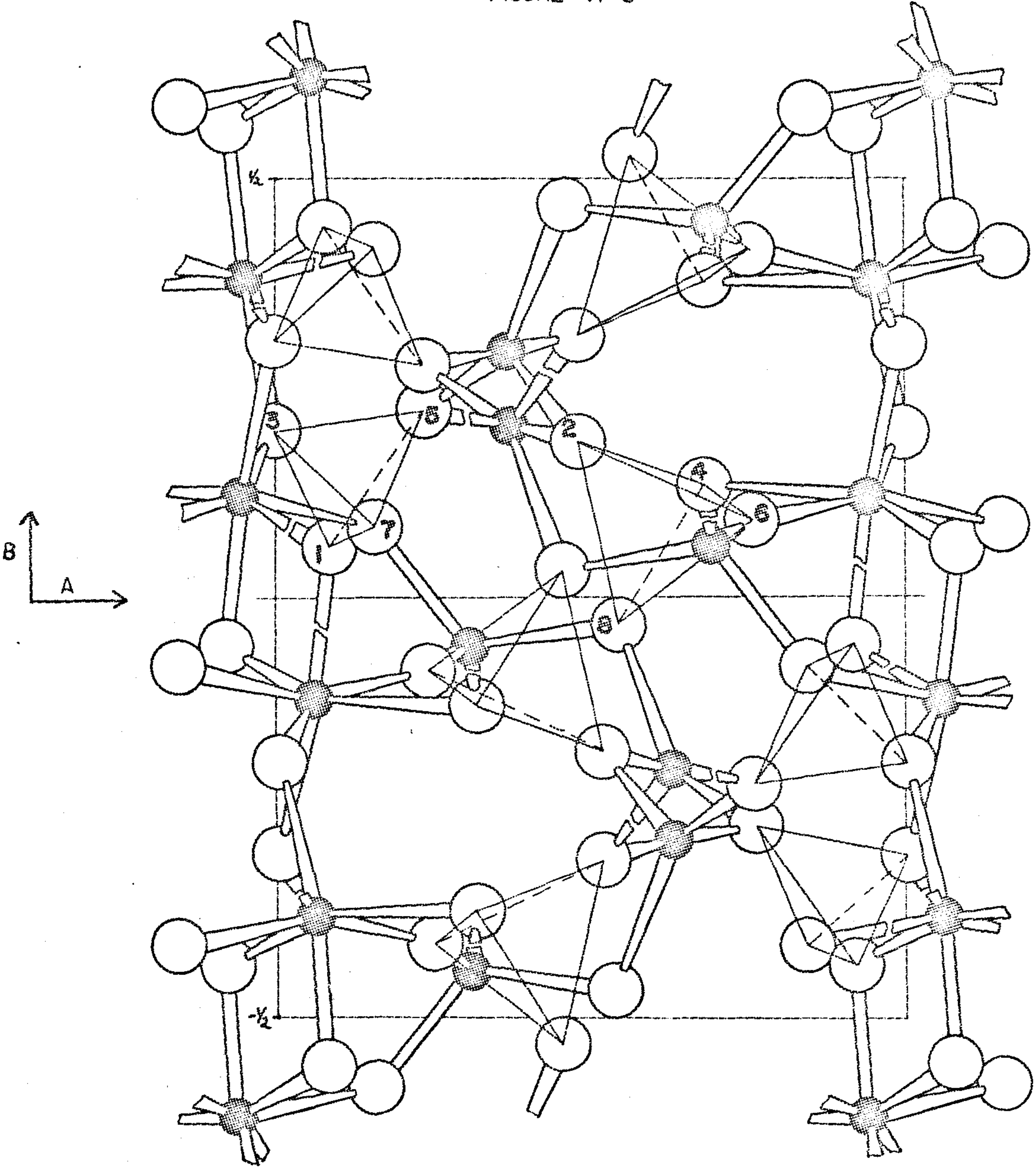
½
3
5
2
4
6
7
1
8
B
A
-½

The two PO_4 tetrahedra are slightly irregular, with average P-O bond distances of 1.538±0.015 Å and 1.545±0.019 Å respectively. The average O-P-O angle is 109.5° in each tetrahedron. The largest of these angles is 112° and the smallest 104°. Not all of the oxygen atoms in these two groups attain a planar environment to the degree found in β-$Zn_3(PO_4)_2$. The angles subtended at each oxygen atom and their sums are listed in Table (VI-6), where it can be seen that only O(2), O(6), O(7) and O(8) lie very close to the ligand plane. The widespread occurrence of this planarity had suggested that it might be useful in determining the probable positions of the oxygen atoms. The success of the procedure used in this determination supports this supposition, despite the fact that B-graftonite contains the largest deviations from planarity found in any of the divalent metal ion ortho- and pyrophosphate(38) structures studied to date.

MILLS MEMORIAL LIBRARY
McMASTER UNIVERSITY

TABLE (VI-6)

Bond angles subtended at the oxygen atoms in B-graftonite

Bonded atoms	Angle (°)	Sum of angles (°)	Bonded atoms	Angle (°)	Sum of angles (°)
M(1)-O(1)-M(1)'	101.8		M(3)-O(2)-M(3)'	99.6	
M(1)-O(1)-P(1)	126.2	350.8	M(3)-O(2)-P(2)	136.9	359.7
M(1)'-O(1)-P(1)	122.8		M(3)'-O(2)-P(2)	123.2	
M(1)-O(3)-M(1)'	126.3		M(1)-O(4)-M(2)	111.1	
M(1)-O(3)-P(1)	118.0	340.5	M(1)-O(4)-P(2)	97.6	336.2
M(1)'-O(3)-P(1)	96.2		M(2)-O(4)-P(2)	128.5	
M(3)-O(5)-M(3)'	104.6		M(1)-O(6)-M(2)	133.5	
M(3)-O(5)-P(1)	118.5	352.2	M(1)-O(6)-P(2)	97.1	358.2
M(3)'-O(5)-P(1)	129.1		M(2)-O(6)-P(2)	127.6	
M(1)-O(7)-M(2)	130.2		M(2)-O(8)-M(3)	108.1	
M(1)-O(7)-P(1)	100.4	357.0	M(2)-O(8)-P(2)	119.0	357.0
M(2)-O(7)-P(1)	129.4		M(3)-O(8)-P(2)	129.9	

CHAPTER VII

DISCUSSION AND SUMMARY

A. Discussion

The structures of the divalent metal ion orthophosphates will be discussed in terms of two types of polyhedron; the anion polyhedron, consisting of the PO_4^{3-} group, and the cation polyhedron, which comprises the cation and its near-neighbour oxygen atoms. The anion polyhedra are nearly regular tetrahedra in all the extensively refined structures presented here. The apparent irregularities in the P-O bond lengths in β^1-$Cd_3(PO_4)_2$ and to a lesser extent in β^1-$Mn_3(PO_4)_2$ are undoubtedly a consequence of the lower degree of refinement of these structures due to the limited amount of intensity data collected. Three dimensional data were not recorded for either of the β^1 structures and the decreased resolution inherent in projection data is also reflected in the much larger esd's calculated for the parameters of these structures then for the atomic parameters in β-$Zn_3(PO_4)_2$. The esd's for the oxygen atom parameters are considerably higher for β^1-$Cd_3(PO_4)_2$ than for β^1-$Mn_3(PO_4)_2$, even though the least squares residuals and overdeterminacy factors are comparable for these two refinements. This is due to the fact that the oxygen atoms in $Cd_3(PO_4)_2$ make up a much smaller fraction of the total electron density than they do in $Mn_3(PO_4)_2$ and their positions are therefore less well determined in the former structure.

The effective overdeterminacy in the β^1 structure was too low to permit meaningful anisotropic temperature factors to be determined. In the refinement of β^1-$Cd_3(PO_4)_2$ the isotropic temperature factors were not varied in the refinement, but were set to the values determined for the corresponding β^1-$Mn_3(PO_4)_2$ atoms. Thus the two β^1 structures have not been determined with sufficient accuracy to support a discussion of the deviations from regularity which are found in the PO_4 tetrahedra.

The B-graftonite structure is also not a suitable one on which to base such a discussion because two different cations, Cd^{++} and Zn^{++}, enter the same site, M(1), in the crystal. The detailed environment of each M(1) site will be dependent upon whether it is occupied by a Cd^{++} or a Zn^{++} ion, and the oxygen atom positions thus determined correspond to an "average" over all the M(1) sites. This positional disorder will be found around any site that is occupied by more than one atomic species.

Only for β-$Zn_3(PO_4)_2$ is the refinement accurate enough to warrant a discussion on the significance of the deviation from regularity of the PO_4 tetrahedra. Here, the shortening of the P-O bond to an oxygen atom which is strongly bonded to only one cation is quite significant. Despite the shortening of two bonds within the one tetrahedron, $P(2)O_4$, the average P-O bond length is only 0.006 Å shorter than that found for the $P(1)O_4$ group, and only 0.01 Å less than the average P-O bond distance found in other accurately determined orthophosphate structures(29). This constancy of the average P-O bond length, and the variation in length of the individual P-O bonds due to further bonding of the oxygen atoms, has been considered by Cruickshank$^{(31)}$ in his model of π-bonding within tetrahedral anions such as PO_4^{3-}.

This model proposes that, in an "isolated" PO_4 tetrahedron, there is a π-bonding system set up which utilizes the $3d_{z^2}$ and $3d_{x^2-y^2}$ orbitals of the phosphorus atom, and the $2p_x$ and $2p_y$ orbitals of each oxygen atom (the oxygen atom z axis is taken to be along the bond direction). This scheme provides a π-bond order of 1/2, in addition to the σ-bond of order unity, between the phosphorus atom and each oxygen atom. If an oxygen atom's $2p_x$ and/or $2p_y$ orbitals are required in making bonds to other atoms, the order of the π-bond to the phosphorus atom will be reduced, resulting in an increase in the P-O bond length. The phosphorus $3d_{z^2}$ and $3d_{x^2-y^2}$ orbitals can now be utilized more fully in the π-bonds to the remaining oxygen atoms of the tetrahedron, resulting in a decrease in these P-O bond distances. If the relationship between bond order and bond length is assumed to be linear, the average P-O bond distance should remain constant, as the total π-bond order is a constant (2). While this linearity has not been predictly theoretically, the approximate constancy of the average P-O bond length is well known.

In the divalent metal ion orthophosphates, the PO_4 tetrahedra are only approximately isolated. In a nuclear magnetic resonance (nmr) study of $LiMnPO_4$, Mays$^{(39)}$ found evidence for a superexchange effect which required the delocalization of electrons along the Mn-O-P-O-Mn paths in the crystal. The shortening of the P-O bonds in the cases of O(4) and

0(6) in β-$Zn_3(PO_4)_2$ shows the effect of a change in the environment about this "isolated" PO_4 group. These changes in P-O bond lengths are of smaller order than those cited by Cruickshank for the cases where an oxygen atom is shared between two PO_4 groups (pyro- and metaphosphates), for example, but the predictions of his model apply equally well here. Although the oxygen atom positions in B-graftonite, especially those around M(1), may not be very accurately determined, the same shortening of the P-O bonds involving oxygen atoms less strongly bonded to the cations is apparent (Table (VI-5)), but not as significant as in β-$Zn_3(PO_4)_2$.

There is a significant tendency for the oxygen atoms to lie close to the planes defined by their three nearest neighbours in these structures. In Table (IV-6) the sums of the bond angles subtended at the oxygen atoms are used to indicate the planarity of these atoms which in β-$Zn_3(PO_4)_2$ is very good. In β-^{1}-$Mn_3(PO_4)_2$ and B-graftonite the planarity is not as good, as indicated by Table (V-10) and Table (VI-6) respectively. It is worth noting that although B-graftonite provides the worst example of this planarity (β-^{1}-$Cd_3(PO_4)_2$ is not considered due to the incomplete state of refinement), the majority of the oxygen atoms were successfully located by assuming that they did lie in their ligand planes.

This planar arrangement of the two nearest cations and the phosphorus atom could be the result of their mutual electrostatic repulsions (phosphorus carries a nominal charge of +5 in a PO_4^{3-} anion), but it could also imply the existence of directed orbital overlap between the oxygen atoms and their neighbouring cations. Evidence for this further electron delocalization to the cations has been found in the nmr studies mentioned above. This planar oxygen atom environment has been found in other divalent metal orthophosphate structures, such as α-$Zn_3(PO_4)_2$ and γ-$Zn_3(PO_4)_2$, and also occurs with the terminal oxygen atoms in such pyrophosphates as α-$Mg_2P_2O_7$(40) and α-$Cu_2P_2O_7$(41). Thus it appears that a planar environment is a general feature of phosphate oxygen atoms that are shared by only two cations, and although this planarity is not rigourously maintained in each case it does provide an important packing constraint.

The great stability of the tetrahedral PO_4^{3-} anion, as attested to by the widespread occurrence of phosphate minerals, provides an even more severe constraint to the manner in which these structures can be formed and still satisfy the coordination preferences of the cations. Apparently, the increase in energy as a PO_4 tetrahedron is distorted is considerably greater than the energy differences associated with different cation environments. The regularity of the anion polyhedra is therefore maintained at the expense of the constancy of these cation environments.

All of the structures studied here display irregular cation coordination. It appears that the energy balance between the different orthophosphate phases is determined by the preference of the different cations for a particular environment, within the constraints in packing imposed by the PO_4 tetrahedra.

Zn^{++} is found in four-fold coordination in all the cation sites in α-$Zn_3(PO_4)_2$(8), and in four and five-fold coordination in β-$Zn_3(PO_4)_2$.

In the other orthophosphate phases, it exists in higher coordination only in a mixed compound such as B-graftonite or γ-$Zn_3(PO_4)_2$ where these sites are selectively occupied by a second cation such as Cd^{++} or Mg^{++}. Calvo(9) has shown that Mg^{++} dissolves preferentially in the octahedral cation site in γ-$Zn_3(PO_4)_2$ and it is presumed that Mn^{++} and Cd^{++} do also. In B-graftonite the segregation of Cd^{++} into the M(1) site is virtually complete. It is therefore apparent that, relative to Mn^{++}, Cd^{++} and Mg^{++}, Zn^{++} prefers sites of low coordination number, namely four or five.

From this observation one can begin to understand the relative stabilities of the different orthophosphate phases. These phases can be separated into four classes, which are listed in Table(VII-1). The α-$Zn_3(PO_4)_2$ structure occurs only with pure $Zn_3(PO_4)_2$ and is unstable, relative to γ-$Zn_3(PO_4)_2$, with the presence of more than a few mole per cent of Cd^{++}, Mn^{++} or Mg^{++}. The stability of the α phase is presumably marginal, and depends strongly on the Zn^{++} ions' preference for tetrahedral coordination. The stability of the γ phase cannot be attributed simply to a high expenditure of energy necessary to insert Mg^{++}, for example, into a tetrahedral site, as pure $Mg_3(PO_4)_2$ has this structure[†], and 2/3 of the cation sites are tetrahedrally coordinated(9).

In β-$Zn_3(PO_4)_2$ the cations have a slightly higher average coordination than in the α structure, but this structure is stable only near its melting point. Although the transition to the α phase is

---

[†] $Co_3(PO_4)_2$ also has the γ-$Zn_3(PO_4)_2$ structure. This has been confirmed(42) on the basis of single crystal photographs.

TABLE (VII-1)

The four structure classes among the small divalent metal ion orthophosphates

α-$Zn_3(PO_4)_2$	β-$Zn_3(PO_4)_2$	α-$Zn_3(PO_4)_2$	graftonite
α-$Zn_3(PO_4)_2$	β-$Zn_3(PO_4)_2$	$(Zn,Mg)_3(PO_4)_2$	$(Fe,Mn,Ca)_3(PO_4)_2$
	$\beta\overset{1}{-}Mn_3(PO_4)_2$	$(Zn,Mn)_3(PO_4)_2$	B-$(Zn,Cd)_3(PO_4)_2$
	$\beta\overset{1}{-}Cd_3(PO_4)_2$	$(Zn,Cd)_3(PO_4)_2$	C-$(Zn,Cd)_3(PO_4)_2$
	[β-$Cd_3(PO_4)_2$]	$Mg_3(PO_4)_2$	$Mn_3(PO_4)_2$
		$Co_3(PO_4)_2$	$Fe_3(PO_4)_2$

reversible, its sluggish nature suggests that a considerable rearrangement takes place in the bonding, and from an examination of these two structures, no clear mechanism for this transition has been deduced. The β^1 structures of $Mn_3(PO_4)_2$ and $Cd_3(PO_4)_2$ are similar to β-$Zn_3(PO_4)_2$, but the average cation coordination is again increased. Table (VI-9) shows that not all of the analogous β-$Zn_3(PO_4)_2$ bonds are maintained.

Hummel$^{(4)}$ reported a possible order-disorder phase transition in $Cd_3(PO_4)_2$ at approximately 900°C on the basis of some modest intensity changes in X-ray powder diagrams, and the presence of a peak in differential thermal analyses of the compound near this temperature. The phase occurring above this transition is probably the cadmium analogue of β-$Zn_3(PO_4)_2$, without the tripling of the c axis which occurs in β^1-$Cd_3(PO_4)_2$. If this is the case, the proposed "β-$Cd_3(PO_4)_2$" probably corresponds more closely to the average (small cell) β^1 structure, than to β-$Zn_3(PO_4)_2$, due to the preference of Cd^{++} for higher coordination numbers than Zn^{++}. No single-crystal X-ray studies have been undertaken on this phase, and this structure should be determined in order to obtain more information regarding the environmental preferences between Zn^{++} and Cd^{++}.

One might expect that a tripled "β^1-$Zn_3(PO_4)_2$" structure would be more stable than β-$Zn_3(PO_4)_2$ at temperatures below the stability region of the α phase. A photograph was taken of a β-$Zn_3(PO_4)_2$ single-crystal at low temperatures (<-100°C). No new reflections or significant intensity changes were seen. This failure to observe a β^1 phase does not rule out the possibility of its existence as there might have been insufficient thermal energy at these low temperatures to initiate a transition.

The graftonite-like structures are typified by the existence of the multi-coordinated cation site, M(1). In all examples of this structure which occur with mixed cation composition, there is a pronounced preferential solubility connected with this site. In B and C-graftonite(43), Cd^{++} exhibits a decided preference for this site, and in the mineral, Ca^{++} enters this site preferentially(43). In the mineral, site M(2), which in B-graftonite is tetrahedrally coordinated, has gained a fifth ligand. This is again consistent with the greater preference of Zn^{++} for tetrahedral coordination than that shown by Mn^{++} and Cd^{++}. The assignment of $Fe_3(PO_4)_2$ to the graftonite structure category is based on X-ray powder data(44) which exhibits a strong resemblence to the powder pattern of Mn-graftonite.

The stability of the graftonite structure in mixed orthophosphate systems where the M(1) site is preferentially filled by a large divalent cation suggest that other compounds such as $Zn_2Sr(PO_4)_2$, might also have this structure. X-ray powder data have been reported for this compound(45) but there is no pronounced similarity to the powder data of either B or C-graftonite(4). A single-crystal study of the zinc-strontium phosphates is of some importance if the stability criteria for these cations is to be fully understood.

There is a fifth class of divalent orthophosphate structures not included in the studies undertaken here, which is characteristic of the orthophosphates of large cations such as Ba^{++} and Sr^{++}. In the structures of $Ba_3(PO_4)_2$ and $Sr_3(PO_4)_2$(46), which are of high symmetry ($R\bar{3}m$), there are two cation sites, one 12-fold and the other 10-fold coordinated, which arise from the cations occupying two types of interstices in close-packed layers of PO_4 tetrahedra. $Ca_3(PO_4)_2$ forms two stable phases(47). The low temperature (whitlockite) phase forms a structure related to that of $Ba_3(PO_4)_2$. The structure of the α phase of $Ca_3(PO_4)_2$ which is stable above 1180°C has not been completely determined(47).

In the orthophosphate structures studied here it is difficult to talk of coordination number in a meaningful way as the cation environments are irregular. One cannot state when an interatomic distance is too great for the atoms to be "bonded". The value of 2.45 Å, for example, which was used to distinguish between "weakly" and "strongly" bonded oxygen atoms in the description of β^1-$Mn_3(PO_4)_2$, clearly lacks a quantitative justification.

This difficulty in defining the coordination number of an irregularly bonded cation makes the "coordination number hypothesis", regarding the correlation of Mn^{++} luminescence with the coordination number of the Mn^{++} ion, difficult to substantiate. A second difficulty arises from the fact that only the environments of the cation sites in the host lattice are known from a structure determination, and assumptions must be made concerning the sites that the Mn^{++} ions enter and the distortions which arise in these sites as a result. In β-$Zn_3(PO_4)_2$, for example, in which Mn^{++} should attain an octahedral environment according to its red luminescence, only the site occupied by Zn(2), where there is a sixth ligand weakly bonded to the cation, could be suitable, Preliminary electron paramagnetic resonance (epr) studies$^{(48)}$ of β-$Zn_3(PO_4)_2$:Mn, however, indicate that Mn^{++} enters at least two sites in the crystal, yet the luminescent bandwidth$^{(2)}$ does not suggest that more than one coordination number is involved. It is not possible for a Mn^{++} ion to attain six-fold coordination in either the Zn(1) or Zn(3) site without major distortions in the environments of these sites. Similarly in B-graftonite there are no sites which could lead to an octahedrally coordinated Mn^{++} ion, and it is extremely doubtful that Mn^{++} would enter an interstitial site as pure $Mn_3(PO_4)_2$ exists with this structure, and the mineral itself contains approximately 28 mole per cent $Mn_3(PO_4)_2$$^{(11)}$. Thus it would appear that no reliable conclusions about the cation environments in a host crystal can be made from the luminescent behaviour of Mn^{++}.

Coordination number is, in itself, too naive a concept on which to base an understanding of Mn^{++} luminescence. The effect of different environmental symmetries on the energy levels in the perturbed ion is not describable solely in terms of the number of ligands surrounding the ion. The re-emission process takes place after a length of time ($\simeq 10^{-8}$ seconds) which is long compared with the time the Mn^{++} environment requires to "relax" to a point near the minimum in the excited state potential function. This relaxation accounts for the large energy difference between the absorption and emission processes in the ion (the former corresponds to radiant energy in the ultra-violet part of the spectrum, while the latter occurs at 6380 Å in the case of $\beta\text{-}Zn_3(PO_4)_2$.

The extent of this relaxation, which depends on the effect of the ligand field on the excited state energy levels, must be calculated for the specific environment of the luminescing ion. In the first of a series of such calculations(49) made for a $[MnO_6]^{10-}$ complex with O_h and D_{4h} symmetries, the lowest excited states were found to be unstable with respect to a change in the ligand distance. Thus only through quantitative calculations of the ligand fields at the site of the luminescing ion, and through detailed analyses of the electronic energy levels under the influence of these fields, will a reliable correlation between crystal structure and luminescence be obtained.

B. Summary

The studies reported here have resulted in the determination of the crystal structure of $\beta\text{-}Zn_3(PO_4)_2$, the related $\beta^1\text{-}Mn_3(PO_4)_2$ and $\beta^1\text{-}Cd_3(PO_4)_2$ structures, and the structure of B-graftonite. The orthophosphates of small divalent metal ions have been grouped into four classes and some considerations regarding the stability criteria of each class have been discussed. Zn^{++} was found to exist most frequently in sites of low coordination number, four or five, while Mn^{++} and Cd^{++} achieved coordination numbers approaching six. The inadequacy of the coordination number hypothesis has also been discussed.

There are several areas in which further studies are required. The uncertainty in the preparation of $\beta^1\text{-}Mn_3(PO_4)_2$ should be resolved, and the stability of this phase relative to Mn-graftonite should be investigated. An extension of this phase study into the quaternary (Mn, Fe, Ca, Mg)$_3$(PO$_4$)$_2$ system is also necessary to determine the stability criteria for the graftonite structure; particularly the stability of this structure relative to that of the mineral sarcopside. Sarcopside and graftonite are found intergrown in nature, and chemical analyses(11) have indicated that Ca^{++} is excluded from sarcopside and that Mg^{++} is preferentially taken up instead. The information obtained in such a phase study, together with the determination of the detailed differences in the cation environments among all of the graftonite-like phases, is of paramount importance in understanding the stability criteria for these structures.

A single crystal study of Zn$_2$Sr(PO$_4$)$_2$ should also be undertaken as an inspection of the powder pattern is inconclusive in determining if this compound does crystallize with the graftonite structure. The proposed β-Cd$_3$(PO$_4$)$_2$ structure should also be investigated, and additional intensity data recorded to permit more extensive refinement of the β^1-Cd$_3$(PO$_4$)$_2$ structure.

An extension of these studies to the investigation of the crystal structures of M$_3$(XO$_4$)$_2$ compounds in general would be of value. It would be of particular interest to determine whether the orthoarsenates and orthovanadates of divalent metal ions of small radius such as Zn^{++}, Cd^{++}, Mn^{++} etc., have the same structures as the orthophosphates discussed here. This might be expected on the basis of constraints imposed by the tetrahedral AsO$_4^{3-}$ and VO$_4^{3-}$ anions, similar to those imposed by the PO$_4^{3-}$ anions. Accurate determinations of these structures would provide information on the regularity and resistance to distortion of these anions relative to PO_4^{3-}. This in turn would permit a more complete evaluation of the structural constraints imposed by such anions.

BIBLIOGRAPHY

1. F. L. Katnack, F. A. Hummel; J. Electrochem. Soc., 105, 125 (1958).
2. F. A. Hummel, F. L. Katnack; ibid, 105, 528 (1958).
3. A. L. Smith; ibid, 98, 363 (1951).
4. J. J. Brown, F. A. Hummel; ibid, 110, 1218 (1963).
5. J. F. Sarver, F. L. Katnack, F. A. Hummel; ibid, 106, 960 (1959).
6. S. H. Linwood, W. A. Weyl; J. Opt. Soc. Am., 32, 443 (1942).
7. J. H. Schulman; J. Appl. Phys., 17, 902 (1946).
8. C. Calvo; Can. J. Chem., 43, 436 (1965).
9. C. Calvo; J. Phys. & Chem. of Solids, 24, 141 (1963).
10. D. S. McClure; "Solid State Physics", Vol. 9, Academic Press, New York (1959).
11. C. S. Hurlbut; Am. Miner., 50, 1698 (1965).
12. International Tables for X-ray Crystallography, Vol. 2, Kynoch Press, Birmingham (1959).
13. International Tables for X-ray Crystallography, Vol. 3, Kynoch Press, Birmingham (1962).
14. A. L. Patterson; Phys. Rev., 46, 372 (1934).
15. M. J. Buerger; "Vector Space", John Wiley & Sons, New York (1959).
16. M. M. Woolfson; "Direct Methods in Crystallography", Clarendon Press, Oxford (1961).
17. H. Lipson & W. Cochran ; "The Crystalline State", Vol. 3, ed. by L. Bragg, "The Determination of Crystal Structures", G. Bell & Sons, London (1953).

18. International Tables for X-ray Crystallography, Vol. 1, Kynoch Press, Birmingham (1952).

19. C. Calvo; Private communication.

20. D. W. J. Cruickshank, D. E. Pilling, A. Bujosa, F. M. Lovell , M. R. Truter; in "Computing Methods and the Phase Problem in X-ray Crystal Analysis", ed. by R. Pepinsby, J. M. Robertson & J. C. Speakman, Pergamon Press, New York (1961).

21. M. J. Buerger; "Crystal Structure Analysis". John Wiley & Sons, New York (1960).

22. L. E. Alexander, G. S. Smith; Acta Cryst., 15, 983 (1962).

23. B. E. Robertson; M. Sc. Thesis, McMaster University, (1966).

24. W. Cochran ; Acta. Cryst., 3, 268 (1950).

25. "Physical Methods of Organic Chemistry", ed. by A. Weissberger, Vol. I, part 1, Interscience Publishers, New York (1949).

26. D. T. Cromer, K. Herrington; J. Am. Chem. Soc., 77, 4708 (1955).

27. M. J. Buerger, "X-ray Crystallography", John Wiley & Sons, New York (1962).

28. A. S. Cooper; Acta. Cryst., 15, 578 (1962).

29a. M. Fehlmann, S. Ghose, J. J. Finney; J. Chem. Phys. 41, 1910 (1964).

29b. S. C. Abrahams, J. L. Bernstein; ibid, 44, 2223 (1966).

29c. H. Cid-Dresdner; Z. Krist., 121, 87 (1965).

30. K. Lonsdale; Mineral. Mag., 28, 14 (1947).

31. D. W. J. Cruickshank; J. Chem. Soc., (1961), 5486.

32. C. Calvo; Private communication.

33. M. L. Lindberg; Am. Miner, 35, 59 (1960).

34. B. E. Robertson; M. Sc. Thesis, McMaster University, (1966).

35. M. E. Mrose, D. E. Appleman; Prog. Am. Cryst. Assoc. Ann. Meet.,(1961).

36. H. B. Dyer; Acta. Cryst., 4, 42 (1951).

37. M. J. Buerger; "X-ray Crystallography", John Wiley & Sons, New York (1962).

38. C. Calvo; Private communication.

39. J. M. Mays; Phys. Rev., 131, 38 (1963).

40. C. Calvo; Acta. Cryst., in press (1967).

41. B. Robertson, C. Calvo; ibid, in press (1967).

42. C. Calvo; Private communication.

43. C. Calvo; Private communication.

44. J. Korinth, P. Royen; Z. Anorg. Allg. Chem., 313, 121 (1961).

45. J. F. Sarver, M. V. Hoffman & F. A. Hummel; J. Electrochem. Soc., 108, 1103 (1961).

46. W. H. Zachariasen; Acta. Cryst., 1, 263 (1948).

47. A. L. Mackay; ibid, 6, 743 (1953).

48. C. V. Stager; Private communication.

49. L. L. Lohr; J. Chem. Phys., 45, 3611 (1966).

APPENDIX A

Dead-time Correction Evaluation

Let the true integrated intensity, I, of a reflection have a Gaussian profile, so that the true count rate is given by

$$i(t) = \frac{I \exp(-t^2)}{\sqrt{\pi}} \tag{A-1}$$

Let the observed integrated intensity be

$$I' = i'(t)\, dt = \frac{i(t)\, dt}{1 + i(t)\tau} \tag{A-2}$$

Substituting Eqn. (A-1) into Eqn. (A-2), and expanding the denominator of the integral by means of a Binomial expansion and integrating term by term, yields

$$I' = I \sum_{n=o} \left(\frac{-I\tau}{\sqrt{\pi}}\right)^n \frac{1}{\sqrt{n+1}} \tag{A-3}$$

which is valid when $\frac{I\tau}{\sqrt{\pi}} < 1$, for which values the series is rapidly convergent.

Table (A-1) shows the values of I' calculated for different values of I, with a value for τ of 1.0×10^{-6}. The largest value of I and the corresponding value of I' have been used to calculate the effective resolution time ψ, which in turn has been used to calculate the corrected intensities I_c, where

$$I_c = \frac{I'}{I - I'\psi} \qquad \text{(Eqn. III-3)}$$

The coincidence losses $\frac{I - I'}{I}$, and the discrepancies between I and I_c, $\frac{I - I_c}{I}$, are listed for each set of tabulated values of I and I'.

TABLE A-1

Dead-time correction evaluation

I ($\times 10^4$)	I' ($\times 10^4$)	I_c ($\times 10^4$)	$\frac{100(I - I')}{I}$	$\frac{100(I - I_c)}{I}$
100.0	72.5	100.0	27.5	0.00
80.0	61.3	79.79	23.4	0.26
60.0	48.7	59.75	18.8	0.41
40.0	34.6	39.83	13.5	0.43
20.0	18.5	19.94	7.3	0.30
10.0	9.62	9.984	3.8	0.16
5.0	4.90	4.995	1.9	0.09
1.0	0.996	0.999^+	0.4	0.02